STUDY OF DIELECTRIC BARRIER DISCHARGE PLASMA JET (DBDJ) FOR BACTERICIDAL IN CONTAMINATED WOUNDS

PIPATH PORAMAPIJITWAT

MASTER OF SCIENCE IN NANOSCIENCE AND TECHNOLOGY

MAEJO UNIVERSITY

2019

STUDY OF DIELECTRIC BARRIER DISCHARGE PLASMA JET (DBDJ) FOR BACTERICIDAL IN CONTAMINATED WOUNDS

PIPATH PORAMAPIJITWAT

A THESIS SUBMITTED IN PARTIAL FULFILLMENT
OF THE REQUIREMENTS FOR THE DEGREE OF MASTER OF SCIENCE
IN NANOSCIENCE AND TECHNOLOGY
GRADUATE SCHOOL MAEJO UNIVERSITY
2019

STUDY OF DIELECTRIC BARRIER DISCHARGE PLASMA JET (DBDJ)
FOR BACTERICIDAL IN CONTAMINATED WOUNDS

PIPATH PORAMAPIJITWAT

THIS THESIS HAS BEEN APPROVED IN PARTIAL FULFLLMENT
OF THE REQUIREMENTS FOR THE DEGREE OF MASTER OF SCIENCE
IN NANOSCIENCE AND TECHNOLOGY

APPROVED BY **Advisory Committee**

Chair .....
(Dr. Sureeporn Sarapirom)
...../...../.....

Committee .....
(Dr. Keratiya Janpong)
...../...../.....

Committee .....
(Associate Professor Dr. Wasin Charerntantanakul)
...../...../.....

Program Chair, Master of Science .....
in Nanoscience and Technology (Assistant Professor Dr. Viruntachar Kruefu)
...../...../.....

CERTIFIED BY GRADUATE SCHOOL .....
(Associate Professor Dr. Kriangsak Mengamphan)
Dean of Graduate School
...../...../.....

ชื่อเรื่อง การศึกษาพลาสมาเจ็ทแบบไดอิเล็คทริกแบร์ริเออร์ดิสชาจ์นเพื่อการฆ่าเชื้อแบคทีเรียในแผลติดเชื้อ
ชื่อผู้เขียน นายพิพัฒน์ ปรมาพิจิตรวัฒน์
ชื่อปริญญา วิทยาศาสตรมหาบัณฑิต สาขาวิชาวิทยาศาสตร์และเทคโนโลยีนาโน
อาจารย์ที่ปรึกษาหลัก อาจารย์ ดร.สุรีย์พร สราภิรมย์

บทคัดย่อ

พลาสมาความดันบรรยากาศ (CAPP) เป็นเทคนิคที่ได้รับการยอมรับการใช้งานทางด้านการแพทย์ ซึ่งเป็นนวัตกรรมใหม่ที่มีการนำไปใช้งานทางด้านการแพทย์ เช่น การเพิ่มประสิทธิภาพของการรักษาแผลติดเชื้อพร้อมกับบรรเทาอาการเจ็บปวดของผู้ป่วยไม่มีผลข้างเคียง แผลติดเชื้อเป็นปัญหาสุขภาพที่สำคัญในหลายประเทศ ปัจจัยที่เป็นสาเหตุของปัญหาสุขภาพของผู้ป่วย ได้แก่ โรคเบาหวาน บาดแผลที่ปนเปื้อนแบคทีเรียและอื่น ๆ ผู้ป่วยต้องทนทุกข์ทรมานและต้องใช้เวลานานในการบำบัดรักษาด้วยยาปฏิชีวนะหรือวิธีการรักษาอื่น ๆ นอกจากนี้การใช้ยาปฏิชีวนะเป็นระยะเวลานานจะก่อให้เกิดการดื้อยาของแบคทีเรียเกิดขึ้น เช่น methicillin-resistant *Staphylococcus aureus* (MRSA) โดยเชื้อแบคทีเรียนั้นมีขีดความสามารถในการพัฒนาความต้านทานต่อยาปฏิชีวนะได้รวดเร็วกว่าการที่เราจะทำการพัฒนายาปฏิชีวนะตัวใหม่ออกมา ด้วยเหตุนี้จึงเป็นปัญหาหลักในการรักษาแผลติดเชื้อ ในการศึกษานี้จะใช้พลาสมาเจ็ทแบบไดอิเล็คทริกแบร์ริเออร์ดิสชาจ์น (DBDJ) ในการฆ่าเชื้อแบคทีเรียและทดลองกับ Primary Human Dermal Fibroblasts Adult (HDFa) cells เพื่อศึกษาผลข้างเคียงของ DBDJ ต่อเซลล์ โดย DBDJ กำเนิดด้วยเงื่อนไขที่ไฟฟ้าแรงดันสูงความถี่ 20 กิโลเฮิร์ทซ์และอัตราการไหลของก๊าซฮีเลียม 1 ลิตรต่อนาที กำลังของพลาสมาในช่วงระหว่าง 0.27 วัตต์ ถึง 0.50 วัตต์และระยะเวลาในการทดลองระหว่าง 15 วินาที ถึง 60 วินาที อนุมูลในพลาสมาจะใช้เครื่องมือวิเคราะห์สเปกตรัมทางแสง (OES) ในการตรวจวัด ผลสเปกตรัมจาก OES พบกลุ่มของ NO และ OH ซึ่งเป็นอนุมูลที่สำคัญต่อการรักษาบาดแผลที่เกิดจากเชื้อแบคทีเรีย การเพิ่มขึ้นของปริมาณอนุมูลอิสระในพลาสมาขึ้นอยู่กับกำลังของพลาสมา โดยวิธี Colony Forming Unit (CFU) จะใช้เพื่อตรวจสอบประสิทธิภาพของการฆ่าแบคทีเรีย *Staphylococcus aureus (S. aureus)* และ *Pseudomonas aeruginosa (P. aeruginosa)* ซึ่งใช้ในการศึกษาประสิทธิภาพการฆ่าเชื้อแบคทีเรีย ผลการทดลองแสดงให้เห็นว่ากำลังของพลาสมาและระยะเวลาที่ใช้เป็นปัจจัยสำคัญในการฆ่าเชื้อแบคทีเรีย เมื่อใช้กำลังพลาสมาที่ 0.50 วัตต์และ ณ เวลาที่ 60 วินาที ผลของการฆ่าเชื้อแบคทีเรียเพิ่มขึ้นถึง 100% ดังนั้นจึงเลือกที่สภาวะการทดลองดังกล่าวในการศึกษาผลกระทบของ

พลาสมาต่อแบคทีเรียไบโอฟิล์มและเซลล์ HDFa ผลการทดลองจากกล้องจุลทรรศน์แบบฟลูออเรสเซนต์ โดยใช้เทคนิค live/dead assay แสดงให้เห็นว่าพลาสมามีประสิทธิภาพสูงในการกำจัดแบคทีเรียไบโอฟิล์ม การศึกษาผลกระทบของ DBDJ ต่อเซลล์ HDFa จะใช้กล้องจุลทรรศ์แบบเชิงแสง เทคนิค live/dead assay และเครื่อง Muse Cell Analyzer ร่วมกับชุด Muse Count & Viability Assay Kit และ Muse Annexin V and Dead Cell Assay Kit ผลที่ได้แสดงให้เห็นว่า DBDJ มีประสิทธิภาพสูงในการฆ่าเชื้อแบคทีเรียโดยไม่ก่อให้เกิดผลกระทบข้างเคียงต่อเซลล์ HDFa ภายใต้สภาวะเงื่อนไขเดียวกัน ดังนั้น DBDJ ที่กำลังพลาสมา 0.50 วัตต์และ ณ เวลา 60 วินาที มีประสิทธิภาพสูงในการฆ่าเชื้อแบคทีเรีย การกำจัดแบคทีเรียไบโอฟิล์มและไม่ก่อให้เกิดความเสียหายหรือผลข้างเคียงต่อ การมีชีวิตของเซลล์ การเกิดอะพอพโทซิส และการตายของเซลล์ HDFa ในการทดลองซึ่งเป็นสิ่งที่สำคัญ

คำสำคัญ : พลาสมาเจ็ทแบบไดอิเล็คทริกแบร์ริเออร์ดิสชาจ์น, เซลล์ไฟโบรบลาสต์, การฆ่าเชื้อแบคทีเรีย, การรักษาแผล, แบคทีเรียไบโอฟิล์ม, แผลติดเชื้อ

Title STUDY OF DIELECTRIC BARRIER DISCHARGE PLASMA JET (DBDJ) FOR BACTERICIDAL IN CONTAMINATED WOUNDS

Author Mr. Pipath Poramapijitwat

Degree Master of Science in Nanoscience and Technology

Advisory Committee Chairperson Dr. Sureeporn Sarapirom

ABSTRACT

The cold atmospheric pressure plasma (CAPP) technique has been recognized in medical fields to bring a new innovative approach in biomedical applications such a contaminated wound healing enhancement as well as relieving the patient's pain without side effects. Contaminated wounds are a major health problem in many countries. Factors of patient health problems are such as diabetes, contaminated wounds, bacteria as well as others. The patients endures pain and requires long treatment periods using antibiotics or other therapies. Moreover, using antibiotics for a long period of time bacterial resistance occurs, such as methicillin-resistant *Staphylococcus aureus* (MRSA). Bacteria have the ability to develop resistance to antibiotics faster than one can develop new drugs. This being the main problem in contaminated wound healing. In this study, the dielectric barrier discharge plasma jet (DBDJ) was used for bactericidal and treated the Primary Human Dermal Fibroblasts Adult (HDFa) cells to study the side effect of DBDJ. This DBDJ is driven by high voltage dc pulse at 20 kHz and using 1 L/min of helium (He) as plasma gas. The DBDJ plasma varied the plasma dissipated power from 0.27 W to 0.50 W and the exposure time 15 s to 60 s. Plasma radical species were utilized by using an optical emission spectroscopy (OES). The results of the OES study found NO and OH radical groups, which play an important role in bactericidal and contaminated wound healing. The increase of radical plasma density depends on the plasma dissipated power. The Colony Forming unit (CFU) method was used to monitor the efficiency of bacteria

killing. *Staphylococcus aureus (S. aureus)* and *Pseudomonas aeruginosa (P. aeruginosa)* were used in the vitro bacteria killing test. The results showed that the plasma dissipated power and exposure time were major factors in bactericidal. When increasing the plasma dissipated power to 0.50 W and exposure time to 60 s, the effect of bacteria killing increased to 100%. Therefore, this condition was choosing to study the effect of plasma on bacteria biofilm and HDFa cells. The result from fluorescent images by live/dead assay showed that DBDJ had high efficiency to removed biofilm. Studying the effects of DBDJ on HDFa cells using optical microscopes, live/dead assay and Muse Cell Analyzer with the Muse Count & Viability Assay Kit and Muse Annexin V and Dead Cell Assay Kit, the result showed the DBDJ being highly efficient for bactericidal as well as not having any side effects on HDFa cells under the same conditions. Therefore, the DBDJ at plasma dissipated power 0.50 W and exposure time 60 s has a high efficiency to kill bacteria, destroy bacteria biofilm by without damage cell and also without side effect to cell viability, apoptosis and death of HDFa cells as in vitro is essential for clinical use.

Keywords : Dielectric Barrier Discharge Plasma Jet, Human Dermal Fibroblasts adult cells, Bactericidal, Wound Healing, Bacterial Biofilms, Contaminated Wounds

ACKNOWLEDGEMENTS

The authors are thankful to the following contributors: Plasma Medicine project in supporting the equipment and budget. The Dielectric Barrier Discharge Plasma Jet (DBDJ) from Dr.Chanchai Chutsirimongkol to investigate the bactericidal in contaminated wounds as in vitro. Thailand Institute of Scientific and Technological Research (TISTR) for support bacterial stain in my research. Thailand Center of Excellence in Physics (ThEP), STEM (Science, Technology, Engineering, Mathematics) Workforce and Graduate School Maejo University for my scholarships. Plasma and Beam Physics research facility (PBP) for equipment, laboratory, suggestion, guidelines and help in my research.

I would like to thank my thesis advisor Dr. Sureeporn Sarapirom for supporting, suggesting and giving me an opportunity to do this new subject research. The door of her office was always open whenever I ran into a trouble spot or had a question about my research or writing. She consistently forced me that this paper to be my own work and steered me in the right direction. Dr. Keratiya Janpong and Assoc. Prof. Dr. Wasin Charerntantanakul my thesis co-advisors in reading and publishing of my thesis, to them I am grateful and indebted for their valuable comments. A special mention to, Assoc. Prof. Dr. Dheerawan Boonyawan for my scholarship and budget in my research.

Finally, I must express my gratitude to my parents for their supporting and continuous encouragement throughout my years of study. This accomplishment would not have been possible without them. Thank you.

Pipath Poramapijitwat

TABLE OF CONTENTS

Page

LIST OF TABLES

Page

LIST OF FIGURES

Page

CHAPTER 1
INTRODUCTION

1.1 Background

In recent years, the over-prescription and incorrect use of antibiotics has led to a rise of bacterial resistant to antibiotic. Antibiotic resistance in bacteria is a major problem and is on the rise worldwide, making some previously treatable infections incurable or even life-threatening. Bacteria are prokaryotic micro-organisms which have great adaptability to changing environments. Bacteria is the main cause of illnesses, wound infections, contaminated wound, meningitis, pneumonia etc. Bacteria can be divided into two groups according to the cell wall structure. Gram-positive bacteria have a relative thick peptidoglycan (20 to 80 nm) cell wall, while gram-negative bacteria have a thinner peptidoglycan (< 10 nm) cell wall (Lin et al., 2016; Mai-Prochnow et al., 2016). The difference of bacterial cell wall leads to different properties to the cell, especially the cell responses to external stressors such as heat, UV radiation and also antibiotics. One of the gram-positive bacterial strains is *Staphylococcus aureus* (*S. aureus*) and one gram-negative bacterial strains is *Pseudomonas aeruginosa* (*P. aeruginosa*). These strains are causing public health concerns in postsurgical patients. The *S. aureus*, *P. aeruginosa* and methicillin-resistant *Staphylococcus aureus* (MRSA) are the most commonly identified bacterium in wounds (Mohd Nasir et al., 2016). Therefore, there is a growing need for the discovery and development of new antibacterial methods of sterilization. Preferably these methods should be easy to use, be cost effective, have low toxicity and no resistance from bacteria (Mai-Prochnow et al., 2015). One of those techniques is cold atmospheric pressure plasma treatment (CAPP). CAPP was widely studied and reported to have high efficiency to eradicate a wide range of pathogens such as fungi, viruses and bacteria. The CAPP sources have been operated at an excitation frequency, either in the several tens of kilohertz ac range or in the radio frequency (RF) range. Various factors including temperature, charged particle, ion and radical species can be manipulated to find suitable conditions. Therefore, it is important to understand the basics of physical and chemical

properties in plasma, such as power deposition and consumption, electromagnetic, electrical characteristics, optical emission spectrum, gas temperature and other parameter in plasma (Kim et al., 2009).

In this study, effects of plasma radicals on *S. aureus*, *P. aeruginosa*, bacteria biofilm and Primary Human Dermal Fibroblasts adult (HDFa) cells were investigated for contaminated wound healing model as in vitro.

1.1.1 Atmospheric pressure plasma (APP)

When more energy or heat is added to atoms or molecules, they turn to be ionized. An electron may gain enough energy to escape from an atom. After the escape of electron, atoms turn into ions. In adequately heated, energy to gas, ionization happens many times, creating clouds of ions and free electrons. This ionized gas mixture comprises of ions, electrons and neutral atoms, called "Plasma". Plasma is the fourth state of matter.

Among the many distinctions between different kinds of plasmas, one is between thermal plasma and non-thermal plasma. Within thermal plasmas the electrons and the ions have the same energy. Non-thermal plasma gains its reactivity from the high energy electrons, while the ions and neutral species remain near room temperature (von Woedtke et al., 2013). Example of thermal plasma are sun and laser fusion plasma. Non-thermal plasma divides two kinds, vacuum pressure plasma or low-pressure plasma and atmospheric pressure plasma. APP is generated by applying an electrical field to a neutral gas or gas mixture. Low-pressure plasma is such as arc plasma, plasma torch, metal vapor vacuum arc and filtered cathodic vacuum arc. APP is such as dielectric barrier discharge (DBD), corona plasma, plasma effluent downstream and plasma jets.

1.1.2 Plasma medicine

Plasma medicine is a new way of plasma application. Physical plasmas are excited ionized gases, which contain different concentrations of low molecular reactive atoms, ions and molecules and emit several kinds of electromagnetic radiation including infrared, visible and ultraviolet (UV) light which are generated by energy

supplied to a neutral gas. Non-thermal plasma or low-temperature plasma (LTP) attributes are mostly technical ones whose composition and temperature are adjustable in a wide range by parameters like type of energy source, power of generator, type of gas, pressure of gas, rate of gas flow and composition. In most cases CAPP technical applications are generated by applying an electrical field to a neutral gas or gas mixture (von Woedtke et al., 2013).

In earlier stages, direct plasma applications on living cell in electro-surgery were based on very harsh interactions of plasma with cells and tissue leading finally to cellular eradication and local “sealing” of tissue. The new research field of plasma medicine considers the advantages and effects of LTP or CAP techniques, with much more differentiated interaction of specific plasma components and specific structural elements along with functionalities of living cells which can probably lead either to stimulation or inhibition of cellular function (Figure 1) (von Woedtke et al., 2013).

In CAPP sources, the main reactive components will consist of reactive neutral species such as reactive oxygen and nitrogen species and are called “reactive oxygen-nitrogen species (RONS)”, UV- radiation and electrical field. In some cases, charged species and electromagnetic fields may also play a role.

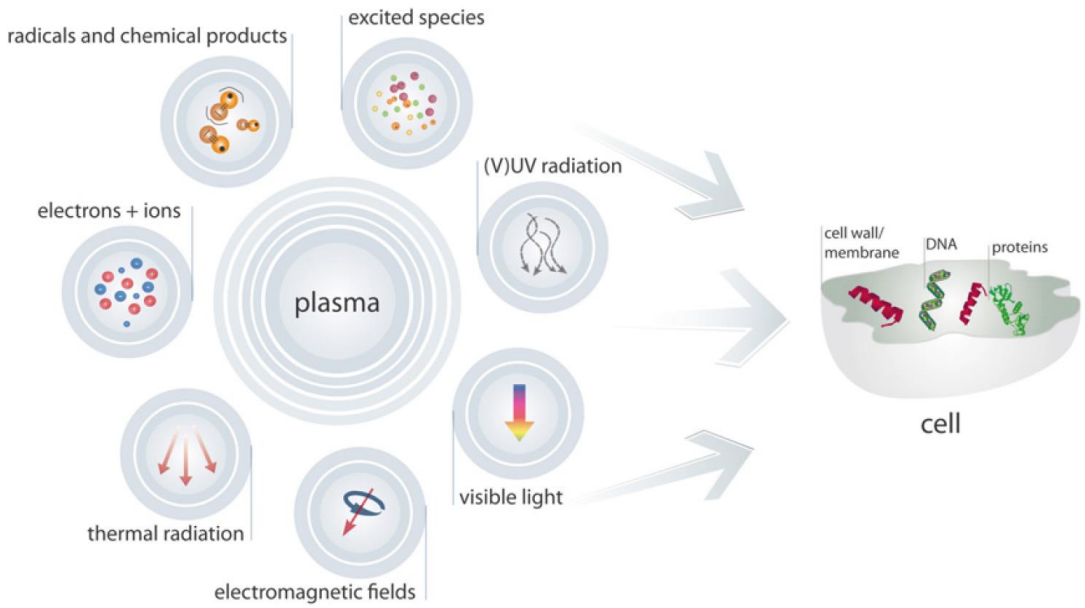

Figure 1 The plasma applications on living tissue (von Woedtke et al., 2013).

About 1% of the population in developed nations suffer from contaminated wounds (Etufugh and Phillips, 2007). Contaminated wounds may result from venous diseases, arterial diseases, diabetes mellitus, pyoderma gangrenosum, carcinoma and other factors. As the population ages, this occurrence is likely to increase. CAPP may help with the treatment though it is unlikely that plasmas will "heal" the underlying disease, The eliminating of bacterial and fungal infections by plasmas may well reduce the suffering, support the treatment and accelerate the recovery (Kong et al., 2009). In recent year, CAPP has shown potential to bactericidal and optimize wound healing process by RONS, free radicals, charge particles and ion in plasma.

It is interesting to note that physical plasma has been coined by Irving Langmuir. In repeating the characteristics of ionic liquids extensively in biology and medicine they are like the characteristics of ionized gas. Despite this historical connection, applications of plasma in medicine has not been explored until recently (Laroussi et al., 2003). This situation will surely change and in this research DBDJ were used to effectively treat bactericidal and bacteria biofilm without damaging HDFa cells in vitro.

1.2 Objectives

1.2.1 Optimize condition of dielectric barrier discharge plasma jet (DBDJ) for bactericidal as in vitro.

1.2.2 Dielectric barrier discharge plasma jet (DBDJ) for eradicated bacteria, bacterial biofilm and without side effect to Primary Human Dermal Fibroblasts adult (HDFa) cells as in vitro.

1.3 Expectation

The optimum condition of dielectric barrier discharge plasma jet (DBDJ) in killing bacteria, destroying bacterial biofilm by without damage cell and also without side effect to cell viability, apoptosis and death of HDFa cells as in vitro is essential for clinical use.

CHAPTER 2
THEORY AND LITERATURE REVIEW

2.1 Plasma

The first time the term "plasma" for an ionized gas was presented in 1927 by Irving Langmuir (1881-1957) (Mott-Smith, 1971). The American chemist, who won the Nobel Prize in 1932, studied electric discharges and their fluid characteristics at General Electric Research and Development Center. Natural plasma phenomena on earth such as lightning and the aurora borealis, a diffuse light displayed in the sky close to the polar circles, when the magnetosphere collide with atoms in the air by high energy charged particles initiated from solar wind.

Plasma refers to an "ionized gas," in which approximately electrons and ions are of equal numbers. It has macroscopic viewpoint of an electrically neutral state. The electron density (n_e) and ion density (n_i) are extremely equal, and relative to the plasma density. Because within plasma electrons can move freely and have a conductive property. When applied radiofrequency (RF) power to a couple of electrodes in an etch chamber, electric fields are generated by the RF power and electrons are accelerated, acquire kinetic energy, and collide with atoms and molecules (Figure 2a). If the electron kinetic energy is greater than the ionization energy, the electron in the valence band are ejected from the atom or molecule. Therefore, the neutral atom or the molecule change to ion (Figure 2b). However, the ejected electron from the molecule or the atom, adds to the first colliding electron and hence makes a total of two electrons. These electrons under the electric field are accelerated, collide with other atoms and molecules, and new ions and electrons are generated. The number of ions and electrons increased as in an avalanche and finally exceed a threshold level over which a resulting discharge begins and thus creates a plasma (Nojiri, 2015). This mechanism shows in Figure 3.

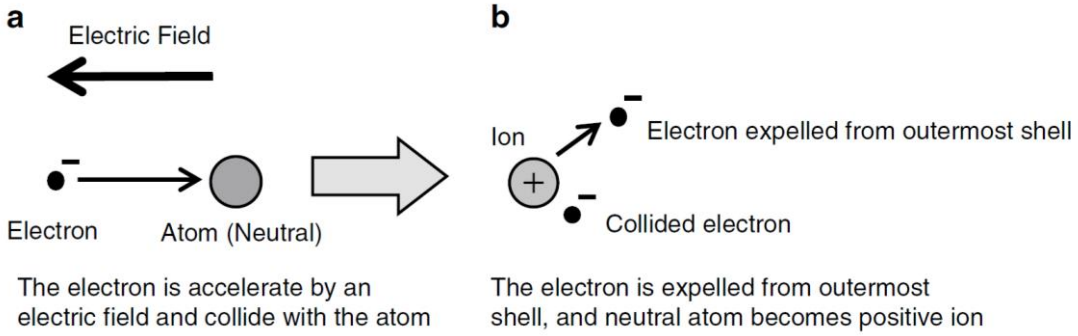

Figure 2 The collision of electrons and neutral atoms generate ion (Nojiri, 2015).

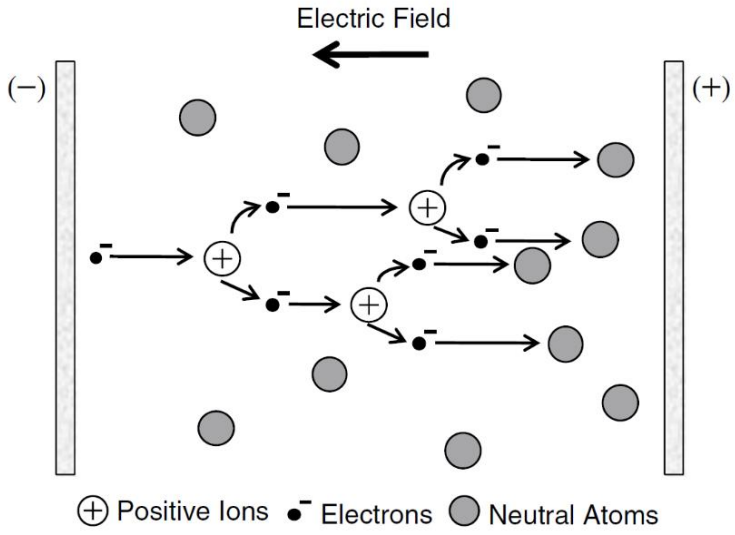

Figure 3 Principle of gas discharge (Nojiri, 2015).

The plasma classification is a completely ionized plasma, in which electrons and ions are ionized 100%, and a weakly ionized plasma with lower degree of ionization and hence a mixture of ions, electrons and where neutral atoms and molecules coexist. Glow discharge plasma is a weakly ionized plasma and consists of the same numbers of positive and negative charges, including electrically neutral atoms and molecules. Figure 3 shows a model of glow discharge plasma. In glow discharge plasma the degree of ionization is in the order of 10^{-6}–10^{-4}. In other words, the degree of ionization is around 1 in 10,000 at most. Most of the particles are neutral and contains only one ion and electron for every 10,000 neutral particles. Consequently, it is called a weakly ionized plasma. At a pressure of 13.3 Pa (100 mTorr) the number of gas molecules is around 3.5×10^{15} cm^{-3} and the plasma density at an

ionization degree of 10^{-4} is 3.5×10^{11} cm^{-3}. In the glow discharge plasma, the plasma density is within a range of 10^{-11} cm^{-3} (Nojiri, 2015).

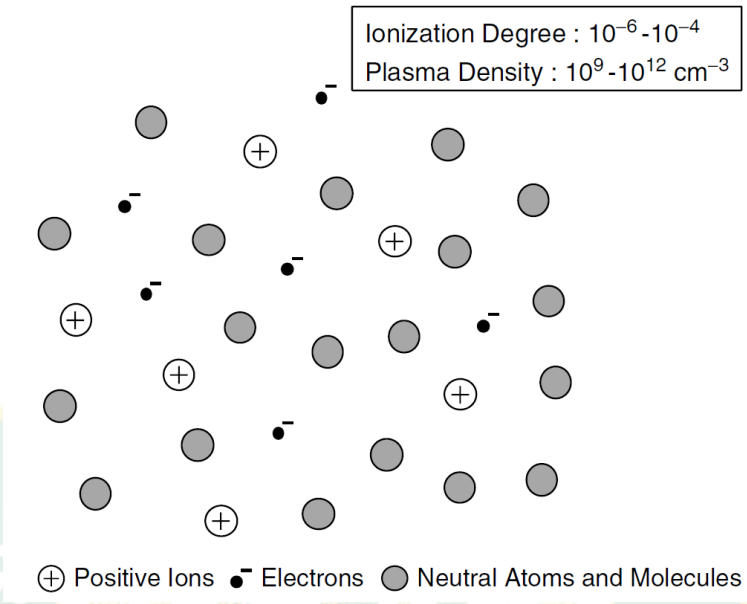

Figure 4 Model of glow discharge plasma (Nojiri, 2015).

CAPP has been used for disinfection in many ways such as medical equipment, packaging in the food industry, implants, blood coagulation, etc. (Fridman et al., 2008). CAPP has a high efficiency in eliminating bacteria which is partly due to their easy access into narrow and pent up spaces (Laroussi, 2002). In recent years, CAPP has a temperature lower than 40 °C and CAPP sources have been developed that provide the possibility to extend plasma treatment to soft tissue cells. CAPP can be generated in several way such as RF, microwave frequencies, high voltage AC or DC, etc. Excited species and reactive gases may be generated during the non-equilibrium processes and in plasma medical field these species have particular attention (Kong et al., 2009).

Plasma composes of electrons, positive ions, and neutral particles, and can be described based on the ionization degree, density, thermodynamic equilibrium, and so on; in consequence, plasma is classified in many ways.

2.1.1 Classical plasma

A plasma gas or called classical plasma, for plasma kinetic theory which has classical Boltzmann statistics, if the distance between gas particles is adequately large. The distance between electrons in a plasma is adequately large if it is larger than the average electron, of mass m_e and speed v_{th} from its thermal energy, de Broglie wavelength (K. Wiesemann, 2013):

$$\lambda_B = \frac{h}{m_e v_{th}} \tag{1}$$

The de Broglie wavelength explains particles have wave-like properties, a particle of mass m moving at speed v will have the properties of a wave of the de Broglie wavelength, where h is the Planck constant.

Furthermore, a plasma can be explained as an ideal gas, when particles only interact elastically, if the mutual potential energy of electrons and ions is smaller than the average kinetic energy:

$$\frac{3}{2}k_B T_e >> \frac{e^2}{4\pi\varepsilon_0 \lambda_e} \tag{2}$$

If the distance between particles in the plasma large enough is the result to the electrostatic force between particles will be weak. Using the relations of $k_B T_e$ and Debye-Hückel length, λ_e for plasma being in ideal gas state therefore we get the equivalent conditions (K. Wiesemann, 2013):

$$\lambda_D >> \lambda_e = \frac{1}{n_e^{1/3}} \tag{3}$$

2.1.2 Degree of ionization in plasma

The number of ionized atoms or molecules depend on the degree of ionization (normally the number of electrons n_e or ions n_i are equal) as a fraction α of the total number n_t of atoms or molecules:

$$\alpha = \frac{n_e}{n_i} \tag{4}$$

The ionization degree is defined as $\alpha_i = n_i/(n_i + n_n)$, where n_i is the number density of ions and n_n is the number density of neutrals. α_i are determinant factor of the response of any plasma to a magnetic field as well as the electric

conductivity of plasma. Plasma with $10^{-6} < \alpha_i < 10^{-1}$ is weakly ionized. Because the electron temperature in the plasma is determinant to the degree of ionization, weakly ionized plasma is called low-temperature plasma. In common plasma-processing chambers, the degree of ionization is less than 10^{-4}. The degree of ionization of inductively coupled plasma (ICP) and electron cyclotron resonance is a lot higher, about 10^{-2}. Plasma with $\alpha_i \approx 1$ is fully ionized, and is referred to as "hot" plasma or high-temperature plasma. Examples include fusion plasmas, solar wind (interplanetary medium), and stellar interiors (the Sun's core).

Only a small part of the atoms in an electric discharge turn to be ionized, typically one (1) in 10^5–10^6, which at a gas pressure of 133 Pa (1 Torr) corresponds to a particle density of 10^{22} m^{-3} and an electron density of 10^{16} m^{-3}. The variation of the degree of ionization with different temperatures is show in Figure 5.

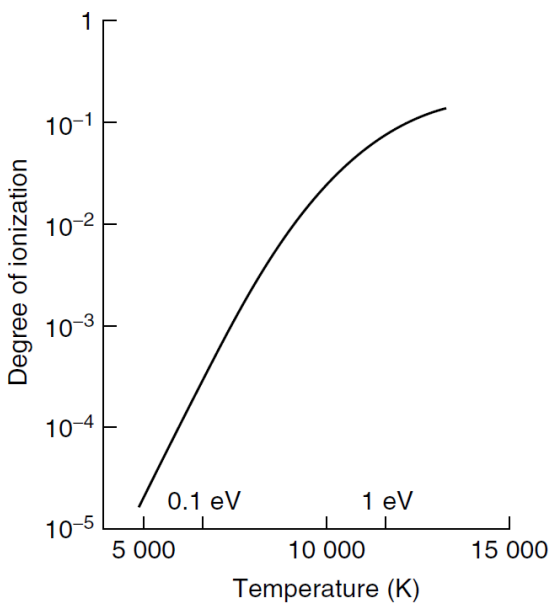

Figure 5 Characteristic variation of the degree of ionization of an atomic gas at atmospheric pressure (Harry, 2010).

2.1.3 Collisions between particles

Collisions of particles may be elastic, in which case momentum is preserved, or inelastic, where momentum is transferred to potential energy. In both cases, energy has exchanged. The energy to collision and the collision frequency

between atomic particles influence the rate at which energy can be coupled with or released from a plasma, the mass of an electron, m_e, is 9.11 × 10^{-31} kg, the nucleus atomic weight of a hydrogen atom (proton), m_p, is 1.67 × 10^{-27} kg.

Figure 6 shows the energy levels of different atomic and molecular transitions. The energy gained by an electron (charge 1.6 × 10^{-19} C) accelerated through a potential of 1V is 1 eV or 1.6 × 10^{-19} J. The Maxwell–Boltzmann distribution indicates the small number of particles available with adequate energy for ionization.

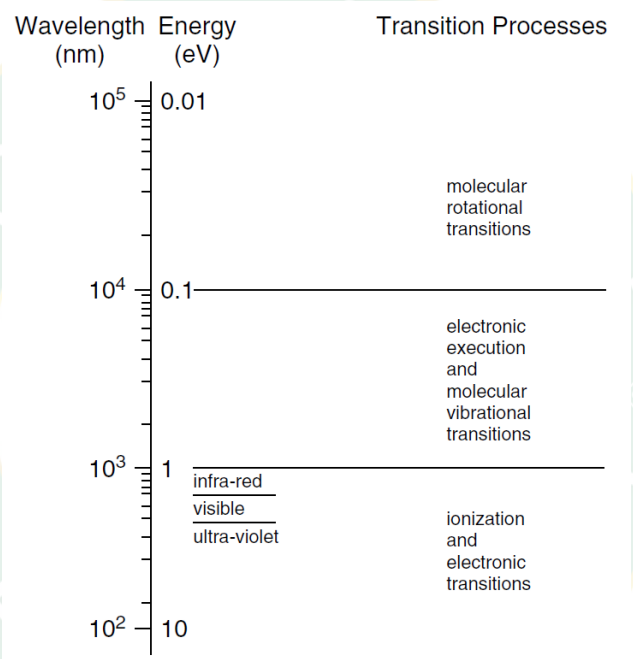

Figure 6 Atomic and molecular energy associated with different energy transitions (Harry, 2010).

The electron small mass results to only an insignificant exchange of kinetic energy from electrons in an elastic collision, both particles conserve the magnitude of their momentum, but its direction will be changed.

2.1.4 Plasma parameters

Table 1 shows commonly values of plasma parameters correlated with an arc discharge plasma or strongly ionized plasma, and a glow discharge plasma or a weakly ionized plasma. A glow discharge plasma is characterized by being without

thermal equilibrium between the electron temperature (T_e) and gas temperature (T_g). An electron temperature correlates with the energy of the electrons, and its relationship to the kinetic energy $\frac{1}{2}m_e v_e^2$ is expressed as

$$\frac{1}{2}m_e v_e^2 = \frac{3}{2}kT_e \quad (5)$$

Where m_e is the electron mass, v_e is the electron velocity, and k is Boltzmann's constant.

Table 1 Types of plasma and plasma parameters (Nojiri, 2015).

Type of plasma		Plasma density (cm^{-3})	Electron temperature T_e (K)	Ion temperature T_i (K)	Gas temperature T_g (K)
Arc discharge	Strongly ionized plasma (high-temperature plasma)	$>10^{14}$	6,000	6,000	6,000
Glow discharge	Weakly ionized plasma (low-temperature plasma)	10^9-10^{12}	~10^4	300-1,000	300

Since electrons are very lightweight, electrons are accelerated by an electric field and receive large kinetic energy. The average electron energy in a glow discharge plasma is several electron-volts. Example the electron energy is 2 eV; then the electron temperature T_e is 23,200 K, according to (5). On the contrary, the temperature of the neutral atoms and molecules has a gas temperature T_g, which is near room temperature (293 K). Otherwise, $\frac{T_e}{T_g}$ is around 80, and the electron temperature T_e and gas temperature T_g are not in a thermal or non-thermal equilibrium. While the electrons have an energy level equal to a high temperature of 10^4 K or higher, the temperature of the etch chamber and the wafer are low because the electrons have small mass. Therefore, a glow discharge plasma is also referred to as a low-temperature

plasma. Because electrons have enough energy that result in the excitation, ionization, and dissociation of atoms and molecules, with the gas temperature remaining near to the room temperature, various types of reactions are possible at low temperature.

An arc discharge is a strongly ionized plasma, and its plasma density is 10^{14} cm^{-3} or greater. The electron temperature T_e, ion temperature T_i, and gas temperature T_g are in a thermal equilibrium, and T_e=T_i=T_g is approximately 6,000 K. For this reason, the arc discharge is referred to as a high-temperature plasma (Nojiri, 2015).

2.1.5 Plasma thermal equilibrium

Considering relative temperatures between electrons, ions, and neutrals, plasmas are classified as thermal equilibrium and nonthermal equilibrium.

2.1.5.1 Thermal equilibrium plasma

The electron temperature (T_e), ion temperature (T_i), and neutral temperature (T_n) are identical in thermal equilibrium plasma. This is attributed to the frequent collisions between electrons and ions/neutrals inside high-temperature and high-density plasma. Examples include the natural fusion reactor (Sun), a magnetic field (of tokamak design), or inertial (laser) confinement of a plasma.

2.1.5.2 Nonthermal equilibrium plasma

In nonthermal equilibrium plasma, the momentum transfer between light electrons and heavy particles (ions and neutrals) is not efficient enough and the power applied to plasma favors electrons. Therefore, the electron temperature (T_e) is extremely higher than in ions (T_i) and neutrals (T_n), being, T_e >> T_i, T_n. Nonthermal equilibrium plasmas are generated by corona discharge, glow discharge, arc discharge, capacitively coupled discharge, inductively coupled discharge, wave heated plasma, etc. Applications of nonthermal plasma have expanded to cover many fields including environmental engineering, aeronautics and aerospace engineering, biomedicine, textile technology, and analytical chemistry.

2.1.6 Plasma source

The plasma source comprises of a needle on which the voltage is applied and surrounded by a quartz glass tube. Flow rate of gas normally at 1 to 2 L/min of helium or argon, sometimes with a gas mixture, is flow through the glass tube to force the gas and the plasma out to the air. Since having the high electric field on the needle tip the plasma can be generated either with inert gas, an argon or a helium flow (Hofmann, 2013).

Table 2 shown lists of various reactions that can take place at a surface exposed to a plasma. The first two show etching and deposition processes that are in turn enhanced by the arrival of energy brought by other particles.

Table 3 and Table 4 list phenomena that take place in the gas phase, where particles are ionized, some molecular gases are broken up and others agglomerate (oligomerize). The last process is the first stage in the formation of particulate matter in plasmas.

Table 2 Surface reactions (Braithwaite, 2000).

Reactions	Description	Evidence
$AB+C_{solid} \rightarrow A+BC_{vapour}$	Etching	Material erosion
$AB \rightarrow A+B_{solid}$	Deposition	Thin film formation
$e^-+A^+ \rightarrow A$	Recombination	Major loss process
$A^* \rightarrow A$	De-excitation	
$A^* \rightarrow A+e^-$ (from surface)	Secondary emission	Auger electrons
$A^+(fast) \rightarrow A+e^-$	Secondary emission	Auger electrons

Table 3 Gas phase reactions involving electrons (Braithwaite, 2000).

Reactions	Description	Evidence
$e^-+A \rightarrow A+e^-$	Elastic scattering	Thermal electrons
$e^-+A \rightarrow A^++e^-+e^-$	Ionization	Conductivity
$e^-+A \rightarrow A^*+e^-$	Excitation	
$e^-+A^* \rightarrow e^-+A+h\nu$	De-excitation	Light emission
	Two-step ionization	Ionization efficiency

Reactions	Description	Evidence
$e^-+A^* \rightarrow A^++e^-+e^-$	Fragmentation	Residual gas analysis
$e^-+AB \rightarrow A+B+e^-$	Dissociative ionization	
$A^++e^-+B+e^-$	Dissociative attachment	
A^-+B	Volume recombination	Plasma decay and steady-state
$e^-+A^++B \rightarrow A+B$		

Table 4 Gas phase reactions involving ions and neutrals (Braithwaite, 2000).

Reactions	Description	Evidence
$A^++B \rightarrow B^++A$ 'resonant' for B=A	Charge exchange	Ion energy spectra
$A^++B \rightarrow B+A^+$	Elastic scattering	Ion energy spectra
$A^++B \rightarrow A^++B^*+e^-$	Excitation	Ionization efficiency
$A^++B \rightarrow A^++B^++e^-$	Ionization	Ionization efficiency
$A+B^* \rightarrow A^++B+e^-$	Penning ionization	Ionization efficiency
$A^++BC \rightarrow A^++B+C$	Fragmentation/dissociation	Residual gas analysis
$e^-+A^++B \rightarrow A+B$	Volume recombination	Plasma decay
$A^{\pm}+B \rightarrow AB^{\pm}$	Oligomerization	Ion mass spectra
$A+B \rightarrow AB$	Oligomerization	Residual gas analysis

2.1.7 Atmospheric pressure plasma (APP)

For generated plasma at atmospheric pressure or ambient air can overcome the drawbacks of the low-pressure plasma. However, high voltage for gas breakdown is required and for enhanced collisions between electrons and gas molecules. In avoiding arcing and gas temperatures is low in APP to attain low-temperature sources, several models have been developed via properly scheming electrode configurations and discharge-excitation voltage waveforms for limit discharging duration. Major methodologies for avoiding arch and hot gas include dielectric barrier discharge (DBD) and pulsed voltage or high frequency (HF) voltage was used for excitation of discharge

rather than direct current (DC) voltage (Setsuhara, 2016). Another method is to apply a voltage with a high frequency, usually RF (Park et al., 2001) in order to reduce the operation voltage. In most cases these RF plasmas are capacitively coupled plasmas, i.e. generated between two electrodes at radio frequency 13.56 MHz. With this configuration and at these frequencies the current is mainly eradication current, compared to the usually much smaller ohmic current. The last method is to apply the voltage and switch it off before a transition to a spark or arc can emerge, i.e. applying voltages with a duration of pulses of a few hundreds of nanoseconds or less, depending on the electrode geometry.

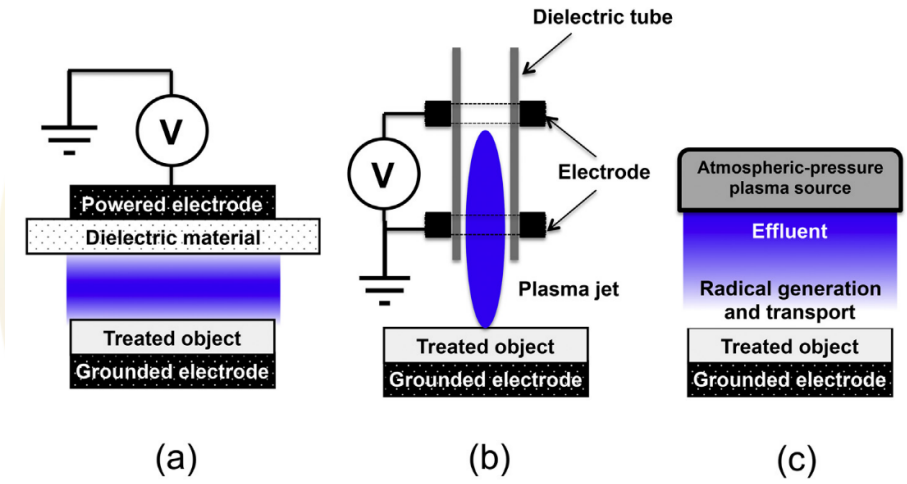

Figure 7 Atmospheric-pressure plasma exposure in biomedical applications; (a) DBD, (b) plasma jet and (c) plasma effluent downstream (Setsuhara, 2016).

APP-irradiation diagram for biomedical applications are shown in Figure 7. In DBD shows in Figure 7 (a). DBD known as a barrier discharge or a silent discharge, is one type of discharge when at least one of the electrodes is covered by a dielectric material. Layer of dielectric play a role current limiter and shield the formation of arc discharge or a spark. The energy of electrical coupled into a DBD plasma is generally transferred to the electrons, meanwhile the neutral gas remains near to ambient temperatures. DBD system is the non-equilibrium plasma that can be operated at high pressures. The treated object act as a counter electrode (grounded electrode) and the

gap distance is in range of mm or much less than several cm. Hence is suited to treating flat areas of skin. In the DBD type has been used in a wide range of plasma-medicine applications for example sterilization of living animal or human tissue, blood coagulation, wounds healing and skin treatments. However, in the DBD type is restricted by the size of the gap distance between HV electrode and target, and thus plasma sources generated in open space for expanding the flexibility of applications are required.

Other method of open-space exposure has been realized by the plasma-jet in Figure 7 (b). The atmospheric pressure plasma jets (APPJ) are prone to arcing. An arc is a thermal plasma that forms when a current is heated up through the electrodes creating high energy enough. If the temperature at the electrode is high enough more electrons escaping from atom are created due to thermionic emission, which leads to a very high current at low voltage at gas high temperatures. Arcs are very energetic and need to be evaded in many applications. The most significant sources which create non- arcing atmospheric pressure plasmas are dielectric barrier discharges (DBDs), corona discharges and cold atmospheric pressure plasma jets (CAPPJs) (Hofmann, 2013). Plasma is generated in the discharge tube with barrier discharge sustained in flows of noble gases such as He and Ar gas, when flown along dielectric tubes with cylindrical configurations comprise of electrodes and a dielectric tube. In plasma jet, the ionization wave was generated in the discharge tube blown from the discharge tube toward the object. The different designs of atmospheric pressure plasma jets remain (Schutze et al., 1998). The special feature of all of them is that usually inert gas such as helium or argon is blown through a nozzle, dimension size um or mm. In most cases enclosing this nozzle one electrode is connected to a high voltage source around 0.1 to 100 kV and a grounded electrode. The plasma is then usually generated inside the nozzle between these electrodes and blown out via gas flow. To guard arcing in plasma jets three methods can be implemented either separately or in many combinations. One method is to use the geometry of DBD, with the two electrodes being separated by at least one dielectric barrier, such as glass. The advantage of the dielectric barrier is that the charge, which is generated in the volume of the plasma,

will be deposited on the dielectric. This leads to a local reduction of the electrical field, which will lead to a self-quenching of the discharge (Hofmann, 2013).

There are several advantages of plasma jets over DBD discharges. DBD discharges, especially in air, are in most cases filamentary and are created randomly over the surface, while a plasma jet forms in most cases a stable diffuse seeing discharge without the need of the surface as a secondary electrode. This makes it possible to treat rough surfaces homogeneously in either a direct contact or an indirect mode, which is a challenge in a DBD geometry. The common disadvantages of plasma jets are the relatively small size of the discharges and the need of (expensive) rare gases. While air jets have also been developed (Kolb et al., 2008).

The plasma-effluent downstream shows in Figure 7 (c). The object is located in the downstream of APP sources, when the effects of the electric filed in region of the treated object can be ineffective, and the effluent of the APP into the open-space, ambient air is source for generation of reactive species. The reactive species generate by the effluent of the plasma source when transported to the objects for treatments (Setsuhara, 2016). As mentioned before, many different kinds of electrode configurations and voltage waveforms can and are used in different plasma research groups. Finally, these plasma sources are different in many ways such as size, rate of gas flow, electrode, etc. A direct contrast of the different plasma sources is in most cases extremely challenging if not impossible without a lot of detailed information of plasma properties (Hofmann, 2013).

2.2 Bacteria

2.2.1 Bacterial cells

One type of prokaryotes are bacteria. Bacteria are simple single cell organisms without cell nucleus or other membrane- bound organelles, unlike eukaryotes. Ordinarily bacteria have a size of around 100 nm and have many shapes, such as rods, spheres, and spirals. The chromosomal DNA of bacteria is a single loop that forms a deformed structure in the cytoplasm known as the nucleoid. Moreover,

bacteria can also carry plasmids, that are small circular DNA molecules providing supplementary genes that are not important to the bacteria, but can assist in their survival in severe environments which are the reasons that make bacteria resistant to antibiotics. All of bacteria cells have a cell membrane in the form of a lipid bilayer. A barrier between the cell interior and cell membrane is known as cytoplasm, and the external world, and molecules can selectively be transported pass it. Furthermore, the lipid membrane, bacterial cells have a cell wall that prevents the cell from pressure produced by osmotic flow of water into the cell (Laroussi et al., 2012).

2.2.2 *Staphylococcus aureus*

In the 1880s *Staphylococcus aureus* (*S. aureus*) was the first time introduced to the scientific community and *S. aureus* have potential to cause skin and wound infections. Moreover, *S. Aureus* is a unique bacterium as it has the potential to adapt to for antibiotics resistance leading to the development of methicillin-resistant *Staphylococcus aureus* (MRSA) in the 1960s. About 25% of population has *S. aureus* living in the nasal cavities, which being its major reservoir and the most important source for infection. Transportation of *S. aureus* is affected by genetic and environmental factors, along with cell-wall lipoteichoic acid, hormonal status, and antimicrobial activity of nasal secretions (Boost et al., 2008). Therefore, *S. aureus* is one of the most poisonous and also dangerous pathogens for human life. *S. aureus* is the cause of various deep-seated invasive and toxin-mediated illnesses including superficial infections. The broad range of clinical conditions results from a diversity of extracellular components, as well as surface proteins, capsule, biofilm formation, enzymes, and toxins (Petinaki and Spiliopoulou, 2012). MRSA is a major health pathogen problem worldwide which has significantly increased over the last decade.

2.2.3 *Pseudomonas aeruginosa*

Pseudomonas aeruginosa (*P. aeruginosa*) is opportunistic pathogen in most cases of humans and animals, leading to severe infections whereby the immune system is compromised (Fergie et al., 1994), or after long time of antibiotic treatments, injuries and medical process (Strateva and Yordanov, 2009) . *P. aeruginosa* is

opportunistic pathogen in gram-negative type ubiquitously present in water and soil. It has a natural potential to be resistant to penicillin and aminopenicillins, and the cephalosporin of first and second generations. Moreover, it is normally sensitivity to aminoglycosides, fluoroquinolones, lipopeptides, ureidopenicillins, carboxypenicillins, carbapenems and the third generation of cephalosporin. Furthermore, *P. aeruginosa* can develop resistance to against any antibiotic faster than that we are able to develop antibiotic. (Strateva and Yordanov, 2009).

2.3 Mechanisms of CAPP to bactericidal

The fact that RONS are created by cells and released extracellularly in inflammatory response to infections, tumors, and wounds supports the claim that RONS must be the main active mechanism in CAPP. That is to say RONS are believed to be a part of an intracellular signaling pathway. This class of RONS are called primary species and they are well controlled in the cell and their reactions with biomolecules are reversible. The signaling mechanisms consist of modifications of the intracellular redox state and proteins in signaling pathways by oxidation. One more class of RONS are secondary species and they are toxic and cause irreversible damage by their reactions with biomolecules. The primary RONS comprise of superoxide (O_2^-), hydrogen peroxide (H_2O_2), and nitric oxide (NO), and the secondary RONS include hydroxyl (OH) and peroxynitrite ($ONOO^-$). The secondary species only generate in the cell in case primary species react with one another or with a transition metal. The formation of hydroxyl from hydrogen peroxide is catalyzed by iron ions and known as the Fenton reaction. Interestingly, a reaction lead to oxidative damage to pathogen membranes upon immune response, known as lipid peroxidation, the cleavage of lipid peroxides is catalyzed by ferrous ions, which is similar to the Fenton reaction. Another way of forming hydroxyl is through the Haber-Weiss reaction, where O_2 is transformed into H_2O_2 which is then transformed to OH. Peroxynitrite is formed in a reaction between superoxide and nitrogen oxide. The reaction between peroxynitrate and amino acids leads to the formation of nitrated amino acids which causes oxidative damage to proteins (Kong et al., 2009). Therefore, RONS generated in CAPP can both act as an

immune response (primary RONS) and a highly reactive damaging species (secondary RONS).

RONS in CAPP have been reported to have oxidative effects on the outer structures of the cells, that is on the membrane and the cell wall, affecting their structural integrity. Ozone (O_3) interferes with cellular respiration, OH (hydroxyl radical) compromises the function of unsaturated fatty acids in the lipid membrane, H_2O_2 (hydrogen peroxide) has oxidative effect on proteins, lipids, and DNA, and atomic oxygen, metastable oxygen molecules, and superoxide (O_2^-) can oxidize proteins (Laroussi et al., 2012). However, the way RONS affect cells depends on their concentration. For example, H_2O_2 (hydrogen peroxide) can activate cell proliferation or restrain it and induce cell apoptosis and Nitric oxide (NO) which play an important role as an anti-inflammatory agent at low concentration, but at higher concentration it can damage cells (Kong et al., 2009). When the concentration of RONS are overwhelming to the cell, it is said to be in a state of oxidative stress, damaging lipids, protein, and DNA (Zhang et al., 2016).

As to the metabolic part, ATP (Adenosine triphosphate), the molecule used as the energy currency for life, is the descriptor of the metabolic activity in cells and can be used to observe how bacterial cells in form biofilm react to the stress that follows a CAPP exposure. For short exposure times, bacteria have been shown to try to handle with the stress by either increasing respiration and consequently the ATP production or to uncouple the ATP production from respiration (Joaquin et al., 2009). In a liquid condition, RONS have been shown potential to cause acidification and therefore inactivation of suspended bacteria (Suschek and Opländer, 2016).

Heinlin et al., study in Plasma medicine: possible applications in dermatology. Experiments shown CAPP have efficient, contact-free and painless disinfection, even in microscopic view without damage to healthy tissue. Plasma have affected the biochemical processes and offer new probability for the selective application of individually designable medical active substances application. For dermatology, new ways are being opened for wound healing, tissue regeneration, therapy of skin disinfection and probably other pathogen (Heinlin et al., 2010).

Daeschlein et al., study in Skin decontamination by low- temperature atmospheric pressure plasma jet and dielectric barrier discharge plasma. The APPJ and DBD have a high efficiency in eradicating physiological (PF) and artificially (AF) from the fingertips of healthy participant. Moreover, in the investigation plasma-resistant isolates were not found. CAP has shown to have potential for inactivation skin disease. For the purpose of hand hygiene, the times of plasma exposure should be decreased significantly by technical means (Daeschlein et al., 2012).

Lin et al., study in Ar/O_2 Argon-Based Round Atmospheric-Pressure Plasma Jet on Sterilizing Bacteria and Endospores. A round argon-based non-thermal atmospheric-pressure plasma jet (APPJ) for sterilization application was developed and characterized. The APPJ temperature at the tube outlet is lower than 37 °C, so as not to induce damage to normal tissue. The absorbed power of plasma is around 2.7 W. The OES data shown that APPJ has high intensity of hydroxyl radicals (OH) in glow discharge region. Additionally, this device was applied to eradicate the bacteria (*E. coli* and *B. subtilis*) and endospore (*B. subtilis* endospore). Furthermore, when feeding additional oxygen (0.04%) into working gas it can not only increase the OH radicals but also accelerate the killing of bacteria and endospore (Lin et al., 2016).

Mohd Nasir et al., study in Cold plasma inactivation of chronic wound bacteria. The researchers used two types of plasma systems to generate cold plasma: a parallel plate dielectric barrier discharge (DBD) and a capillary-guided corona discharge. Parameters for applied voltage, discharge frequency, exposure time and flow rate of the carrier gas affects the cold plasma chemistry and thus change the composition and concentration of plasma species to reaction with the target sample. Chronic wounds failure to heal, often contaminated by multidrug resistant pathogen, make them resistant to healing. Methicillin- resistant *Staphylococcus aureus* (MRSA) and *P. aeruginosa* are the two major bacteria in infection and clinical non-infection wounds. The efficiency of cold plasma generated by the two different designs are based on eradication of three different isolates of MRSA and four isolates of *P. aeruginosa* (Mohd Nasir et al., 2016).

Mai-Prochnow et al., study in Gram-positive and Gram-negative bacteria differ in their sensitivity to cold plasma. The results showed CAP efficiency is direct relative

to the thickness of the cell wall of bacteria in various species. Biofilms of Gram-positive *B. subtilis* cell wall are around 55.4 nm, have ability resistance to CAP, with less than one $\log_{10}$ reduction after exposure time 10 min. On the other hand, biofilms of Gram-negative *P. aeruginosa* cell wall are around 2.4 nm and were almost completely eliminated under the same exposure time conditions. Planktonic cultures of Gram-negative *P. libanensis* also had a higher $\log_{10}$ reduction than Gram-positive *S. epidermidis*. Mixed species biofilms of *P. aeruginosa* and *S. epidermidis* showed the same trend of Gram-positive bacteria as having ability to resistant treatment of CAP. In addition, when grown in co-culture, Gram-negative *P. aeruginosa* have higher resistant to CAP than as a mono-species biofilm. OES spectrum found OH and O in the plasma have ability to break bond structure of cell walls. This study showed cell wall thickness being relative to CAP inactivation times of bacteria, but cell membranes and biofilm matrix have also a likely role (Mai-Prochnow et al., 2016).

Kang et al., study in Portable microwave air plasma device for wound healing. A portable microwave air plasma was developed for safety and effective wound healing process. Generated plasma by a fixed microwave power and two type of gas flows. The result shows the rate of the two air flows define the stability of the plasma jet, gas temperature and including control the concentrations of the reactive species in plasma. Two different system, the NO and ozone system, were identified as acceptable for wound healing without damage from thermal and toxicity. These systems show the same plasma characteristics excluding different concentration of NO and ozone. Both systems show a more than double faster in wound healing process when compared with the untreated case. Speedier potential healing process especially with ozone safety make the NO abundant system the best operation condition for wound healing. The performance of the developed device was monitored by a one-hour continuous generated plasma with a 24 V battery (Kang et al., 2015).

CHAPTER 3

EXPERIMENT

3.1 The Dielectric Barrier Discharge Plasma Jet (DBDJ)

This research has supported commercial Bio-Plasma Dielectric Barrier Discharge Plasma Jet (DBDJ) equipment from Photo Bio Care Co. Ltd, Thailand (Yaopromsiri et al., 2015) and laboratory of plasma and beam physics research facility (PBP), department of physics and materials science, Chiang Mai university, shown in Figure 8. DBDJ have outside diameter 21 mm and inside diameter 8 mm (gas outlet). In Figure 9 DBDJ consist of HV power supply, gas inlet, dielectric housing, electrode, quartz dielectric and plasma glow discharge. DBDJ was fixed at operated conditions at input voltage 40 V, output high voltage dc pulse 20 kHz (DBDJ), flow rate of He gas at 1 L/min for help generate plasma, intensity at 5 and variation generated repetition rate from 50 Hz to 110 Hz or converted to plasma dissipated power from 0.27 W to 0.50 W.

Figure 8 (A) DBDJ, (B) monitor display of power supply and (C) power supply of BIO Plasma.

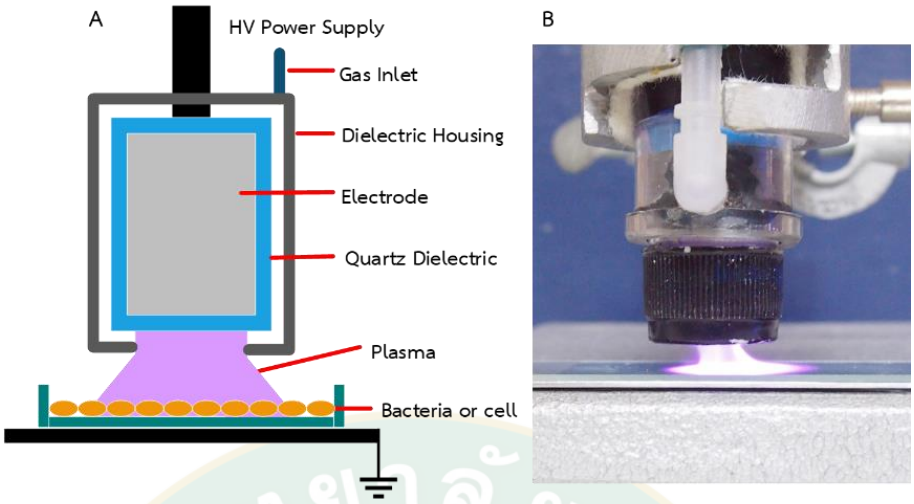

Figure 9 (A) Internal components of DBDJ and (B) Plasma glow discharge of DBDJ.

The experiment diagram shown in Figure 10. The research facilities available for this research at plasma and beam physics research facility (PBP), department of physics and materials science, Chiang Mai university and cell culture laboratory, department of biology, faculty of science, Chiang Mai university. First of all, measurement plasma properties of DBDJ by oscilloscope, OES and gas detector. Second, bactericidal test by spread plate technique and follow up by colony forming unit (CFU) assay. DBDJ was generated at plasma dissipated power from 0.27 W to 0.50 W and time exposure 15 s to 60 s. Third, bacteria biofilm test used live/dead assay and observed by fluorescence microscope. For bacteria biofilm and cell toxicity, plasma dissipated power at 0.50 W and time exposure at 60 s. Lastly, cytotoxicity of HDFa cells monitored by optical microscope to observed morphology, live/dead assay and flow cytometry (Muse Cell Analyzer) with Muse Count & Viability Assay Kit and Muse Annexin V and Dead Cell Assay Kit.

3.2 Plasma properties

DBDJ was operated at high voltage dc pulse 20 kHz (DBDJ), flow rate of He gas at 1 L/min and plasma dissipated power from 0.27 W to 0.50 W. For measurement plasma properties of DBDJ was used oscilloscope with high-voltage probe (Tektronix, P6015A and Hantek, T3100), OES (spectrometer AvaSpec-2048) and gas detector (Shenzhen YuanTe Technology : model SKY2000-NO and SKY2000-O_3).

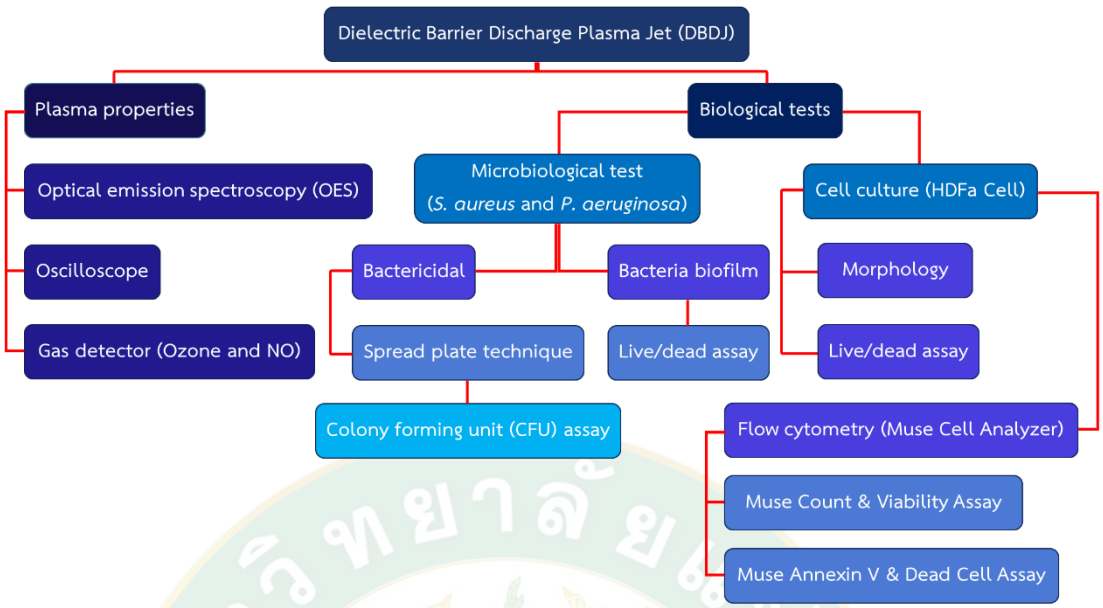

Figure 10 Experiment diagram.

3.2.1 Electrical properties

The setup diagram for measurement electrical properties shown in Figure 11. The intensity of plasma is captured by photo sensor amplifier. The light signal was converted to voltage by amplifier and connects the elements to the digital oscilloscope to provide a signal corresponding to the light intensity of the plasma in real time. When changing the experiment parameters for example supply voltage operated showed instantaneous results in the oscilloscope. In this work the high voltage waveform was determined using a high-voltage probe (Tektronix, P6015A). The plasma dissipated power was estimated by Lissajous figure method or Q-V plot (Cai Yi-xi et al., 2010). The discharge charge was estimated from the voltage across the 1 nF capacitor measured by a HV probe (Hantek, T3100). Equation for calculated plasma dissipated power and dose of plasma refer to (11 and 12). Lassajous figure method (Q-V plots) by Channel 1 is HV probe (1 kV), Channel 2 is capacitor (1 nF) discharge C. When V_1 = 1 kV, f = 20 kHz, C = 1 nF and V_2= 20 V. Area of plasma = πr^2 (when r = 2.1 cm and t = exposure time).

$$Q = CV \tag{6}$$

$$P = IV \tag{7}$$

$$P = \left(\frac{Q}{t}\right) V_1 \tag{8}$$

$$P = \left(\frac{CV_2}{t}\right) V_1 \tag{9}$$

$$P = CV_1V_2f \tag{10}$$

$$P = Area(unit^2)\ (CV_1V_2f)(duty\%)\ W \tag{11}$$

$$Dose = \left(\frac{Pt}{area\ of\ plasma}\right) J/cm^2 \tag{12}$$

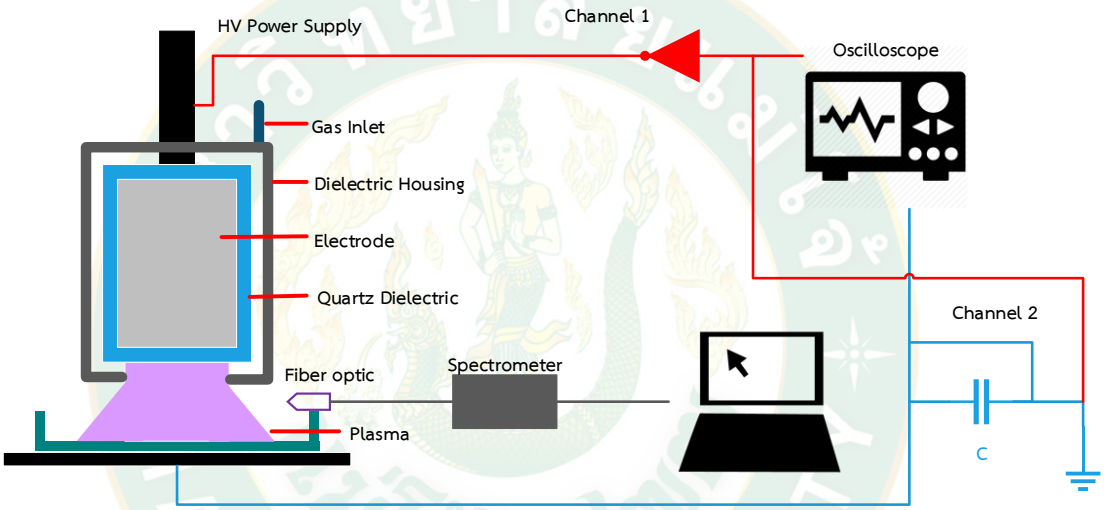

Figure 11 Setup diagram of equipment.

3.2.2 The reactive oxygen nitrogen species (RONS)

Spectrometers used for plasma diagnostics are in principle similar as UV-VIS spectrometers. The major difference is its much higher spectral resolution, better than 0.01 nm and in the case of optical emission spectroscopy (OES). No light source is required inside the spectrometer. The gratings have higher density, more than 300 gr/mm and are used for covering all of broad length spectra. Only older spectrometers use optical prisms. The slits are installed at the entrance of spectrometer for adjustability. The detectors used charge coupled device (CCD) or photomultipliers and photodiodes. Therefore, the spectral record quality and the final spectrometer resolution depends on all of these elements. At present spectrometers are completely controlled by computer and make is easy to use. In this research were used

spectrometer AvaSpec-2048 for measurement light emission spectra in glow discharge plasma. OES used fiber optic spectrometer led light emission spectra of plasma into system by CCD detector. CCD change light emission spectra signal to digital signal shows on computer display by program controller AvaSoft version 7.4. After saving OES data was file exported to Microsoft Excel and data was used to plot graph and mark peaks in OriginPro 2016. OES setup as shown in Figure 11. The properties of spectrometer AvaSpec-2048 shown in Table 5.

The NO and O_3 concentration were measured by using the two gas detectors (Shenzhen YuanTe Technology); model SKY2000-NO for measuring NO concentration and model SKY2000-O_3 for measuring O_3 concentration during DBDJ operation. When operated DBDJ concentration of NO and O_3 stay safety criteria for user were guarantee.

Table 5 Technical data of AvaSpec-2048.

Optical Bench	Symmetrical Czerny-Turner, 75 mm focal length
Wavelength range	200-1100 nm
Resolution	0.05-20 nm, depending on configuration
Stray-light	0.04-0.1%, depending on the grating
Sensitivity	310,000 counts/μW per ms integration time
Detector	CCD linear array, 2048 pixels
Signal/Noise	200:1
AD converter	16 bit, 2 MHz
Integration time	1.11 ms - 10 minutes
Interface	USB 2.0 high speed, 480 Mbps RS-232, 115.200 bps
Sample speed with on-board averaging	1.1 ms /scan
Data transfer speed	1.8 ms / scan (USB2) 430 ms / scan (RS-232)

Digital IO	HD-26 connector, 2 Analog in, 2 Analog out, 3 Digital in, 12 Digital out, trigger, sync.
Power supply	Default USB power, 350 mA or with SPU2 external 12VDC, 150 mA
Dimensions, weight	175 x 110 x 44 mm (1 channel), 716 grams

3.3 Microbiological test

Samples of *Staphylococcus aureus* (*S. aureus*) TISTR 2329 and *Pseudomonas aeruginosa* (*P. aeruginosa*) TISTR 2370 were obtained from Thailand Institute of Scientific and Technological Research (TISTR). First of all, the best condition of DBDJ for bactericidal was found by using spread plate method with plasma dissipated power from 0.27 W to 0.50 W and time exposure 15 s to 60 s. After the best condition was found selected only one condition plasma dissipated power at 0.50 W and time exposure 60 s for destroying bacteria biofilm by using live/dead assay to monitored.

3.3.1 Bactericidal

The sample bacteria of *S. aureus* and *P. aeruginosa* bacteria were grown in 5 mL nutrient broth (NB) using the orbital shaker 150 rpm in incubator at 37 °C for 24 h to obtain a bacterial density of approximately 1×10^{7} to 1×10^{8} CFU/mL. After 24 h serial dilution to 10^{-4} for *S. aureus* and *P. aeruginosa* was used before prepared in Nutrient Agar (NA). Then prepared *S. aureus* and *P. aeruginosa* was used spread plate method 200 uL for DBDJ experiment. DBDJ treated on *S. aureus* and *P. aeruginosa* operated at plasma dissipated power from 0.27 W to 0.50 W and time exposure 15 s to 60 s gap between DBDJ and plate at 0.5 cm. After that DBDJ treatment *S. aureus* and *P. aeruginosa* incubated at 37 °C for 24 h and result of DBDJ treatment was investigated by Colony Forming unit (CFU) method count and calculate efficiency bactericidal of DBDJ according to (13). Count number of control and treatment in circle area. Average efficiency and plot graph when diameter area is 2.1 cm.

$$\%Reduction\ or\ efficiency\ = \left(\frac{Control-Treatment}{Control}\right) x100\% \qquad (13)$$

3.3.2 Bacteria biofilm

The bacterial biofilms both of *S. aureus* and *P. aeruginosa* were prepared in NB. After incubated at 37 °C for 24 h to have density of approximately $1x10^7$ to $1x10^8$ CFU/mL and then moved to 12-well plate at 1 mL/well on the 12 mm coverslip glass with 0.1% of gelatin in Phosphate Buffered Saline (PBS 1X, pH 7.4) 30 min at 4 °C before being used. The bacteria samples were incubated at 37 °C for 48 h and NB had to be changed every 24 h. After 48 h removed NB, plasma exposure on bacteria samples was carried out at plasma dissipated 0.50 W and exposure time 60 s. Live/Dead assay method with double stain Hoechst 33342 and Propidium iodide (PI) was used to monitor immediately after treatment. Prepared double stain HO/PI dilute in deionized water to 1 ug/mL and drop 200 uL on coverslip glass soaked in incubator at 37 °C for 30 min to activate double stain HO/PI and avoid exposing to light. After incubated solution was removed, wash PBS 2 times and plated coverslip glass on cleaned microscope slide with BosterBio antifade mounting medium 20 uL. Performance of DBDJ to destroy bacteria biofilm was observed by Olympus BX51 fluorescence microscope. The magnification for bacteria biofilm image at 1000x oil immersion lens with ZEISS Immersion Oil 518 N was used. For fluorescent imaging of HO/PI image have to be taken at the same spot but using different laser source to activated HO/PI stains. In case of HO which has the ability to bind both of live and dead cell, ultraviolet excitation at 405 nm was used, after emission spectrum maximum at 461 nm in blue fluorescence. In case of PI binding with DNA stain only dead cell and PI cannot cross the membrane of live cells, laser wavelength 488 nm to excitation and emission maximum at 617 nm in red fluorescence was used. After which both of HO/PI image were saved, export file, customize the image color in ACDSee Photo Studio Ultimate 2018 and merge or overlap two images by ImageJ-win64 program.

3.4 Human Dermal Fibroblasts adult (HDFa) cells

Human Dermal Fibroblasts, adult (HDFa) cells Cat. no. C-013-5C purchased from Cascade Biologics™ invitrogen cell culture (GIBCO invitrogen cell culture). Primary human dermal fibroblasts are isolated from adult skin, cryopreserved at the end of the primary culture. Morphology of HDFa cells are spindle-shaped (cells are bipolar and refractile) and passage of HDFa cell for experiments not more than passage 12. Before plasma exposure, HDFa cells have 70-80% confluence, media cover around 2 mm. and gab between DBDJ and cells at 5 mm. DBDJ was operated only one condition at plasma dissipated power 0.50 W and time exposure 60 s.

3.4.1 Cell culture

HDFa cells were cultured in 10% Fetal Bovine Serum (FBS) with Dulbecco's Modified Eagle Medium (DMEM) high glucose supplemented and Antibiotic-Antimycotic (1X) - Thermo Fisher Scientific (Thermo Fisher Scientific, Inc., Waltham, MA, USA) in a humidified atmosphere containing 95% air/5% CO_2 at 37°C. HDFa cells were grown to 70-80% confluence, media removed and washed by Phosphate Buffered Saline (PBS 1X, pH 7.4) 2 times, harvested by add 1 mL (T-25 flask) or 2 mL (T-75 flask) 0.025% trypsin-EDTA (Thermo Fisher Scientific, Inc.) in PBS incubated for 5 min 95% air/5% CO_2 at 37°C. Add completed media (DMEM+10%FBS), after trypsinization and move cell suspension to tube 15 mL for centrifuge. After centrifuge at 1,000 rpm 7 min was media removed, add fresh media seed cells to 6-well plate at volume 2 mL/well for flowcytometry and 12-well plate at volume 1 mL/well on coverslip glass diameter 10 mm. for Live/Dead assay, HDFa cell had confluence 25-30% and media changed every 48 h. HDFa cells before experiment have confluence 70-80%. After that start cell cytotoxicity assay.

3.4.2 Cell morphology

Before to monitored proceed effect of DBDJ to HDFa cell with fluorescent microscope or flow cytometry, we always have to observe cell morphology changes by optical microscope (OM). The morphology of cells culture such as shape and appearance are important for successful cell culture experiments. Moreover, to verify

the healthy status of cells in culture, investigating the cells by eye and a microscope each time they will help to detect any indication of contamination early on and to sterilize it before it spreads to other cells cultures around the laboratory. After HDFa cells ready for experiment were removed media, washed by PBS and fresh media was added to cover HDFa cells around 2 mm. Then DBDJ exposure on HDFa cells and cell morphology of HDFa cells by Olympus CK40 Inverted Microscope with USB portable digital microscope 10x (2 million-pixel camera) were monitored. For cell morphology image magnification at 40x was used.

3.5 Cell cytotoxicity assay

Cell cytotoxicity assay of DBDJ was monitored by live/dead assay, flow cytometry (Muse cell analyzer) with Muse count and viability kit and Muse annexin V dead cell kit. To study effect of DBDJ at the best condition for eradicating bacteria in wound healing model to HDFa cells as in vitro were used. In the experiment, HDFa cells have media cover around 2 mm, gab between DBDJ and cells at 5 mm. Condition in experiment had 4 condition and 3 times in every condition. First of all, negative control or natural control. Secondly, positive control induced by adding 50% Dimethyl sulfoxide (DMSO) with 50% DMEM 2 mL incubated at 37°C 15 min for live/dead assay or 10% Dimethyl sulfoxide (DMSO) with 90% DMEM 2 mL incubated at 37°C 2 h for flow cytometry. DMSO have ability to induce apoptosis and dead cells. Thirdly, treatment control by He gas blow on cells at flow rate 1 L/min. 60 s. Lastly, DBDJ was operated only one condition at plasma dissipated power 0.50 W and time exposure 60 s. After experiment cell cytotoxicity assay was monitored immediately and run assay of all conditions at the same time. Then for data from flow cytometry statistical analysis were used, results reported and ImageJ to process fluorescent image.

3.5.1 Hoechst 33342 and Propidium iodide (PI) double stain

Hoechst 33342 (HO) is a kind of blue-fluorescence dye when bound to DNA both of live/dead cells (excitation/ emission maximum ~350/461 nm). Propidium iodide (PI) is a red-fluorescence dye when bound to DNA, permeant to dead cells only. (excitation/emission maxima ~535/617 nm). After DBDJ experiment was removed

media and add 200 uL double stain HO/PI diluted (1 ug/mL in deionized water) on coverslip glass incubated at 37 °C for 30 min to activate double stain HO/PI avoiding exposure to light. After incubated solution was removed, washed by PBS 2 times and plate coverslip glass on cleaned microscope slide with BosterBio antifade mounting medium 20 uL. Live/dead assay of HDFa cell was observed by Olympus BX51 fluorescence microscope. The fluorescent image of HDFa cells magnification at 200x and 400x were used. For fluorescent imaging of HO/PI have to be taken at the same spot but using different laser source to excitation HO/PI stains. After both of HO/PI image were saved, export file, customize the image color in ACDSee Photo Studio Ultimate 2018 and merge or overlap two images by ImageJ-win64 program.

3.5.2 Muse Cell Analyzer

The Muse Cell Analyzer miniaturized fluorescence detection was used and microcapillary cytometry for deliver single-cell analysis, which as highly quantitative. Preferably, when compared with ordinary methods such as microscopy. The high-performance cell analysis system used microcapillary technology and miniaturized optics. Detector laser-based fluorescence of each cell event can analyze up to 3 cellular parameters: cell size (forward scatter) and 2 colors (detected in the red and/or yellow fluorescence). Therefore, Muse furnish more quantitative results than imaging systems (non-flow based), as it can examine up to two parameters only, take a long time, and furnish less quantitative data. The Muse cell analyzer system uses microcapillary and miniaturized optics. For excitation a green diode laser and uniquely designed series of retro-reflective lenses were used allowing maximum light capture and sensitivity. Therefore, quantitative data effect of DBDJ to HDFa cells, Muse Cell Analyzer with Muse Count & Viability Assay Kit and Muse Annexin V and Dead Cell Assay Kit were used.

3.5.3 Muse Count & Viability Assay

For quantitative analysis of cell count and viability on the Muse Cell Analyzer Muse Count & Viability assay was used. Both of differentially stains live and dead cells depend on their permeability to the two DNA binding dyes stain in the

reagent. Software module automatically calculated and two dot plots shows on display data. A DNA-binding dye stain with cells that have lost their membrane integrity, the dye can stain the nucleus of dead and dying cells. This parameter is shown as viability and is used to differentiate live cells (viable cells that do not stain) from dead or dying cells (non-viable cells that stain). A membrane-permeant DNA staining dye stains all cells with a nucleus. This parameter is shown as nucleated cells and is used to differentiate cells with a nucleus from debris including non-nucleated cells. After plasma exposed HDFa cells, HDFa cells (6-well plate) was harvested in all conditions by removed media, washed PBS 2 mL/well and add 2 mL/well 0.025% trypsin-EDTA in PBS incubated for 5 min 95% air/5% CO_2 at 37°C. Add complete media 2 mL/well cell suspension was moved to tube 15 mL for centrifuge. After centrifuge at 1,000 rpm 7 min was media removed, add fresh media 300 uL, added move cell suspension to 1.5 mL microcentrifuge tubes, Add Muse Count & Viability (7-AAD) Reagent 100 uL to each tube, mixed by vortex mixer and incubate for 5 minutes at room temperature and avoiding exposure to light. Run assay start at positive control, negative control, treatment control and plasma treatment respectively. Start at positive and negative control to set population and threshold of HDFa cells. Set events to acquire of HDFa cells at 10,000 and export PDF file after all testing for statistical analysis.

3.5.4 Muse Annexin V and Dead Cell Assay

Muse Annexin V & Dead Cell Assay was used for quantitative analysis of live, early and late apoptosis, and cell death with the Muse Cell Analyzer. The assay kit was utilizing Annexin V to detect phosphatidylserine (PS) on the external membrane of apoptotic cells. The marker of dead cell 7-AAD was used as an indicator integrity of cell membrane structural. It was excluded from live, healthy cells, including early apoptotic cells. Therefore, four populations of cells in this assay can be differentiated. First, non-apoptotic cells or healthy cells: Annexin V (-) and 7-AAD (-). Second, early apoptotic cells (live cells): Annexin V (+) and 7-AAD (-). Third, late stage apoptotic and dead cells: Annexin V (+) and 7-AAD (+). And last, mostly nuclear debris or necrosis cells: Annexin V (-) and 7-AAD (+). After DBDJ experiment HDFa cells were harvested in all conditions by removed media, washed PBS 2 mL/well and add 2 mL/well 0.025%

trypsin-EDTA in PBS incubated for 5 min 95% air/5% CO_2 at 37°C. Add complete media 2 mL/well move cell suspension to tube 15 mL for centrifuge. After centrifuge at 1,000 rpm 7 min was removed media, add fresh media 100 uL to 15 mL tube, next vortex, move cell suspension to 1.5 mL microcentrifuge tubes, add 100 uL Muse Annexin V & Dead cells and mixed by vortex. Incubated at room temperature 20 min and avoid exposing to light. Then start assay at positive control, negative control, treatment control and plasma treatment respectively. Start at positive and negative control to set population and threshold of HDFa cells (live, early apoptosis, late apoptosis and necrosis or dead cells). Set events to acquire of HDFa cells at 10,000 and export PDF file after all testing for statistical analysis.

3.5.5 Statistical analysis

After export PDF file report of Muse Count & Viability Assay or Muse Annexin V and Dead Cell Assay, key data from report in Microsoft Excel 2016 and used for calculating mean, standard deviation (SD), number of test (n) and standard error (SE). Next, export file from Microsoft Excel 2016 in form text file (.txt) by first column is condition number, mean, SD, n, and SE respectively. Then, R-program x64 ver.3.5.1 with R-Studio ver.1.1.456 were used. Significant differences were evaluated by using repeated measures one-way ANOVA followed by an appropriate post hoc multiple comparison test (Tukey method). If result compared in each condition, one by one condition have *P*-value or probability value < 0.01-0.05 is significant mark * and < 0.01 is significantly mark **. Therefrom, plot graph data in R-Studio and export graph in form PDF file. Import graph pdf file into Adobe Illustrator CC for editing graph, labeling the X-Axis and Y-Axis, marking significant bar and adjusting graph scale. After editing graph finished save graph in form PDF and PNG file for report.

CHAPTER 4
RESULTS AND DISCUSSION

4.1 The Dielectric Barrier Discharge Plasma Jet (DBDJ)

The commercially Bio-Plasma Dielectric Barrier Discharge Plasma Jet (DBDJ) was operated at input voltage 40 V, output high voltage dc pulse 20 kHz (DBDJ), flow rate of He gas at 1 L/min, intensity at 5 and variation generated repetition rate from 50 Hz to 110 Hz (plasma level 1 to 7) or converted to plasma dissipated power from 0.27 W to 0.50 W. For measuring plasma properties of DBDJ oscilloscope was used to calculate plasma dissipated power and dose, optical emission spectroscopy (OES) to detect elements in plasma, gas detector NO and Ozone.

4.1.1 Electrical properties

First of all, measuring electrical properties of DBDJ oscilloscope was used for calculating truly plasma dissipated power applied at different repetition rates 50 Hz to 110 Hz. By finding value of current (*I*) by the voltage across capacitor (channel 2), area in Figure 13 B and %duty cycle in Figure 12 (A or B), when voltage (channel 1), frequency (*f*) in Figure 12 (F), capacity (*c*), voltage (channel 2) are constant. After that, we can find truly plasma dissipated power and dose of DBDJ at repetition rate 50 Hz to 110 Hz, by used the equation (11 and 12).

The Lissajous figure of DBDJ is shown in Figure 13. At applied frequency 20 kHz, the plasma dissipated power at 0.27 W. Therefore, when increasing repetition rate to DBDJ the percentage of duty cycle, power and dose of DBDJ increased. These factors have influence on the intensity of radicals in DBDJ. Intensity of radicals in plasma played an important role for bactericidal and wound healing process.

Figure 14 shown increasing of plasma dissipated power of DBDJ influenced by plasma level 1 to 7 or repetition rate 50 Hz to 110 Hz. When increasing plasma level from 1 to 7 (50 Hz to 110 Hz) the value of area (Lissajous figure) and %duty cycle increased. Leading to plasma dissipated power increased from relative of equation (11) and DBDJ have a plasma dissipated power maximum at 0.50 W.

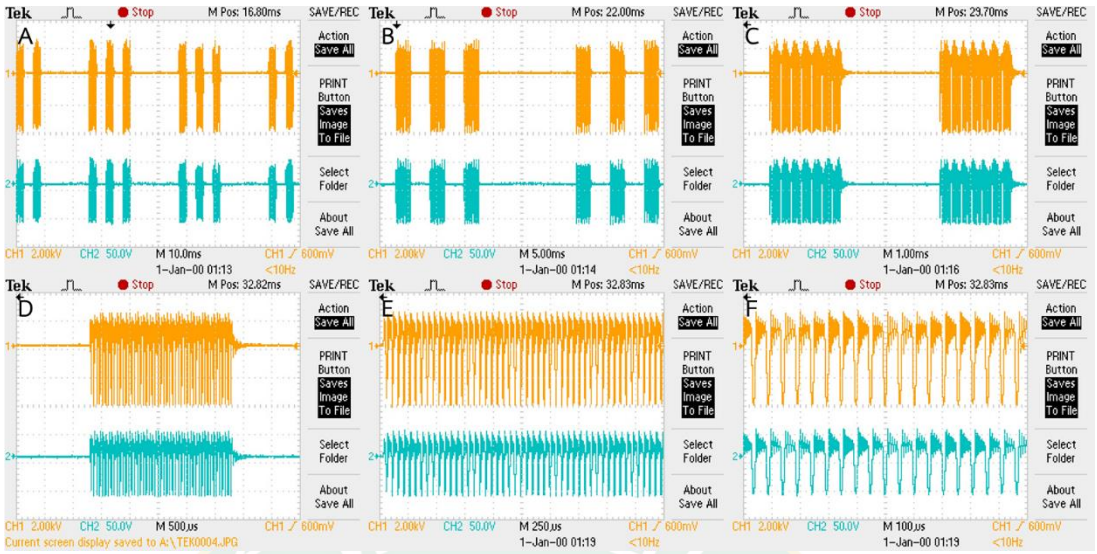

Figure 12 The Lissajous figure of DBDJ at repetition rate 50 Hz or plasma dissipated power 0.27 W. (A) t = 10 ms, (B) t = 5 ms, (C) t = 1 ms, (D) t = 500 us, (E) t = 250 us and (F) t = 100 us.

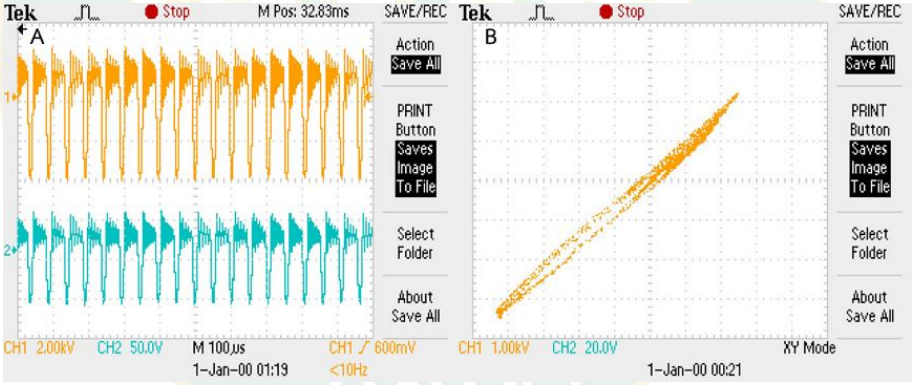

Figure 13 A) The applied voltage signal (channel 1) the voltage across the 1 nF capacitor (channel 2) and B) the Lissajous figure of DBDJ the plasma dissipated power at 0.27 W.

Moreover, plasma dissipated power has influence on the intensity of reactive oxygen nitrogen species (RONS) in DBDJ and its effect on efficiency for bactericidal. Dose of plasma depend on plasma dissipated power and exposure time from the equation (12). Table 6 shown relative of DBDJ lv.1 to lv.7 or repetition rate 50 Hz to 110 Hz to %duty cycle, area (Lissajous figure), plasma dissipated power and

dose. Plasma dissipated power and exposure times involves to value of dose as shown in Table 7. Therefore, Intensity of RONS in plasma and dose of plasma depends on value of plasma dissipated power and exposure time. They play an essential role in the efficiency of bactericidal and wound healing process.

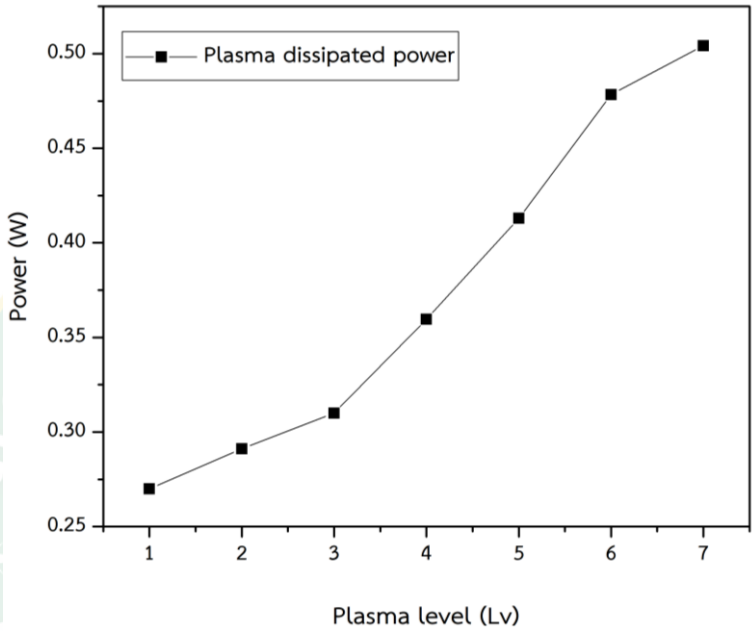

Figure 14 Increasing of plasma dissipated power influenced by plasma level 1 to level 7 (repetition rate at 50 Hz to 110 Hz).

Table 6 Duty%, area (Lissajous figure), plasma dissipated power and dose of DBDJ lv.1 to lv.7.

Plasma Lv.	Duty %	Area	Power (W)	Dose (J/cm^2)
1	0.24	3.08	0.27	0.0195
2	0.23	3.07	0.29	0.0209
3	0.25	2.96	0.31	0.0224
4	0.28	3.18	0.36	0.0260
5	0.32	3.39	0.41	0.0296
6	0.37	3.52	0.48	0.0347
7	0.38	3.24	0.50	0.0361

Table 7 Relative of dose to plasma dissipated power and exposure times.

Power (W)	Dose (J/cm^2)			
	15 s	**30 s**	**45 s**	**60 s**
0.27	0.29	0.59	0.88	1.17
0.29	0.31	0.63	0.94	1.26
0.31	0.34	0.67	1.01	1.34
0.36	0.39	0.78	1.17	1.56
0.41	0.44	0.89	1.33	1.78
0.48	0.52	1.04	1.56	2.08
0.50	0.54	1.08	1.63	2.17

4.1.2 The reactive oxygen nitrogen species (RONS)

The reactive oxygen and nitrogen species (RONS) played an important role in bactericidal (Kang et al., 2015). These radicals and electrostatic force of ions break down bacteria cell, damage DNA and charge particles accumulated leading to cell rupture or lysis. The main bactericidal that could kill bacteria was RONS. Figure 15 shows the broad range of OES spectra with plasma dissipated power 0.27 W to 0.50 W. The emission spectrum of DBDJ in wavelength range of 200 to 900 nm, found the peak of NO at 297.61 nm, OH at 308.99 nm, N_2 at 337.54 nm and He at 706.54 nm as shown in Figure 16. The NO lines are primarily from the NO A–X (γ) in the ultraviolet region at wavelength 200 to 300 nm but will very low intensity. The N_2 C-B (2^{nd} positive system at 334.27 nm) and N^+_2 B-X (1^{st} negative system at 406.24 nm) was observed between wavelength 300 to 450 nm because the excitation processes is like the electron impact excitation from the ground state N_2 (X1Σ g+) and the first metastable state N_2 (A3Σ u+) and pooling reaction (Kang S. K. et al., 2015). Also found OH at 308.99 nm and He at 706.54 nm. The Figure 17 showed that when increasing the plasma dissipated power from 0.27 W to 0.50 W the intensity of RONS increased. The increasing of NO intensity is significant but ineffective for the intensity of OH in Figure 18.

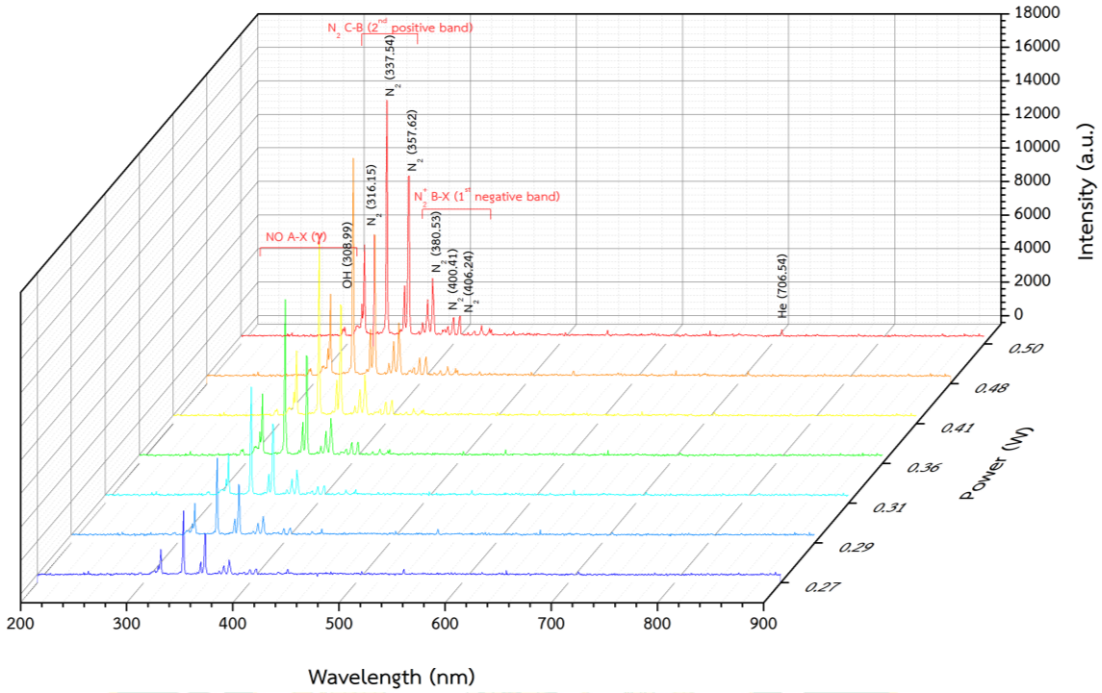

Figure 15 The emission spectra of DBDJ with plasma dissipated power 0.27 W to 0.50 W.

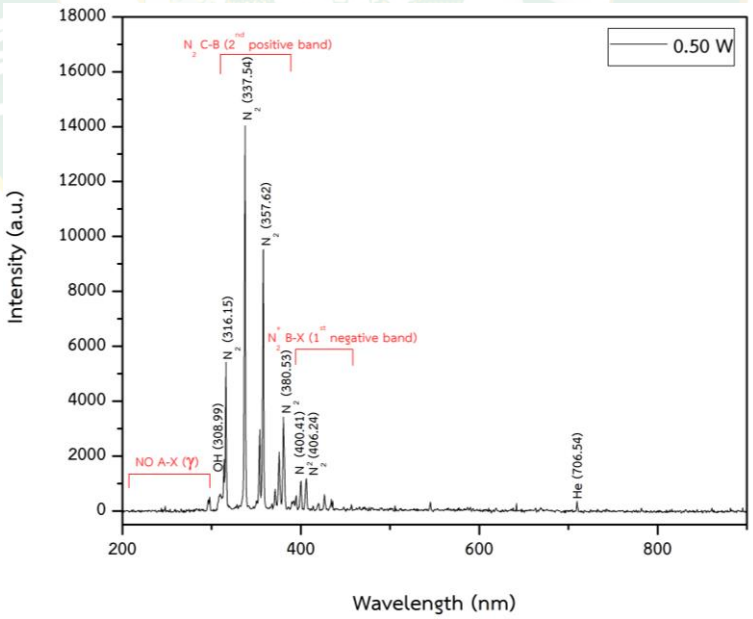

Figure 16 The emission spectra of the plasma dissipated power at 0.50 W.

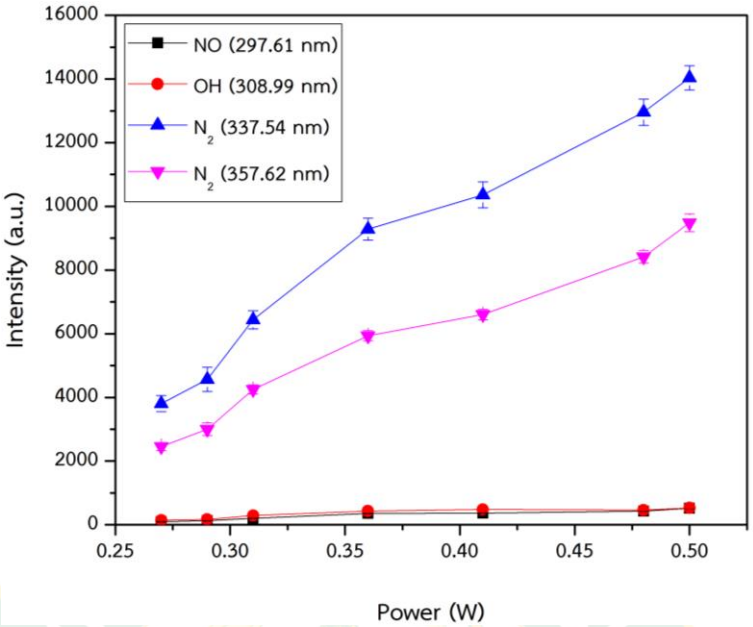

Figure 17 The relative of the RONS intensity and the plasma dissipated power.

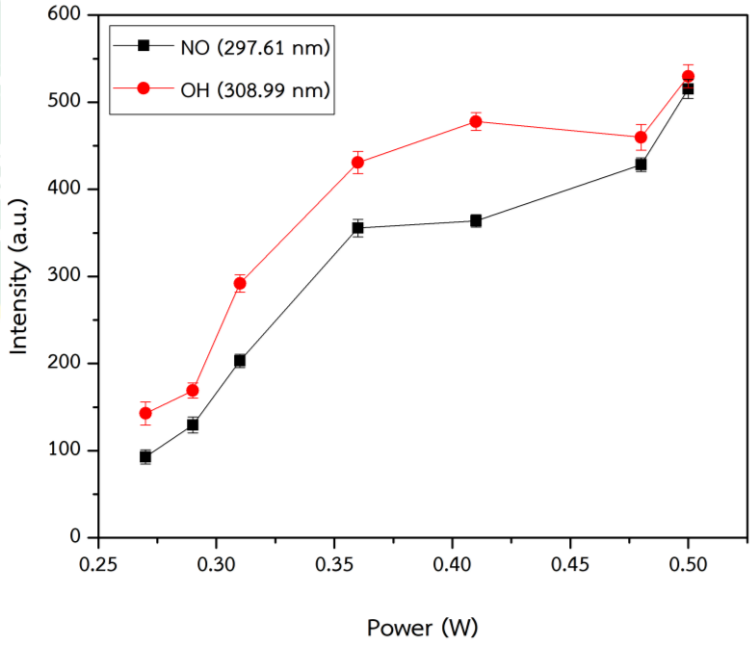

Figure 18 NO and OH intensity and the plasma dissipated power.

The intensity of the OES spectrum increases by increasing the applied plasma dissipated power as shown in Figure 15 and Figure 17. This result shows plasma dissipated power at 0.27 W has a low intensity of RONS. At the higher plasma dissipated

power at 0.50 W higher intensity of RNS and ROS or RONS was found. The intensity on all of radical in plasma depends on applied plasma dissipated power to DBDJ.

Regarding NO, as seen in Figure 19, NO concentration exhibits a remarkable increase with the plasma dissipated power, When increased from 1 ppm at 0.25 W to 5 ppm at 0.5 W. Whereas, O_3 concentration shows an infinitesimal value, less than 0.5 ppm. In biomedical applications, concentration of O_3 and NO should not be higher than 8 h. TWA 0.1 ppm and TWA 25 ppm, respectively, otherwise it could adversely affect the respiratory system.

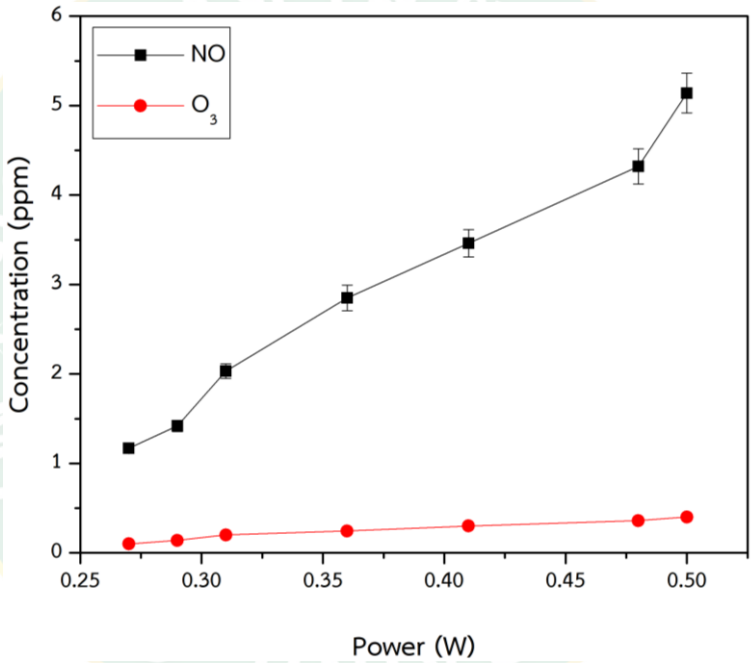

Figure 19 The relative between NO and O_3 concentration and the plasma dissipated power.

The existence of these molecules implied curative properties of the studied plasma because reactive nitrogen species (RNS) and reactive oxygen species (ROS) known as reactive oxygen nitrogen species (RONS) were found to play an major role in bactericidal (Kim et al., 2009). RONS have 3 important effects on cells including protein oxidation, lipid peroxidation and oxidation of DNA. Regarding protein oxidation, ROS can fragment protein and protein-protein cross-linkages by inducing oxidation in both amino acid side chains and protein backbones. In lipid peroxidation, RNS/ROS can

induce electrostatic force in the cell membrane, which therefore steal electron from the lipids in cell membranes, resulting in cell lysis. With regard to DNA, RNS can induce DNA deamination leading to strand breaks (Kong et al., 2009; von Woedtke et al., 2013).

4.2 Microbiological test

After knowing about plasma properties of DBDJ, we have to find the best condition of DBDJ for bactericidal by using prepared spread plate method, samples of *Staphylococcus aureus* (*S. aureus*) TISTR 2329 and *Pseudomonas aeruginosa* (*P. aeruginosa*) TISTR 2370 were used with plasma dissipated power from 0.27 W to 0.50 W and time exposure 15 s to 60 s. Then the best condition was found, only one condition was selected plasma dissipated power at 0.50 W and time exposure 60 s to destroy bacteria biofilm by used live/dead assay with fluorescent microscope.

4.2.1 Bactericidal effect of DBDJ

The efficiency of bactericidal *S. aureus* of DBDJ is shown in Figure 20. At plasma dissipated power 0.27 W and exposure time 15 s to 30 s nothing happened to the bacteria and all of them survived. Increasing the exposure time to 45 s some parts of the bacteria died, almost 30%. At exposure time of 60 s a larger clear zone was achieved than at 45 s. This exposure time was enough to eradicate bacteria at nearly 80%. At plasma dissipated power 0.50 W and exposure time 15 s some part of bacteria died but some part survived because exposure time was not sufficient to eradicate all of bacteria by RONS, ions and radical. When the exposure time was increased to 30 s more than 80% of the bacteria died and a large clear zone by plasma diffusions was induced. With exposure time increasing to 45 s and 60 s bacteria death had a larger clear zone than at 30 s. Bacteria died more than 90% up to 100% at 60 s as well as has high plasma diffusion due to applying plasma dissipated power to DBDJ to induce ionization. The intensity of radicals in plasma depends on plasma dissipated power

and effects to bactericidal as well as exposure time. When studied at high plasma dissipated power of DBDJ, the efficiency of bactericidal increased at plasma dissipated power 0.41 W to 0.50 W and exposure time at 45 s to 60 s. By increasing exposure time from 45 s to 60 s the bactericidal increased as well; from 90% up to 100% as shown in Figure 21.

The efficiency of bactericidal *P. aeruginosa* by DBDJ is shown in Figure 22. At plasma dissipated power 0.27 W and exposure time 15 s to 30 s some part of bacteria died, clear zone circle occurred. Increasing the exposure time to 45 s the clear zone expands and exposure time 15 s to 30 s more than 60% of bacteria in this condition died. Using a time of 60 s, a larger clear zone was achieved than at 45 s and the exposure time was enough to eradicate bacteria at more than 70%. At plasma dissipated power 0.50 W and exposure time 15 s more than 60% of bacteria died because plasma dissipated power at 0.50 W have high intensities of RONS and RONS play an important role for bactericidal. When the exposure time was increased to 30 s most of the bacteria died and a large clear zone by plasma diffusions was almost 80%. With exposure time increasing to 45 s and 60 s bacteria death was 90% up to 100% had a larger clear zone than at 30 s as well as having high plasma diffusion due to plasma dissipated power being applied to DBDJ in order to induce ionization radicals. These times being enough for bactericidal. For bactericidal the intensity of RONS in plasma depends on applied plasma dissipated power and RONS play an important role in inactivating bacteria. When investigated at height plasma dissipated power of DBDJ, the efficiency of bactericidal increased at plasma dissipated power 0.41 W to 0.50 W and exposure time at 45 s to 60 s. By increasing time, the bactericidal increased as well; from 80% up to 100% when using the exposure time from 45 s to 60 s as shown in Figure 23.

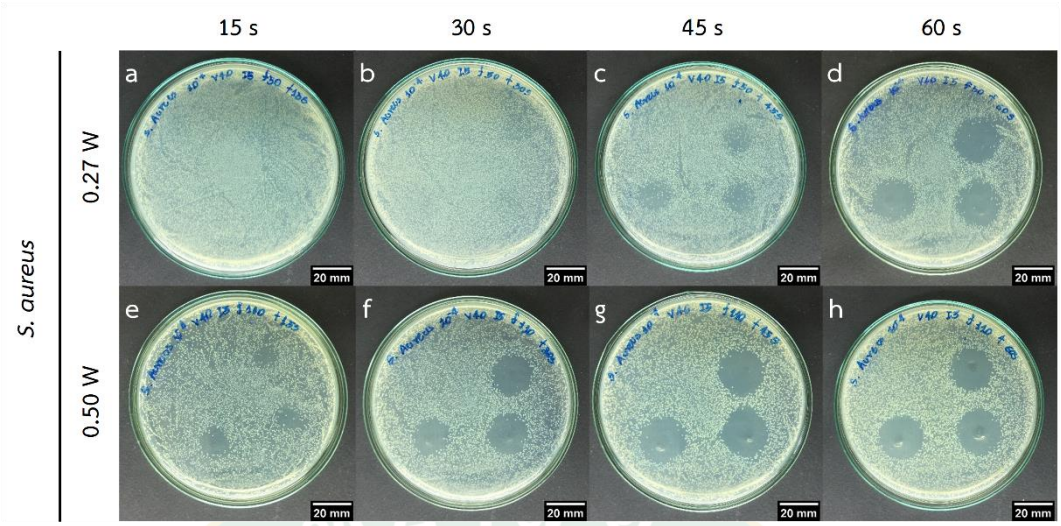

Figure 20 The efficiency bactericidal *S. aureus* of DBDJ, the plasma dissipated power at 0.27 W and exposure time 15 s to 60 s (a, b, c and d), the plasma dissipated power at 0.50 W and exposure time 15 s to 60 s (e, f, g and h).

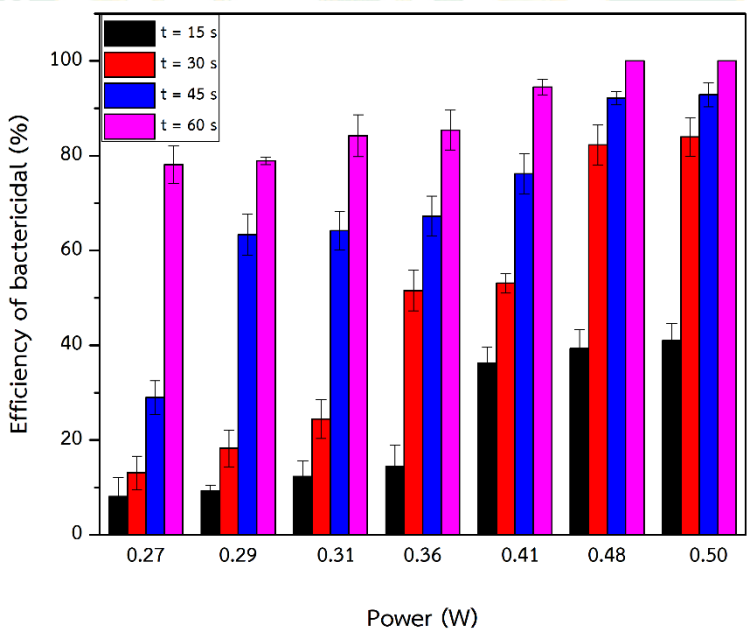

Figure 21 The percentage efficiency of bactericidal *S. aureus* by DBDJ.

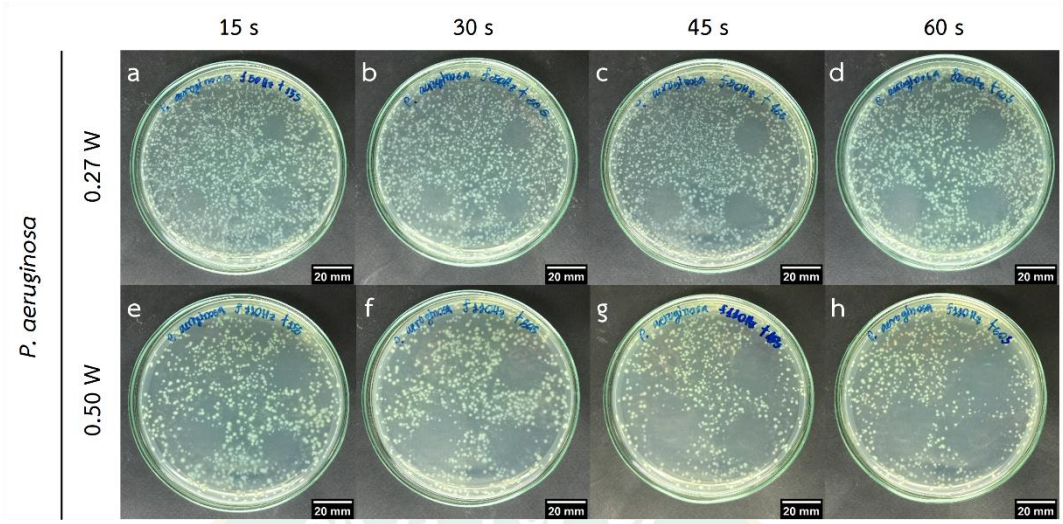

Figure 22 The efficiency bactericidal *P. aeruginosa* of DBDJ, the plasma dissipated power at 0.27 W and exposure time 15 s to 60 s (a, b, c and d), the plasma dissipated power at 0.50 W and exposure time 15 s to 60 s (e, f, g and h).

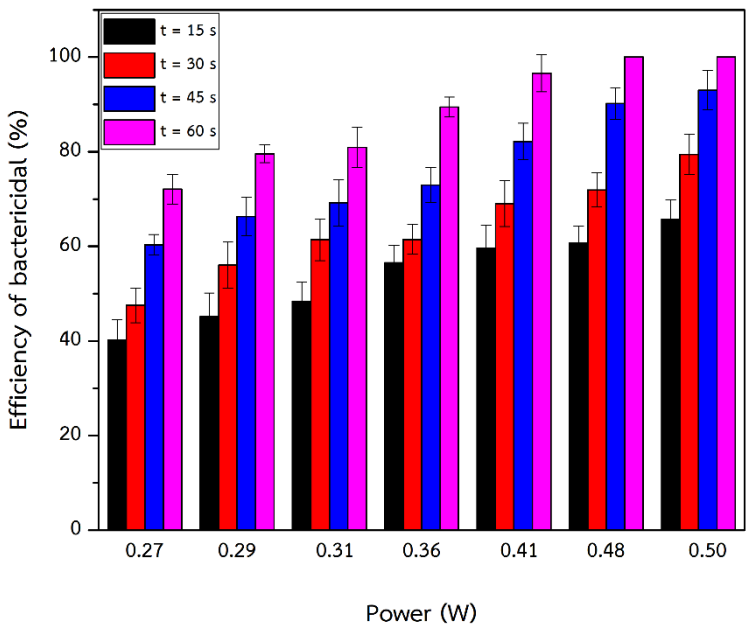

Figure 23 The percentage efficiency of bactericidal *P. aeruginosa* by DBDJ.

Comparing the efficiency of bacterial by DBDJ between *S. aureus* and *P. aeruginosa* applied plasma dissipated power at 0.27 W and 0.50 W, exposure time 15 s to 60 s shows in Figure 24. Figure 24 (C) at applied plasma dissipated power 0.27 W and exposure time 15 s to 30 s in case of *S. aureus* low efficiency bactericidal of less

than 15% was monitored. On the other hand, in case of *P. aeruginosa* high efficiency bactericidal of more than 40% under the same condition was monitored. However, when exposure time increases up to 60 s the bactericidal efficiency of both of them increased more than 70%. Moreover, in Figure 24 (D) when using applied plasma dissipated power 0.50 W and exposure time 15 s to 30 s in case of *S. aureus* bacteria more than 40% and up to 80% died. In addition, in case of *P. aeruginosa* bacteria died more than 60% to 80% under the same condition. Consequently, when using exposure time 45 s to 60 s both of bacteria have high efficiency of bactericidal, being more than 90% and increased to 100% at exposure time 60 s, this because at applied plasma dissipated power 0.50 W a higher intensity of RONS is created than when a plasma dissipated power 0.27 W is applied. When increasing exposure time for bactericidal up to 60 s, this time or dose being enough in order to eradicate both of bacteria by RONS (Dobrynin et al., 2009).

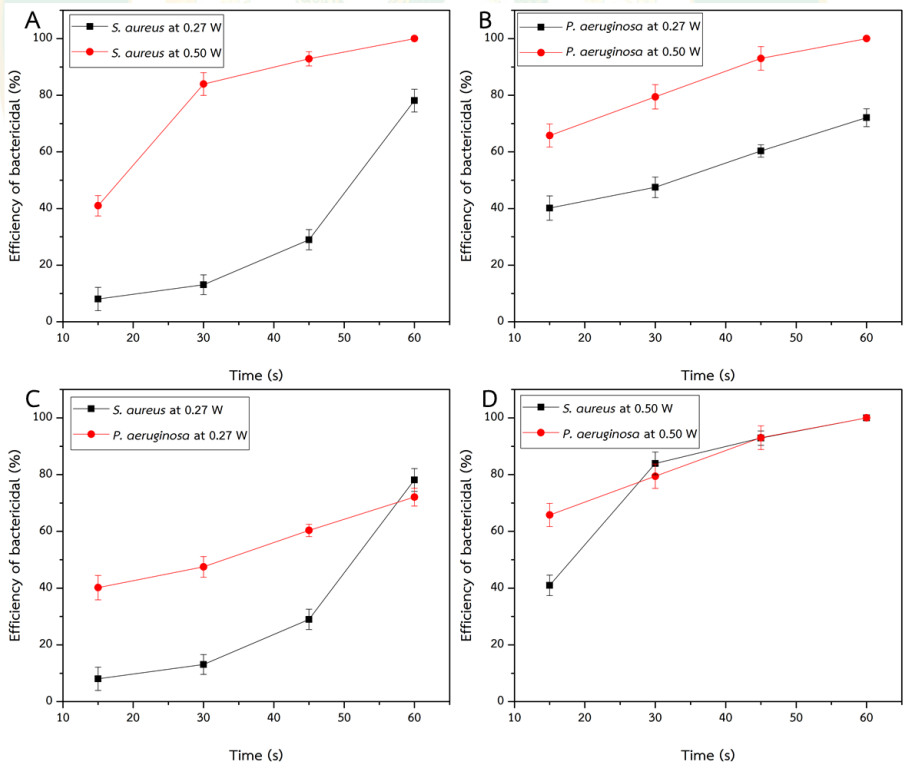

Figure 24 The percentage efficiency bactericidal of DBDJ (A) *S. aureus* with plasma dissipated power at 0.27 W and 0.50 W, (B) *P. aeruginosa* with plasma dissipated power at 0.27 W and 0.50 W, (C) *S. aureus* and *P. aeruginosa* with plasma dissipated power

at 0.27 W and (D) *S. aureus* and *P. aeruginosa* with plasma dissipated power at 0.50 W.

Furthermore, it was found that the *P. aeruginosa* have a higher bactericidal efficiency than *S. aureus* under the same condition. Because of the main difference of the cell wall structure of bacteria. *S. aureus* is gram-positive bacteria and have cell wall thickness ranging from 20 to 80 nm and *P. aeruginosa* is gram-negative bacteria having cell wall thickness between 1.5 to 10 nm. The outer structure of *S. aureus* cell wall is the multi layers of peptidoglycan which is a stronger bonding than the *P. aeruginosa* cell wall. *P. aeruginosa* cell wall consists of phospholipids and lipopolysaccharides, which is influenced by the polarity. Destruction of peptidoglycan through external stresses will lead to cell lysis. The outer membrane is more permeable than the cytoplasmic membrane and the cell wall and therefore potentially easier to penetrate by DBDJ and henceforth probably leading to a higher sensitivity of gram-negative bacteria by DBDJ. In addition, the different thickness of cell wall bacteria effects the diffusion across whereby a thick gram-positive cell wall being slower than a thin gram-negative cell wall leading to a different sensitivity to DBDJ (Mai-Prochnow et al., 2016). Therefore, the different thickness of cell wall between two groups of bacteria, the outer membrane of gram-negative as well as cell appendices of gram-positive bacteria are an important factor to bactericidal of DBDJ (Mai-Prochnow et al., 2016; Vollmer et al., 2008).

4.2.2 Effect of DBDJ on bacterial biofilms

DBDJ plasma operated at plasma dissipated power 0.5 W and exposure time 60 s have high ability to eradicate bacteria shows in Figure 24 (D) and also destroyed bacterial biofilms in Figure 25 and Figure 26. The fluorescent images both of *S. aureus* and *P. aeruginosa* with double stain Hoechst, PI and merge. The result has shown plasma dissipated power at 0.5 W and exposure time 60 s have ability to destroy bacterial biofilm 100% both of *S. aureus* and *P. aeruginosa* in Figure 25 (F) and Figure 26 (F). Moreover, the cause of bacterial biofilm death at height plasma dissipated

power 0.5 W and exposure time at 60 s showed the power of plasma or dose of plasma being enough to eradicate bacterial and destroy bacterial biofilm (Dobrynin et al., 2009) by interaction to cell wall, cell membrane, DNA damage and leading to cell lysis.

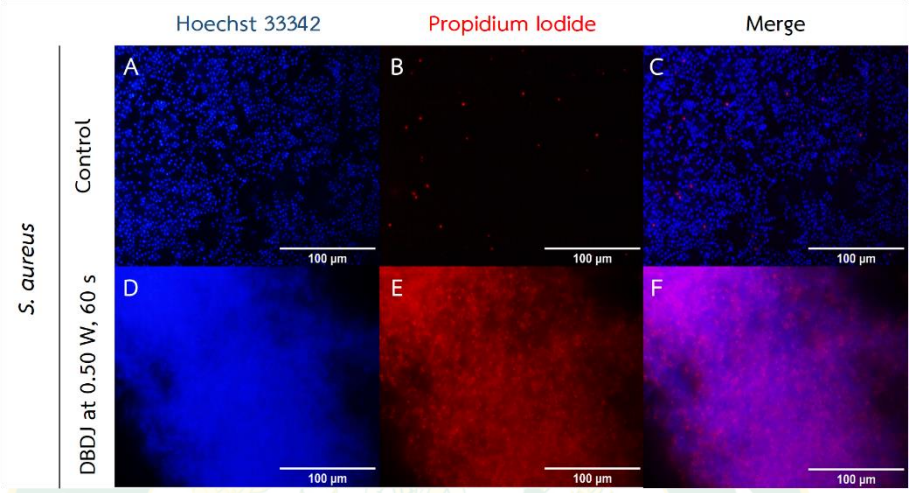

Figure 25 Bacterial biofilm *S. aureus* by Live/Dead assay with double stain Hoechst 33342 and Propidium iodide (PI). Control sample *S. aureus* (A, B and C) and plasma dissipated power at 0.5 W with exposure time 60 s for destroy bacterial biofilm *S. aureus* (D, E and F).

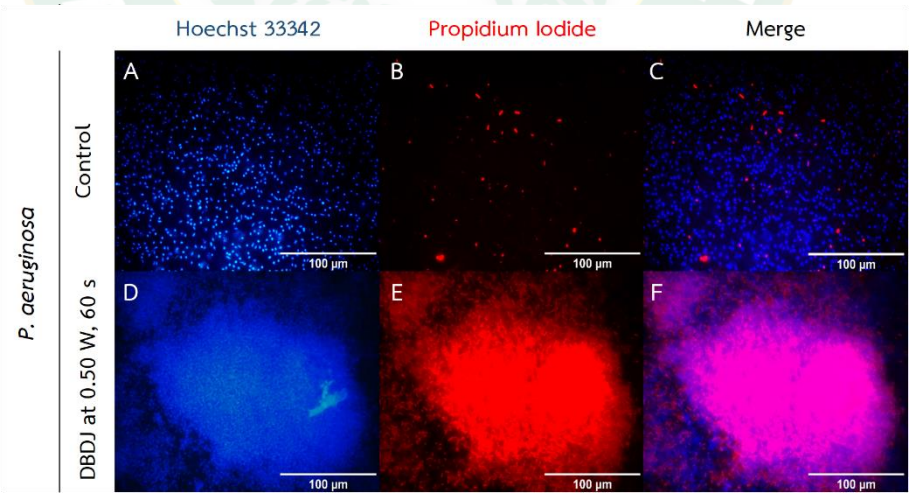

Figure 26 Bacterial biofilm *P. aeruginosa* by Live/Dead assay with double stain Hoechst 33342 and Propidium iodide (PI). Control sample *P. aeruginosa* (A, B and C) and plasma dissipated power at 0.5 W with exposure time 60 s for destroy bacterial biofilm *P. aeruginosa* (D, E and F).

The inactivation of CAPP to bacterial is well-known peroxidation of lipids (Vatansever et al., 2013) and membrane lipids are the most vulnerable to physical stresses because the position is outside of the cell envelope and it is sensitive to RONS. Furthermore, the charged particles in plasma played an important role for bactericidal with the rupture of bacteria cells wall (Fridman et al., 2007; Guo et al., 2015). When the charge particles accumulated on outer surface of the membrane being more than the tensile strength of the membrane it leads to cell rupture by electrostatic force (Laroussi et al., 2003). If no force exists, the repulsive force will only impact on the charges and little damage to the cell membrane will occur. The electric field generated between charge particles have non-uniformity, when time of charge accumulated the transmembrane potential increases. On the other hand, the ions generated in the CAPP couldn't get through the cell membrane. Hence, charge accumulation is still execution. If the intensity of electric field generated form charge particles is strong enough it could change the three dimensional of the protein's structures, separate out the cell membrane and be forceless. Thus, the charge particles forming CAPP has the ability to destroy the proteins and enzymes activity into the cell. Most likely the cytoplasm will leak out the cell through these holes, which was the reason leading to cell death and why the cell dies (Guo et al., 2015; Kong et al., 2009).

The result shows that the efficiency of bactericidal increased by increasing the applied plasma dissipated power and exposure time. When increasing applied plasma dissipated power of DBDJ the increase of intensity of N_2, which depends on the plasma dissipated power applied to DBDJ, is significant, but increasing the applied plasma dissipated power is ineffective to intensity of OH. As can be seem, the RNS has a more important role for bactericidal than RON in this result. RNS induces nitric oxide (NO) and nitric acid influences bacteria cells because bacteria cannot survive in acidic conditions (Heinlin et al., 2010; Suschek and Opländer, 2016). Since the important role of RNS generated NO in host, deference used the exogenous NO as an antibacterial agent as an assistant in healing contaminated wounds. Acidified nitrite has a strong antimicrobial ability on bacteria cell leading to cell death. It has commonly been assumed that the bactericidal effects related to generated nitrous acid and other

unidentified nitrogenous metabolites, but not to nitric oxide. The DBDJ treatment prompts the acidic conditions and accumulation of nitrite and hydrogen peroxide. Consequently, these factors are the main cause for DBDJ to induced toxic effects on bacteria cell (Suschek and Opländer, 2016). Especially the generation of peroxynitrite by nitrite and hydrogen peroxide under acidic conditions play a major role on the bactericidal effects and high intensity of RNS (N_2 and NO_2) causing bacteria cell deaths. Additionally, ROS (OH) were responsible for bacterial cell death as well (Rehman et al., 2016). Consequently, the ROS and RNS or RONS play a major role in bactericidal. Moreover, the electrostatic force in which plasma surrounds bacteria cells had effect to bactericidal in previously research. When the charged particles accumulated around bacteria they break down the cell wall and the cell membrane leading to cell rupture or lysis (Daeschlein et al., 2012; Guo et al., 2015).

4.3 Human Dermal Fibroblasts adult (HDFa) cells

We found the best condition of DBDJ at plasma dissipated power 0.50 W and exposure time 60 s, have high potentially to bactericidal and eradicated bacteria biofilm both of gram-positive bacteria (*S. aureus*) and gram-negative bacteria (*P. aeruginosa*). After that side effect to cell cytotoxicity of this condition were studied. In this work DBDJ treat on Human Dermal Fibroblasts, adult (HDFa) cells was used. Primary human dermal fibroblasts are isolated from adult skin and the results monitored. First of all, observe cell morphology by optical microscope (OM). Then, cell cytotoxicity assay of DBDJ was monitored by live/dead assay, flow cytometry (Muse cell analyzer) with Muse count and viability kit and Muse annexin V and dead cell kit. After which study the effect of DBDJ at the best condition for bactericidal and eradicated bacteria biofilm in wound healing model to HDFa cells as in vitro.

4.3.1 Cell morphology

The result cell morphology of HDFa cell shows in Figure 27. DBDJ treat on HDFa cells, cell morphology remains unchanged when compared with negative control and treatment control. Figure 27 (h) cell morphology are still spindle-shaped and

looked healthy cells after treat at plasma dissipated power 0.50 W and exposure time 60 s. Any change of HDFa cells morphology was not observed except in Figure 27 (d). If cells have damage or side effect, cells going to die and morphology of cells would be changed by shrinkage to sphere, cells detach and death. DMSO have ability to induce cell death and apoptosis pathway. Therefore, result of HDFa cells morphology shown DBDJ at plasma dissipated power 0.50 W and exposure time 60 s without side effect or damage to HDFa cells morphology. The results of optical microscope (OM) shown only the basics of cell health and morphological of cells. On the other hand, this technique cannot observe the reaction inside of HDFa cells pathway. Consequently, we have to do in-depth analysis of HDFa cells by live/dead assay with fluorescent microscope and flow cytometry (Muse cell analyzer) with Muse count and viability kit and Muse annexin V dead cell kit.

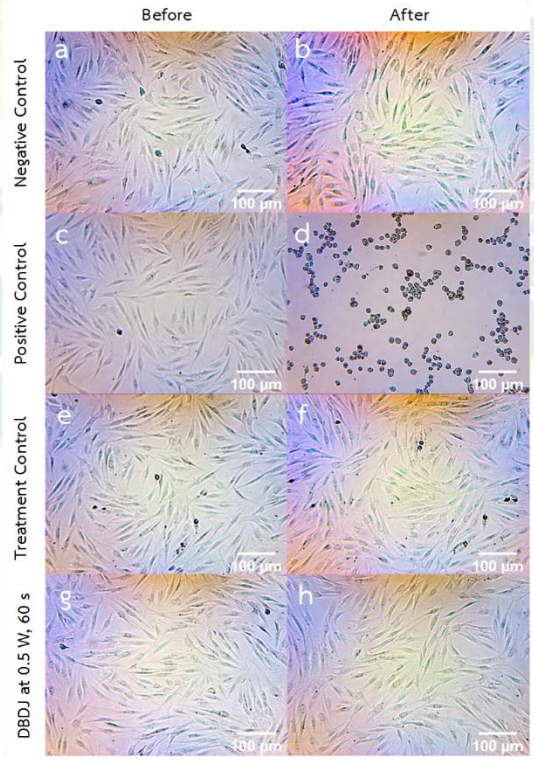

Figure 27 Cell morphology of HDFa cells, (a,b) negative control or natural control as DMEM + 10% FBS, (c,d) positive control as DMEM + 50% DMSO 2 h, (e,f) treatment control as He gas blow 60 s and (g,h) DBDJ at plasma dissipated power 0.50 W with exposure time 60 s.

4.3.2 Live/dead assay of HDFa cells

The fluorescent image of HDFa cells with double stain Hoechst, PI and merge. Hoechst 33342 have ability to bind with live/dead cells and Propidium iodide (PI) is permeant to dead cells only. After merge image together the dead cells will observe. Figure 28 and Figure 29 have shown DBDJ plasma dissipated power at 0.5 W and exposure time 60 s (j, k and l) without damage to cells when compared with negative control as DMEM + 10% FBS (a, b and c) and treatment control as He gas 1 L/min blow on cells 60 s (g, h and i) all of this not differentiated. The positive condition (d, e and f) used DMEM + 50% DMSO for induced cells to cells death for each other to compared.

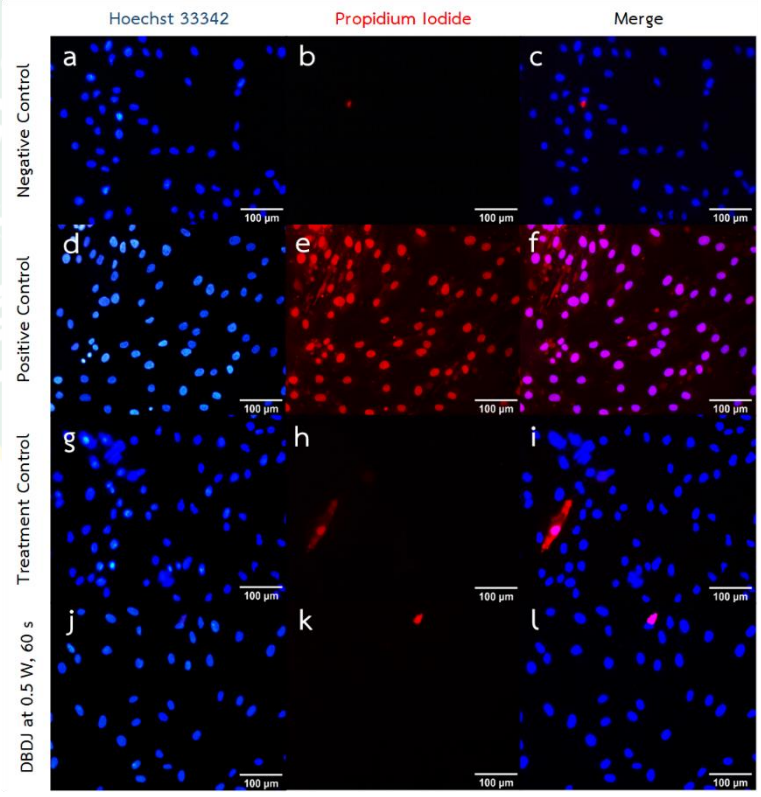

Figure 28 HDFa cells by Live/Dead assay with double stain Hoechst 33342 and Propidium iodide (PI) at magnification 200x. Negative control as DMEM + 10% FBS (a, b and c), positive control as DMEM + 50% DMSO 15 min (d, e and f), treatment control as He gas blow 60 s (g, h and k) and plasma dissipated power at 0.5 W with exposure time 60 s (j, k and l).

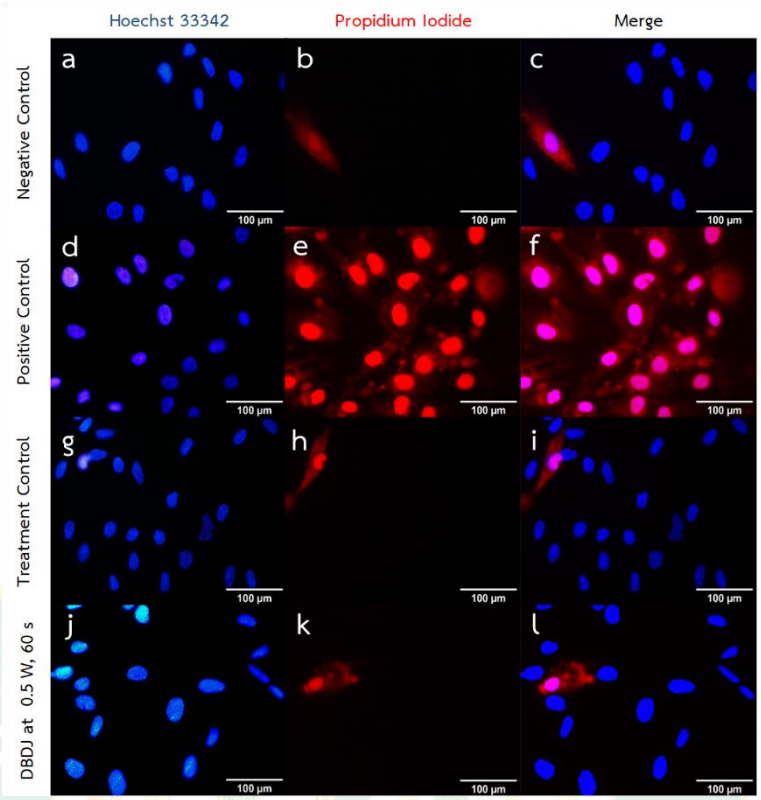

Figure 29 HDFa cells by Live/Dead assay with double stain Hoechst 33342 and Propidium iodide (PI) at magnification 400x. Negative control as DMEM + 10% FBS (a, b and c), positive control as DMEM + 50% DMSO 15 min (d, e and f), treatment control as He gas blow 60 s (g, h and k) and plasma dissipated power at 0.5 W with exposure time 60 s (j, k and l).

The fluorescent image of HDFa cells at differential of magnification (200x and 400x) and spot. The result shows the same trend DBDJ at plasma dissipated power 0.50 W and exposure time 60 s do not induce cells to death not observed significantly. When compared DBDJ treat on HDFa cells condition with negative control and treatment control, cell death did not increase significantly in Figure 28 and Figure 29. Thence, DBDJ operated condition at plasma dissipated power 0.5 W and exposure time 60 s have high potential to killed bacteria and eradication bacteria biofilm without side effect or damage to HDFa cells. The death of the cell does not appear in cells morphology image (OM) and fluorescent image. However, although the result from morphology and fluorescent image shown in the same direction, we cannot draw the

final conclusion that DBDJ operated without any side effect or damage to cells including induce program cells death pathway, unless using other techniques to analyses. In consequence, for quantitative analysis of HDFa cells Muse cell analyzer was used with Muse Count & Viability Assay (monitored percentage of viable cells and dead cells) and Muse Annexin V and Dead Cell Assay (monitored percentage of viable cells, early apoptosis cells, late apoptosis cells and dead cells).

4.3.3 Muse Count & Viability Assay

The result percentage viability of HDFa cells shown in Figure 30 A) HDFa cells was not dead-induced by DBDJ plasma dissipated power at 0.5 W and exposure time 60 s with negative control (DMEM + 10% FBS), positive control (DMEM + 10% DMSO 2 h.) and treatment control (He gas blow 60 s). Figure 30 B) statistical analysis of percentage cell viability using repeated measures one-way ANOVA followed by an appropriate post hoc multiple comparison test (Tukey method). The result has shown plasma dissipated power at 0.5 W and exposure time 60 s, these conditions have high potential to eradicate bacterial and destroy bacteria biofilm without side effects to percentage viability of HDFa cells when compared with negative control and treatment control, all of this not being different after statistical analysis. Positive control used DMEM + 10% DMSO 2 h for induced cells to dead cells for set threshold and compared to each other.

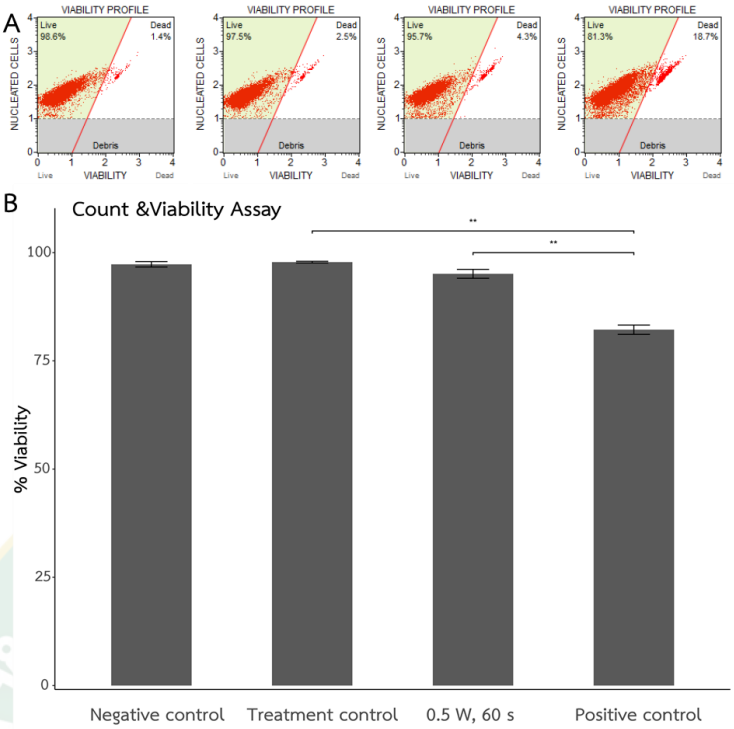

Figure 30 A) Representative figures from flow cytometry of HDFa cells with negative control as (DMEM + 10% FBS), treatment control (He gas blow 60 s), plasma dissipated power at 0.5 W with exposure time 60 s and positive control (DMEM + 10% DMSO 2 h). B) Quantitative analysis of percentage cell viability from flow cytometry. Data are means of 3 replicates and expressed as means ± SD. ** indicates $P<0.01$.

4.3.4 Muse Annexin V and Dead Cell Assay

The percentage total apoptosis of HDFa cells is shown in Figure 31. Accordingly, the apoptosis profile could distinguish 4 cell populations by this method: Live cells (Annexin V−/7-AAD−); early apoptotic cells (Annexin V+/7-AAD−); late apoptotic/dead cells (Annexin V+/7-AAD+); and necrotic cells (Annexin V-/7-AAD+). Figure 31 A) DBDJ plasma dissipated power at 0.5 W and exposure time 60 s increasing percentage total apoptosis of HDFa cells slightly but this not significantly after using statistical analysis in Figure 31 B). The result showed DBDJ plasma did not induce apoptosis and leading cell to death when compared with negative control and treatment control. In positive control DMEM + 10% DMSO were used 2 h for induced cells to apoptosis and dead cells for set threshold and compared to each other.

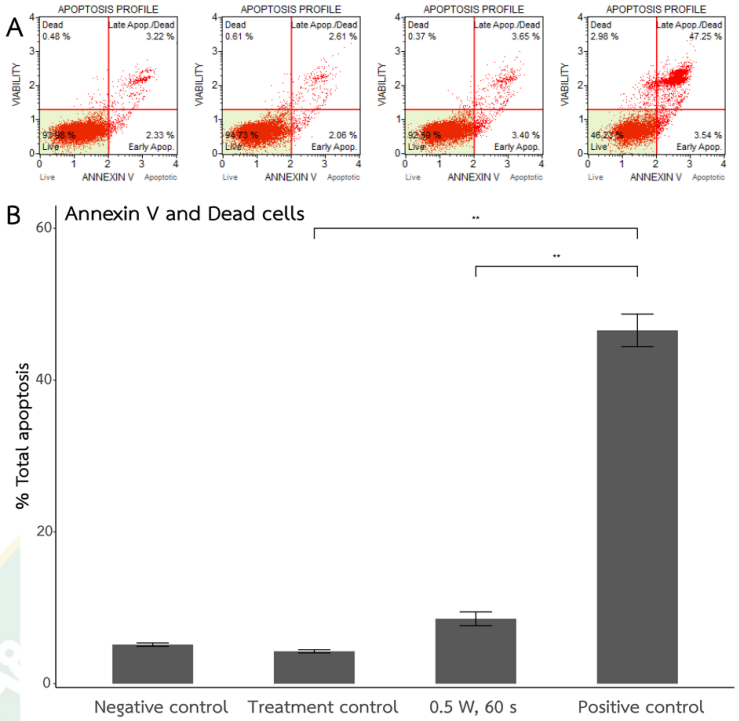

Figure 31 A) Representative figures from flow cytometry of HDFa cells with negative control as (DMEM + 10% FBS), treatment control (He gas blow 60 s), plasma dissipated power at 0.5 W with exposure time 60 s and positive control (DMEM + 10% DMSO 2 h). B) Quantitative analysis of percentage total apoptosis from flow cytometry. Data are means of 3 replicates and expressed as means ± SD. ** indicates $P<0.01$.

The result from morphological of cells, live/dead assay, Muse Count & Viability Assay and Muse Annexin V & Dead Cell Assay shown in the same direction is DBDJ operated at plasma dissipated power 0.50 W and exposure time 60 s have high performance to killed bacteria and destroyed bacteria biofilm both of *S. aureus* and *P. aeruginosa* by without side effect and also without damage to HDFa cells morphology, healthy of cells, percentage of viability cell and not inducing apoptosis or programed cell death leading cell to death of HDFa cell shown in Figure 27 to Figure 31.

CHAPTER 5
CONCLUSION AND RECOMMENDATIONS

5.1 Conclusion

The DBDJ at plasma dissipated power 0.27 W has a low intensity of RONS. At the higher plasma dissipated power 0.50 W, higher intensity of RNS and ROS or RONS were found. The intensity all of RONS and radical in plasma depend on applied plasma dissipated power to DBDJ. All the death of bacteria increased with plasma dissipated power and exposure time. The lager clear zones affected by RONS and charge particles including electrostatic force of ions in plasma play an important role for bactericidal leading to cell lysis of bacteria. Moreover, the difference of cell wall structure between gram-positive and gram-negative bacteria are main factors leading to different sensitivity by DBDJ. The result shows that, DBDJ at plasma dissipated power 0.5 W with exposure time 60 s have high potential to bactericidal, eliminate bacterial biofilms both of *S. aureus* and *P. aeruginosa* by without side effect and also without damage to HDFa cells morphology, health of cells, percentage of viability cell and not inducing apoptosis or programed cell death leading cell to death of HDFa cells in vitro.

Consequently, the best condition of DBDJ are operated plasma dissipated power 0.50 W with exposure time 60 s, dose in that condition being enough to kill bacteria, eradicate bacteria biofilm by without damage and also without side effect to HDFa cells as in vitro is essential for clinical use.

5.2 Recommendations

The DBDJ should be try to be used with other gas besides He gas for so as to have an alternative. The intensity of radical in plasma will use OES with more resolution detail or other advance technique for calculating truly electron temperature, ion temperature and plasma temperature.

For bactericidal effects of DBDJ higher technique should be used to analyses such a flow cytometry for quantitative data. Bacterial Biofilms shall be used with confocal microscopy because bacteria biofilm in form do not live only in a single layer

but they live in form multilayer or agglomerate. Therefore, we need to perform more detailed analysis effects of DBDJ to bacterial and bacteria biofilm.

In cell cytotoxicity assay cells culture time lapse study should be used to observe cells, signaling for example every 6 hours. Moreover, other assay has to be analyzed such as oxidative stress assay, nitric oxide assay and Ki67 proliferation assay; and if possible, imaging flow cytometry shall be used.

REFERENCES

Boost, M. V., O'Donoghue, M. M. & James, A. 2008. Prevalence of Staphylococcus aureus carriage among dogs and their owners. **Epidemiol Infect**, 136(7), 953-964.

Braithwaite, N. S. J. 2000. Introduction to gas discharges. **Plasma Sources Science and Technology**, 9(10.

Cai Yi-xi, Zhang Le-fu, Wang Jun, Rran Dong-li & Jing, W. 2010. Measuring DBD main discharge parameters using Q-V Lissajous figures. **Asia-Pacific Power and Energy Engineering Conference**.

Daeschlein, G., Scholz, S., Ahmed, R., von Woedtke, T., Haase, H., Niggemeier, M., Kindel, E., Brandenburg, R., Weltmann, K. D. & Juenger, M. 2012. Skin decontamination by low-temperature atmospheric pressure plasma jet and dielectric barrier discharge plasma. **J Hosp Infect**, 81(3), 177-183.

Dobrynin, D., Fridman, G., Friedman, G. & Fridman, A. 2009. Physical and biological mechanisms of direct plasma interaction with living tissue. **New Journal of Physics**, 11(11), 115020.

Etufugh, C. N. & Phillips, T. J. 2007. Venous ulcers. **Clin Dermatol**, 25(1), 121-130.

Fergie, J. E., Shema, S. J., Lott, L., Crawford, R. & Patrick, C. C. 1994. Pseudomonas aeruginosa Bacteremia in Immunocompromised Children: Analysis of Factors Associated with a Poor Outcome. **Clinical Infectious Diseases**, 18(3), 390-394.

Fridman, G., Brooks, A. D., Balasubramanian, M., Fridman, A., Gutsol, A., Vasilets, V. N., Ayan, H. & Friedman, G. 2007. Comparison of Direct and Indirect Effects of Non-Thermal Atmospheric-Pressure Plasma on Bacteria. **Plasma Processes and Polymers**, 4(4), 370-375.

Fridman, G., Friedman, G., Gutsol, A., Shekhter, A. B., Vasilets, V. N. & Fridman, A. 2008. Applied Plasma Medicine. **Plasma Processes and Polymers**, 5(6), 503-533.

Guo, J., Huang, K. & Wang, J. 2015. Bactericidal effect of various non-thermal plasma agents and the influence of experimental conditions in microbial inactivation: A review. **Food Control**, 50(482-490.

Harry, J. 2010. **Introduction to Plasma Technology**. Singapore: Fabulous Printers Pte Ltd.

Heinlin, J., Morfill, G., Landthaler, M., Stolz, W., Isbary, G., Zimmermann, J. L., Shimizu, T. & Karrer, S. 2010. Plasma medicine: possible applications in dermatology. **J Dtsch Dermatol Ges**, 8(12), 968-976.

Hofmann, S. 2013. **Atmospheric pressure plasma jets : characterisation and interaction with human cells and bacteria**. Technische Universiteit Eindhoven: Eindhoven : Technische Universiteit Eindhoven, 2013

Joaquin, J. C., Kwan, C., Abramzon, N., Vandervoort, K. & Brelles-Marino, G. 2009. Is gas-discharge plasma a new solution to the old problem of biofilm inactivation? **Microbiology**, 155(Pt 3), 724-732.

K. Wiesemann. 2013. A Short Introduction to Plasma Physics. **CERN Yellow Report CERN**.

Kang S. K., Kim H. Y., Yun G. S. & K., L. J. 2015. Portable microwave air plasma device for wound healing. **Plasma Sources Science and Technology**, 24(3), 035020.

Kang, S. K., Kim, H. Y., Yun, G. S. & Lee, J. K. 2015. Portable microwave air plasma device for wound healing. **Plasma Sources Science and Technology**, 24(3).

Kim, S. J., Chung, T. H. & Bae, S. H. 2009. Characteristic study of atmospheric pressure microplasma jets with various operating conditions. **Thin Solid Films**, 517(14), 4251-4254.

Kolb, J. F., Mohamed, A. A. H., Price, R. O., Swanson, R. J., Bowman, A., Chiavarini, R. L., Stacey, M. & Schoenbach, K. H. 2008. Cold atmospheric pressure air plasma jet for medical applications. **Applied Physics Letters**, 92(24), 241501.

Kong, M. G., Kroesen, G., Morfill, G., Nosenko, T., Shimizu, T., van Dijk, J. & Zimmermann, J. L. 2009. Plasma medicine: an introductory review. **New Journal of Physics**, 11(11), 115012.

Laroussi, M. 2002. Nonthermal decontamination of biological media by atmospheric-pressure plasmas: review, analysis, and prospects. **IEEE Transactions on Plasma Science**, 30(4), 1409-1415.

Laroussi, M., Kong, M. G., Morfill, G. & Stolz, W. 2012. **Plasma Medicine**. Cambridge University Press

Laroussi, M., Mendis, D. A. & Rosenberg, M. 2003. Plasma interaction with microbes. **New Journal of Physics**, 5(41-41.

Lin, Z. H., Tschang, C. Y. T., Liao, K. C., Su, C. F., Wu, J. S. & Ho, M. T. 2016. Ar/O2 Argon-Based Round Atmospheric-Pressure Plasma Jet on Sterilizing Bacteria and Endospores. **IEEE Transactions on Plasma Science**, 44(12), 3140-3147.

Mai-Prochnow, A., Bradbury, M., Ostrikov, K. & Murphy, A. B. 2015. Pseudomonas aeruginosa Biofilm Response and Resistance to Cold Atmospheric Pressure Plasma Is Linked to the Redox-Active Molecule Phenazine. **PLoS One**, 10(6), e0130373.

Mai-Prochnow, A., Clauson, M., Hong, J. & Murphy, A. B. 2016. Gram positive and Gram negative bacteria differ in their sensitivity to cold plasma. **Sci Rep**, 6(38610.

Mohd Nasir, N., Lee, B. K., Yap, S. S., Thong, K. L. & Yap, S. L. 2016. Cold plasma inactivation of chronic wound bacteria. **Arch Biochem Biophys**, 605(76-85.

Mott-Smith, H. M. 1971. History of "plasmas". **Nature**, 233(5316), 219.

Nojiri, K. (2015). Mechanism of Dry Etching. In **Dry Etching Technology for Semiconductors** (pp. 11-30).

Park, J., Henins, I., Herrmann, H. W. & Selwyn, G. S. 2001. Gas breakdown in an atmospheric pressure radio-frequency capacitive plasma source. **Journal of Applied Physics**, 89(1), 15.

Petinaki, E. & Spiliopoulou, I. 2012. Methicillin-resistant Staphylococcus aureus among companion and food-chain animals: impact of human contacts. **Clin Microbiol Infect**, 18(7), 626-634.

Rehman, M. U., Jawaid, P., Uchiyama, H. & Kondo, T. 2016. Comparison of free radicals formation induced by cold atmospheric plasma, ultrasound, and ionizing radiation. **Arch Biochem Biophys**, 605(19-25.

Schutze, A., Jeong, J. Y., Babayan, S. E., Jaeyoung, P., Selwyn, G. S. & Hicks, R. F. 1998. The atmospheric-pressure plasma jet: a review and comparison to other plasma sources. **IEEE Transactions on Plasma Science**, 26(6), 1685-1694.

Setsuhara, Y. 2016. Low-temperature atmospheric-pressure plasma sources for plasma medicine. **Arch Biochem Biophys**, 605(3-10.

Strateva, T. & Yordanov, D. 2009. Pseudomonas aeruginosa - a phenomenon of bacterial resistance. **J Med Microbiol**, 58(Pt 9), 1133-1148.

Suschek, C. V. & Opländer, C. 2016. The application of cold atmospheric plasma in medicine: The potential role of nitric oxide in plasma-induced effects. **Clinical Plasma Medicine**, 4(1), 1-8.

Vatansever, F., de Melo, W. C., Avci, P., Vecchio, D., Sadasivam, M., Gupta, A., Chandran, R., Karimi, M., Parizotto, N. A., Yin, R., Tegos, G. P. & Hamblin, M. R. 2013. Antimicrobial strategies centered around reactive oxygen species--bactericidal antibiotics, photodynamic therapy, and beyond. **FEMS Microbiol Rev**, 37(6), 955-989.

Vollmer, W., Blanot, D. & de Pedro, M. A. 2008. Peptidoglycan structure and architecture. **FEMS Microbiol Rev**, 32(2), 149-167.

von Woedtke, T., Reuter, S., Masur, K. & Weltmann, K. D. 2013. Plasmas for medicine. **Physics Reports**, 530(4), 291-320.

Yaopromsiri, C., Yu, L. D., Sarapirom, S., Thopan, P. & Boonyawan, D. 2015. Effect of cold atmospheric pressure He-plasma jet on DNA change and mutation. **Nuclear Instruments and Methods in Physics Research Section B: Beam Interactions with Materials and Atoms**, 365(399-403.

Zhang, J., Wang, X., Vikash, V., Ye, Q., Wu, D., Liu, Y. & Dong, W. 2016. ROS and ROS-Mediated Cellular Signaling. **Oxid Med Cell Longev**, 2016(4350965.

APPENDIX

APPENDIX A

PLASMA PROPERTIES

A.1 Electrical properties

DBDJ was operated at high voltage dc pulse 20 kHz (DBDJ), flow rate of He gas at 1 L/min and repetition rate 50 Hz to 110 Hz or plasma dissipated power from 0.27 W to 0.50 W. The high voltage waveform was determined using a high-voltage probe (Tektronix, P6015A). The plasma dissipated power was estimated by Lissajous figure method or Q-V plot. Where the discharge charge was estimated from the voltage across the 1 nF capacitor measured by a HV probe (Hantek, T3100) show in Figure A1 and Figure A2 shown plasma glow discharge of DBDJ during experiment.

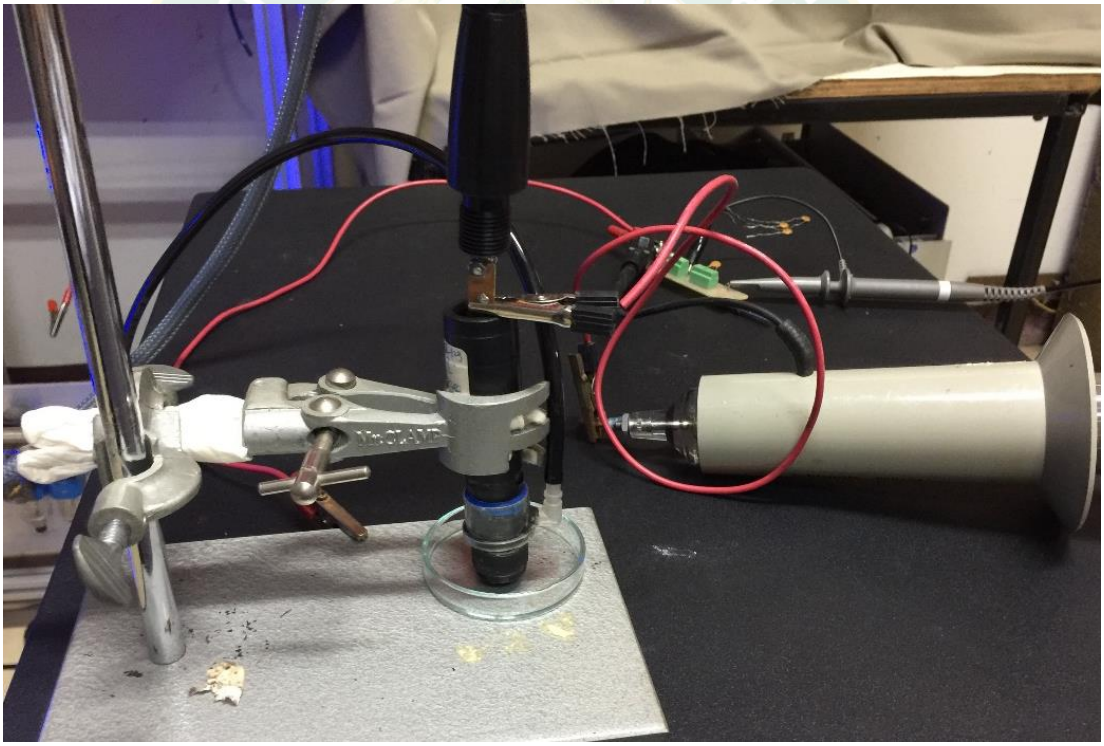

Figure A1 Experiment setup.

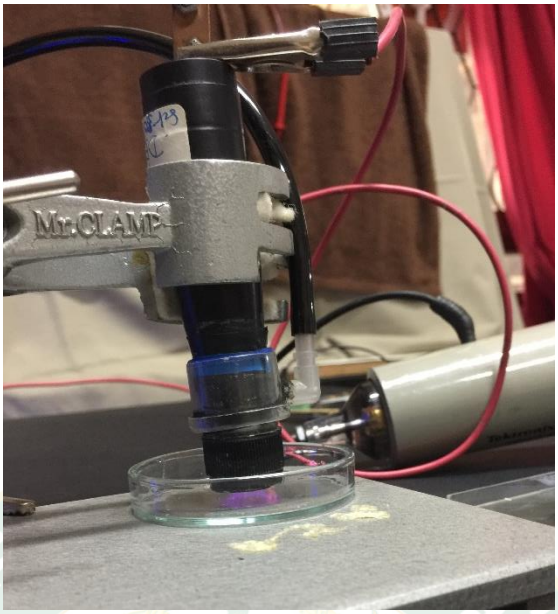

Figure A2 Plasma glow discharge.

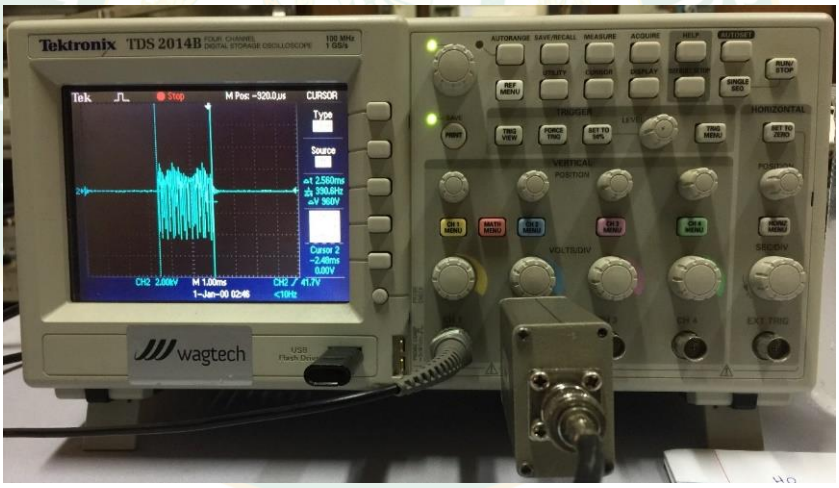

Figure A3 Oscilloscope.

First, save data (duty cycle, frequency, I-V graph and Q-V graph) from oscilloscope and export graph into USB. The raw data from oscilloscope show in Figure A4 to Figure A6 and used this data for calculated plasma dissipated power in Table A1. When value of channel 1, channel 2, capacitor and frequency inside are constant. The relative between repetition rate at 50 Hz to 110 Hz and plasma dissipated power shown in Figure A7.

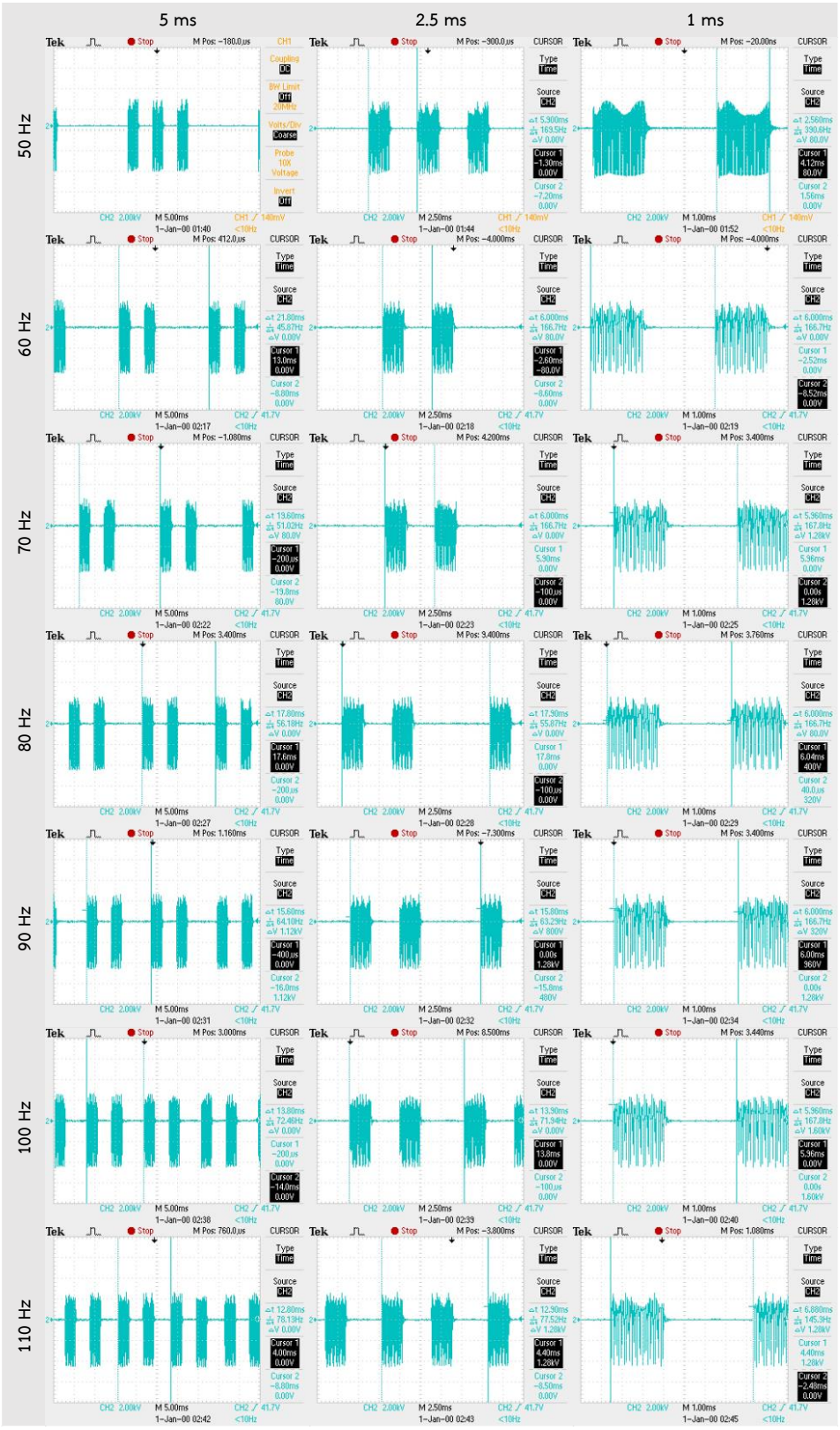

Figure A4 The duty cycle of DBDJ at repetition rate 50 Hz to 110 Hz or plasma dissipated power 0.27 W to 0.50 W with time at 5 ms, 2.5 ms and 1 ms.

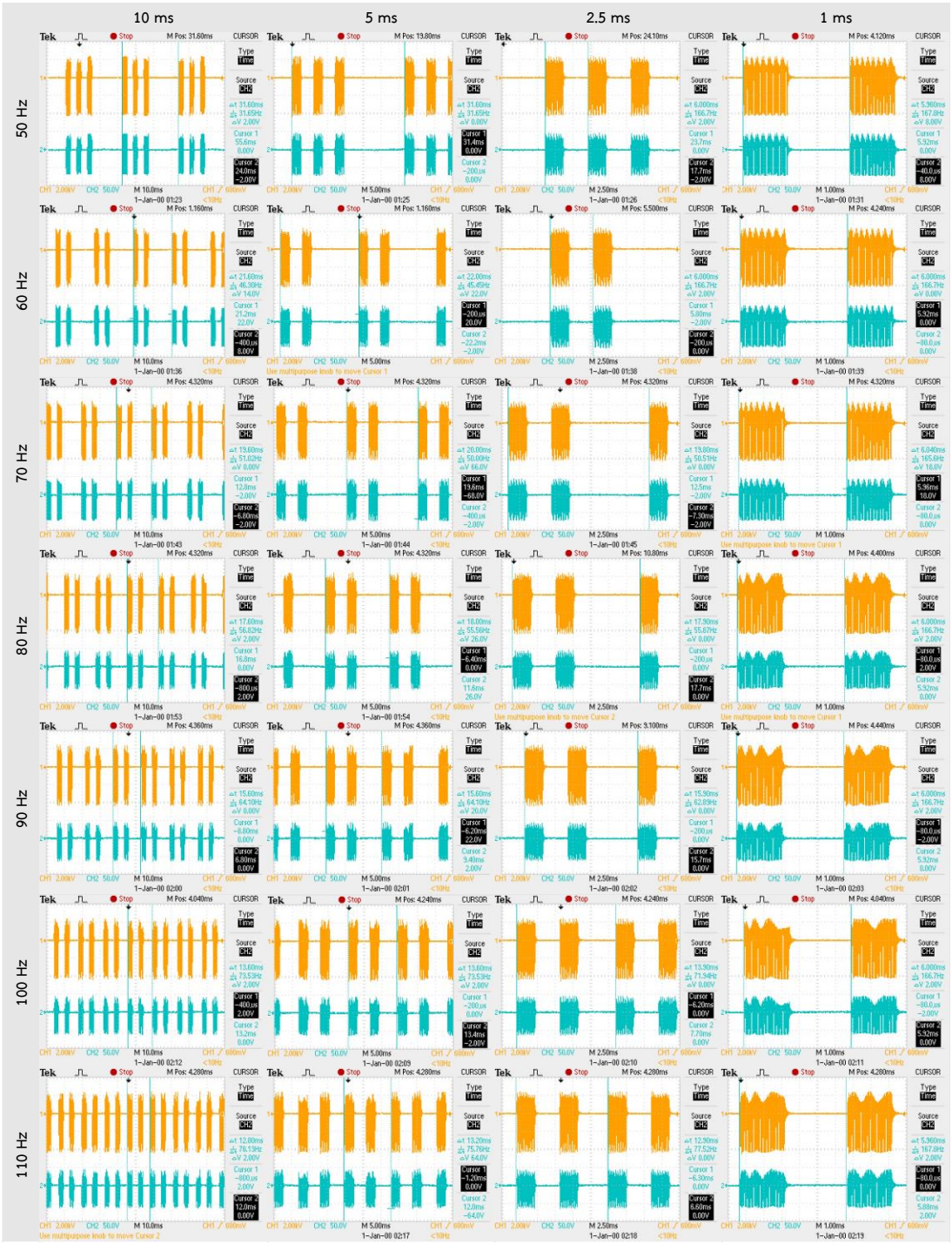

Figure A5 The Lissajous figure of DBDJ at repetition rate 50 Hz to 110 Hz or plasma dissipated power 0.27 W to 0.50 W with time at 10 ms, 5 ms, 2.5 ms and 1 ms.

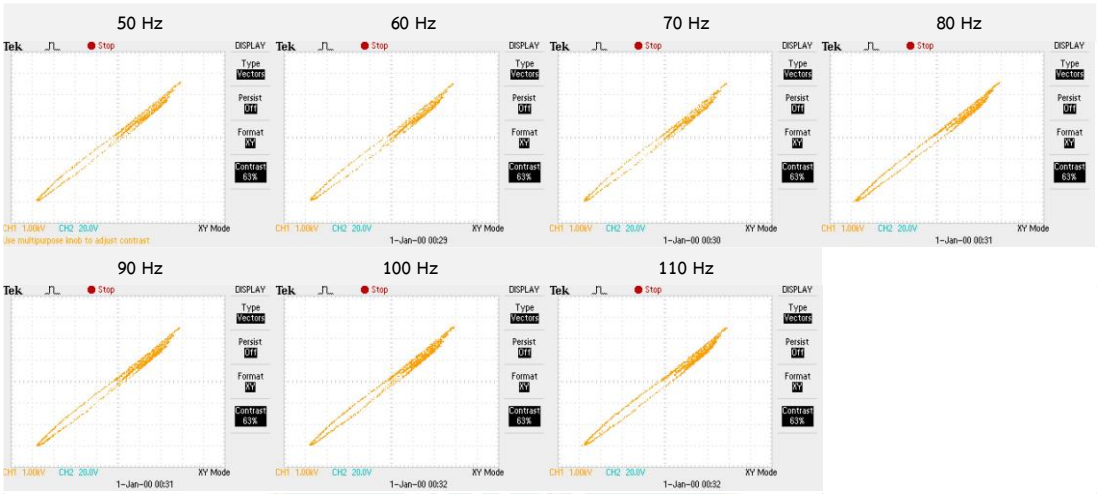

Figure A6 The Lissajous figure of DBDJ at repetition rate 50 Hz to 110 Hz.

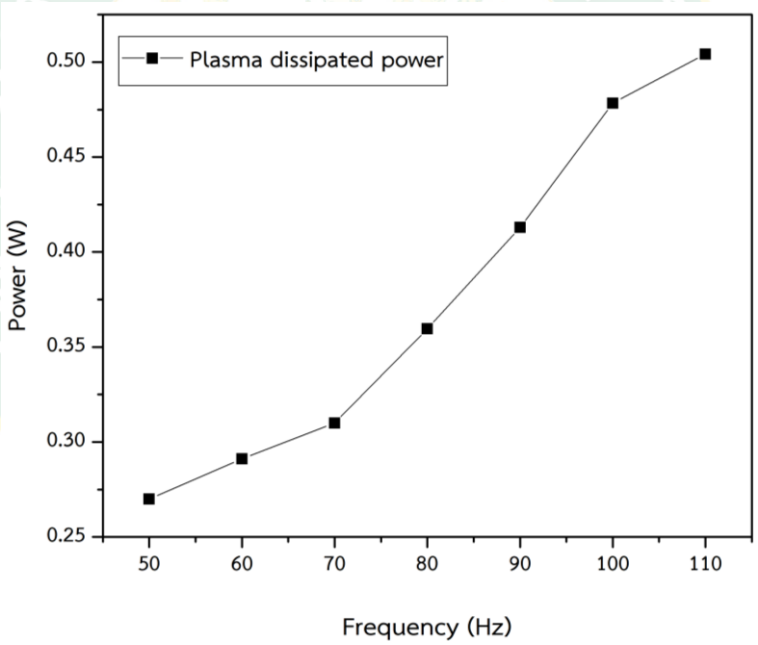

Figure A7 Increasing of plasma dissipated power influenced by repetition rate at 50 Hz to 110 Hz.

Table A1 Plasma dissipated power of DBDJ.

Channel1	*f* (Hz)	Area average	Energy per Cycle (E)	Delta T (ms)	Single Loop (ms)	Number of loop	Total loop (ms)	Duty cycle	Power (W)
1000 V	50	3.085	0.0000617	31.6	2.5	3	7.5	0.237	0.27
Channel2	60	3.070	0.0000614	22.0	2.5	2	5	0.227	0.29
20 V	70	2.961	0.0000592	20.0	2.5	2	5	0.250	0.31
Capacitor	80	3.175	0.0000635	18.0	2.5	2	5	0.278	0.36
1 nf	90	3.393	0.0000679	15.6	2.5	2	5	0.321	0.41
Frequency	100	3.523	0.0000705	13.6	2.5	2	5	0.368	0.48
20 kHz	110	3.244	0.0000649	13.2	2.5	2	5	0.379	0.50

A.2 Reactive Oxygen Nitrogen Species (RONS)

The emission spectrum of RONS and other radicals in plasma was detected by fiber optic spectrometer led light emission spectra of plasma into system by CCD is detector. CCD change light emission spectra signal to digital signal shows on computer display by program controller AvaSoft version 7.4. After saved OES data open file with Microsoft Excel, copy data to plot graph and mark peaks in OriginPro 2016. The emission spectra of the plasma dissipated power at 0.27 W to 0.50 W show in Figure A8 to Figure A14.

Table A2 Intensity RONS of DBD at plasma dissipated power 0.27 W to 0.50 W.

Power (W)	NO (297.61 nm)	OH (308.99 nm)	N_2 (337.54 nm)	N_2 (357.62 nm)
0.27	92.75	142.75	3805.75	2454.75
0.29	129.50	169.00	4564.00	3000.00
0.31	203.00	292.00	6436.25	4245.25
0.36	355.50	430.75	9282.75	5934.75
0.41	363.75	477.75	10362.75	6602.75
0.48	428.25	459.75	12956.75	8417.75
0.50	515.25	529.75	14035.00	9479.75

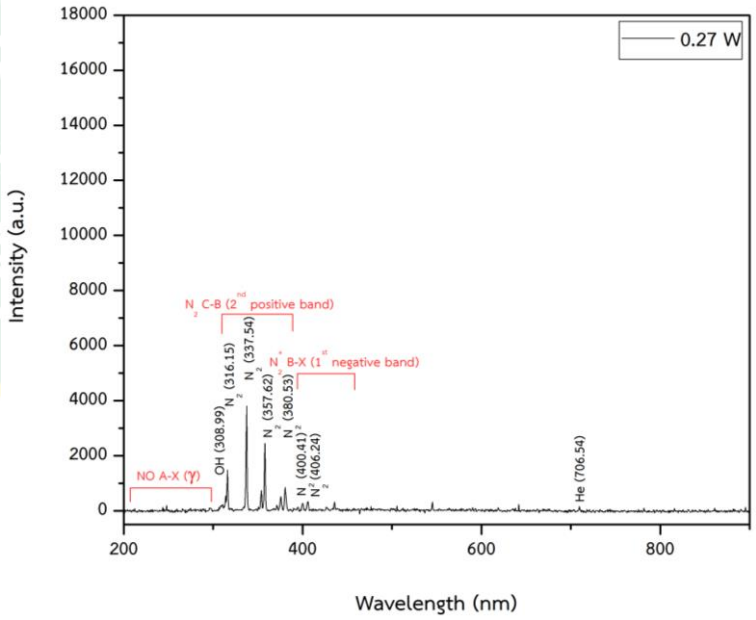

Figure A8 The emission spectra of the plasma dissipated power at 0.27 W.

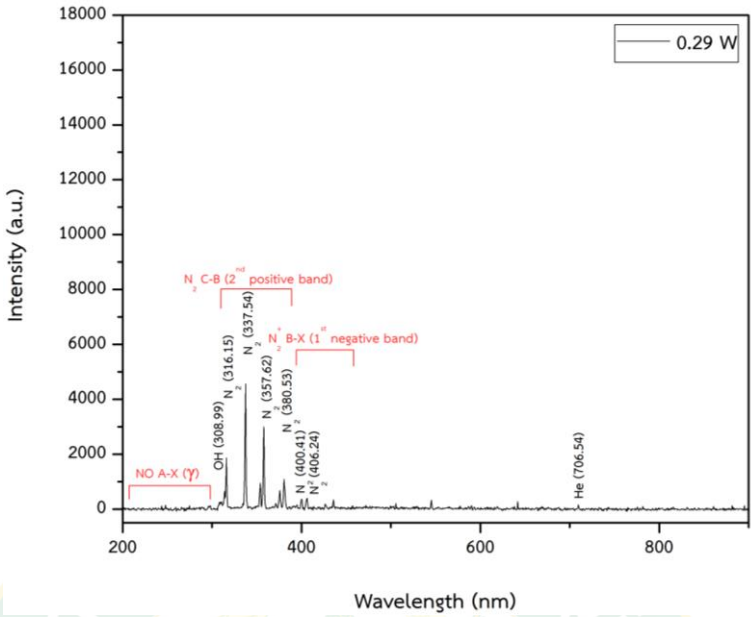

Figure A9 The emission spectra of the plasma dissipated power at 0.29 W.

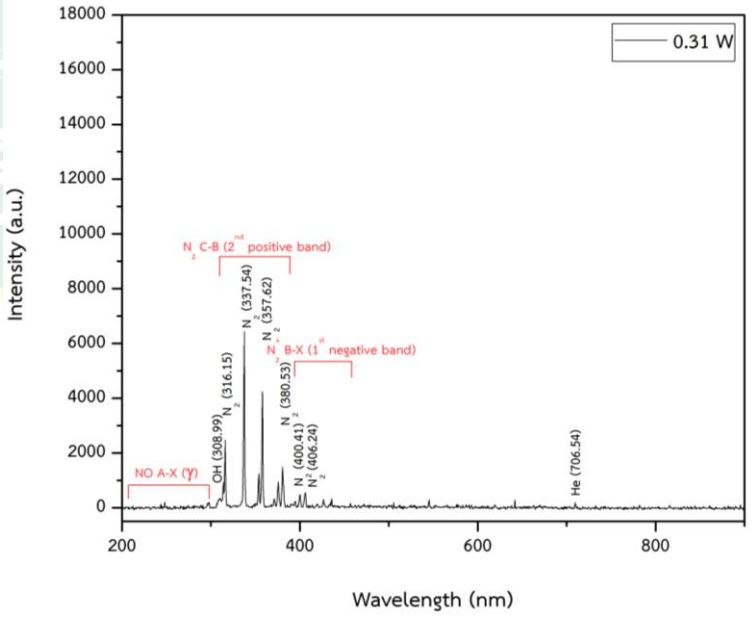

Figure A10 The emission spectra of the plasma dissipated power at 0.31 W.

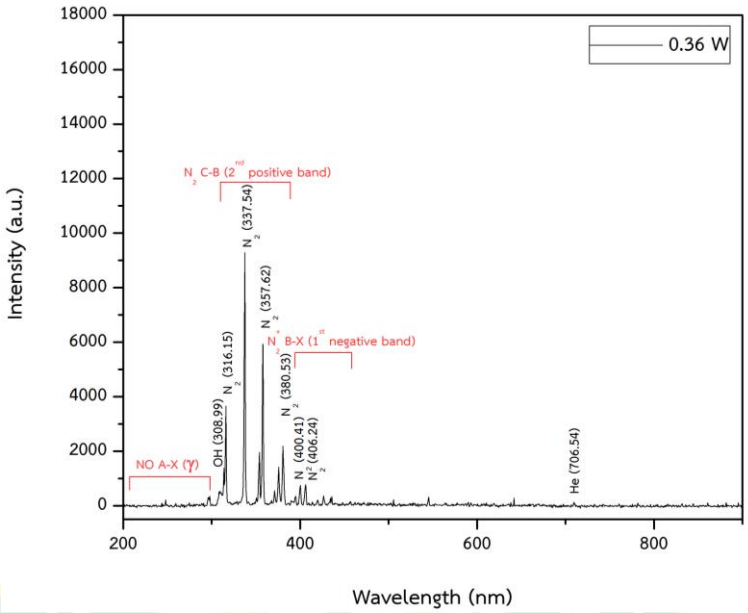

Figure A11 The emission spectra of the plasma dissipated power at 0.36 W.

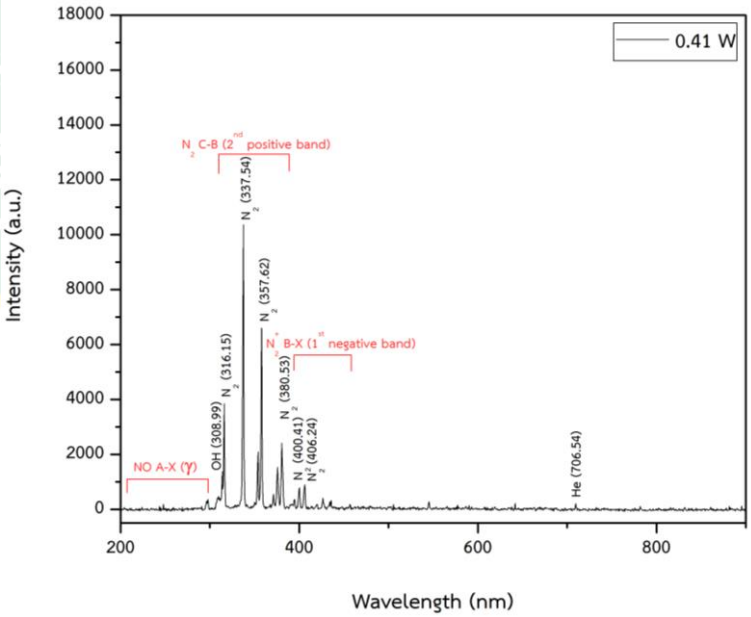

Figure A12 The emission spectra of the plasma dissipated power at 0.41 W.

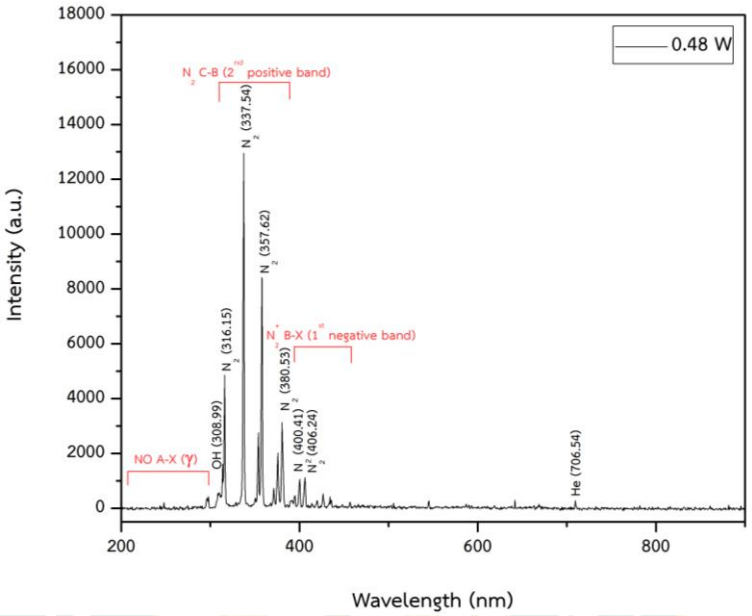

Figure A13 The emission spectra of the plasma dissipated power at 0.48 W.

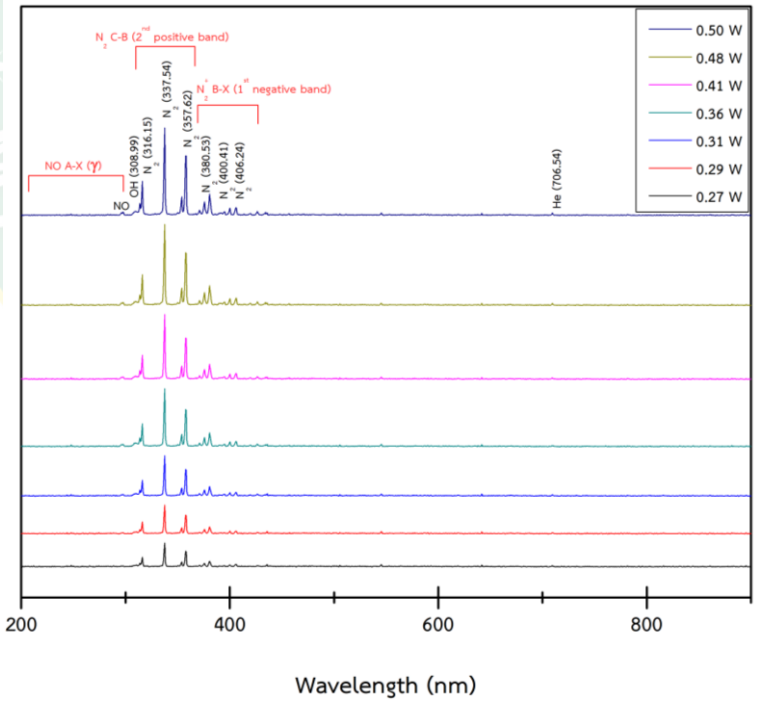

Figure A14 The emission spectra of DBDJ with plasma dissipated power 0.27 W to 0.50 W.

Table A3 Concentration of NO and O_3 at plasma dissipated power 0.27 W to 0.50 W.

Power (W)	NO (ppm)	O_3 (ppm)
0.27	1.17	0.10
0.29	1.42	0.14
0.31	2.03	0.20
0.36	2.85	0.25
0.41	3.46	0.30
0.48	4.32	0.36
0.50	5.14	0.40

APPENDIX B

BACTERICIDAL

B.1 Bacteria preparation

Samples of *Staphylococcus aureus* (*S. aureus*) TISTR 2329 and *Pseudomonas aeruginosa* (*P. aeruginosa*) TISTR 2370 were obtained from Thailand Institute of Scientific and Technological Research (TISTR). The sample bacteria of *S. aureus* and *P. aeruginosa* bacteria were grown in 5 mL Nutrient Broth (NB) in the meantime orbital shaker 150 rpm in incubator at 37 °C for 24 h to obtain a bacterial density of approximately 1×10^{7} to 1×10^{8} CFU/mL. Next 24 h was used serial dilution to 10^{-4} for *S. aureus* and *P. aeruginosa* before prepared in Nutrient Agar (NA). Then prepared *S. aureus* and *P. aeruginosa* was used spread plate method with 200 uL for DBDJ experiment. After that DBDJ treatment *S. aureus* and *P. aeruginosa* incubated at 37 °C for 24 h and investigate result of DBDJ treatment by used Colony Forming unit (CFU) method to counted.

B.2 Bactericidal

The result after plasma expose on bacteria (*S. aureus* and *P. aeruginosa*) show in Figure B1 and B2. Table B1 and Table B2 show percentage efficiency bactericidal of DBDJ. The percentage efficiency bactericidal *S. aureus* and *P. aeruginosa* with plasma dissipated power at 0.27 W and 0.50 W show in Figure B3.

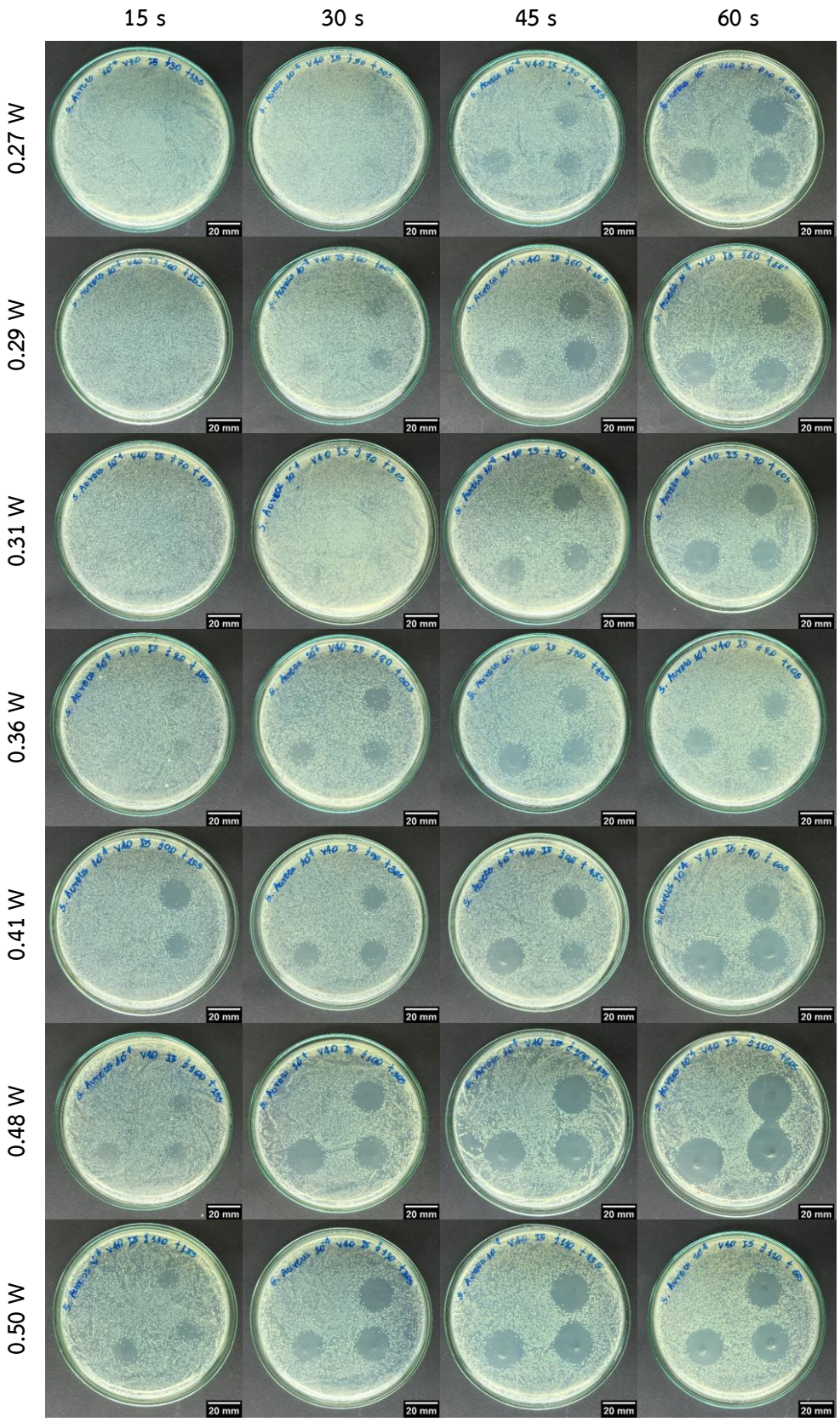

Figure B1 *S. aureus* after exposure by DBDJ.

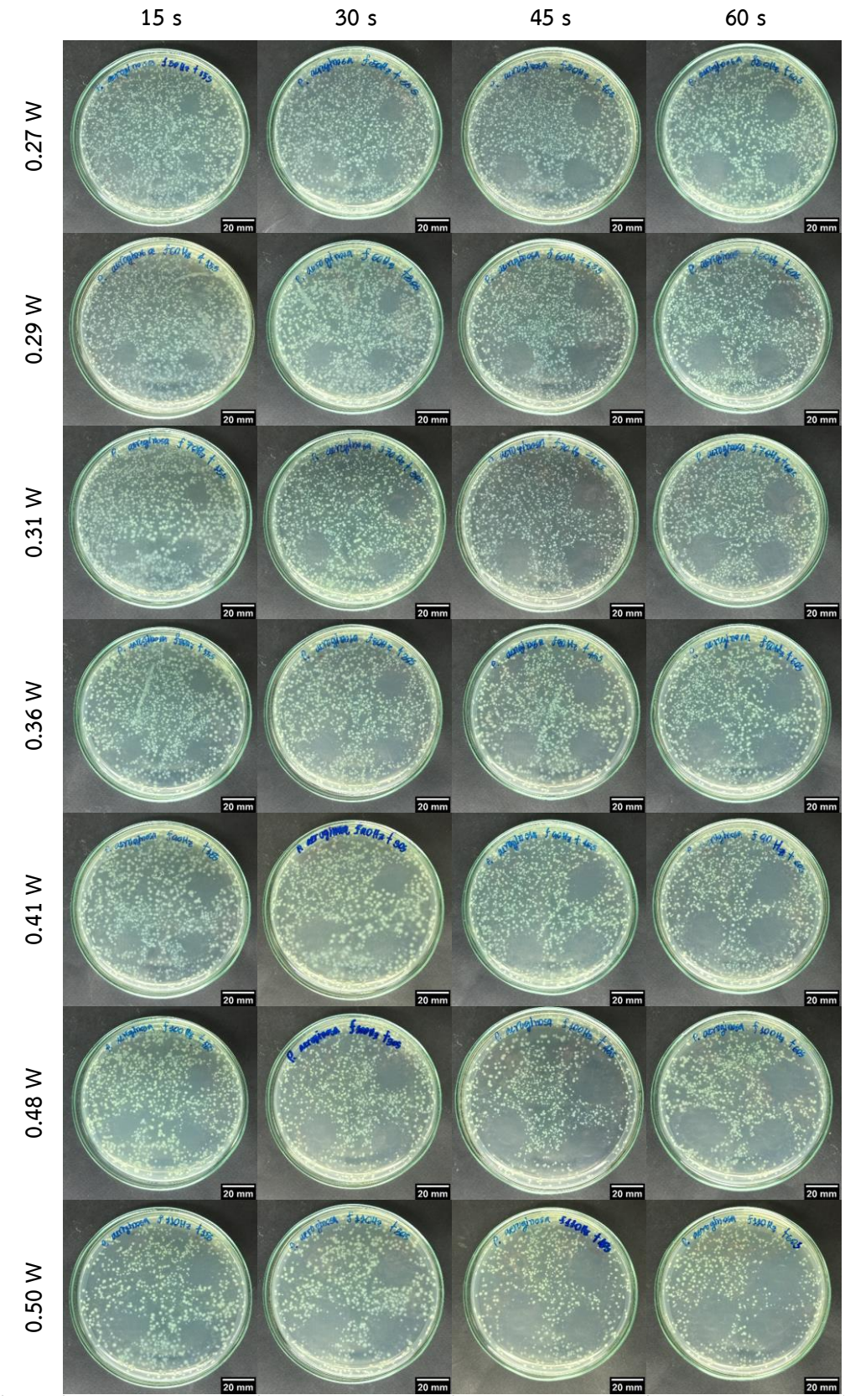

Figure B2 *P. aeruginosa* after exposure by DBDJ.

Table B1 Percentage of Efficiency bactericidal *S. aureus* by DBDJ.

Power (W)	Time 15 s	Time 30 s	Time 45 s	Time 60 s
0.27	8.0	13.1	29.0	78.1
0.29	9.2	18.3	63.3	79.0
0.31	12.3	24.4	64.2	84.2
0.36	14.4	51.5	67.3	85.4
0.41	36.2	53.1	76.2	94.5
0.48	39.3	82.3	92.2	100.0
0.50	41.0	84.0	92.9	100.0

Table B2 Percentage of Efficiency bactericidal *P. aeruginosa* by DBDJ.

Power (W)	Time 15 s	Time 30 s	Time 45 s	Time 60 s
0.27	40.2	47.5	60.4	72.1
0.29	45.1	56.0	66.3	79.6
0.31	48.4	61.4	69.2	81.0
0.36	56.5	61.5	73.0	89.5
0.41	59.7	69.0	82.2	96.6
0.48	60.6	71.9	90.2	100.0
0.50	65.8	79.4	93.0	100.0

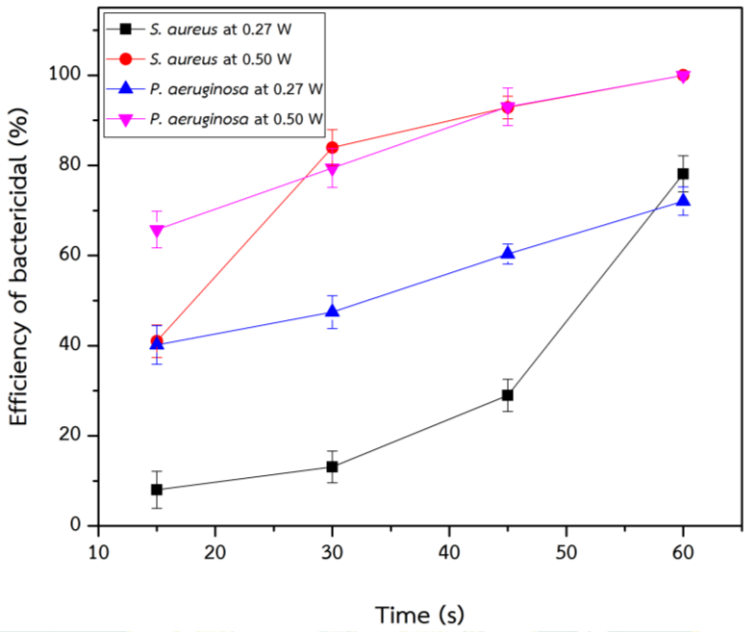

Figure B3 The percentage efficiency bactericidal *S. aureus* and *P. aeruginosa* with plasma dissipated power at 0.27 W and 0.50 W.

APPENDIX C

BACTERIA BIOFILM

C.1 Bacteria biofilm preparation

The bacterial biofilms both of *S. aureus* and *P. aeruginosa* were prepared in NB, after incubated at 37 ℃ for 24 h to have density of approximately $1x10^7$ to $1x10^8$ CFU/mL. Prepare 12 mm sterilized coverslip glass in 12-well plate with 0.1% of gelatin in Phosphate Buffered Saline (PBS 1X, pH 7.4) 30 min at 4 ℃ for coated before use. After 30 min, removed solution, wait for coverslip glass dry and then add bacteria to 12-well plate at 1 mL/well. The bacteria samples were incubated at 37 ℃ for 48 h and NB had to be changed every 24 h. After 48 h removed NB, plasma exposure on bacteria samples was carried out at plasma dissipated 0.50 W and exposure time 60 s. Live/Dead assay method with double stain Hoechst 33342 and Propidium iodide (PI) was used to monitored immediately after treatment. Prepared double stain HO/PI dilute in deionized water to 1 ug/mL and add 200 uL on coverslip glass incubated at 37 ℃ for 30 min to activate double stain HO/PI avoid exposing to light. After incubated was removed solution, wash PBS 2 times and plate coverslip glass on cleaned microscope slide with BosterBio antifade mounting medium 20 uL. Performance of DBDJ to destroy bacteria biofilm was observed by Olympus BX51 fluorescence microscope show in Figure C.1. The magnification for bacteria biofilm image at 1000x was used oil immersion lens with ZEISS Immersion Oil 518 N. For fluorescent imaging of HO/PI have to take at the same spot by used different laser source to activated HO/PI stains. In case of HO have ability to bind both of live and dead cell was used ultraviolet excitation at 405 nm, after emission spectrum maximum at 461 nm in blue fluorescence. In case of PI was used for bind with DNA stain only dead cell and PI cannot cross the membrane of live cells, used laser wavelength 488 nm to excitation and emission maximum at 617 nm in red fluorescence. After saved both of HO/PI image, export file, customize the image color in ACDSee Photo Studio Ultimate 2018 and merge or overlap two images by ImageJ-win64 program.

Figure C1 Olympus BX51 fluorescence microscope.

C.2 Fluorescence image processing

Export JPEG file from computer, customize the image color in ACDSee Photo Studio Ultimate 2018 by adjust Exposure, Highlight Enhancement, Fill light, Contrast, Saturation and Vibrance show in Figure C2 to Figure C5. After optimize both of fluorescent image and save image. Then, open 2 image in ImageJ-win64 program, merge 2 image by Image/Color/Merge Channels and the Merge Channels box will appear. Select the fluorescent images in the appropriate R, G and B channels and the DIC or similar image in gray channel. Select “Create Composite”, click “OK” and save picture show in Figure C6 to Figure C9.

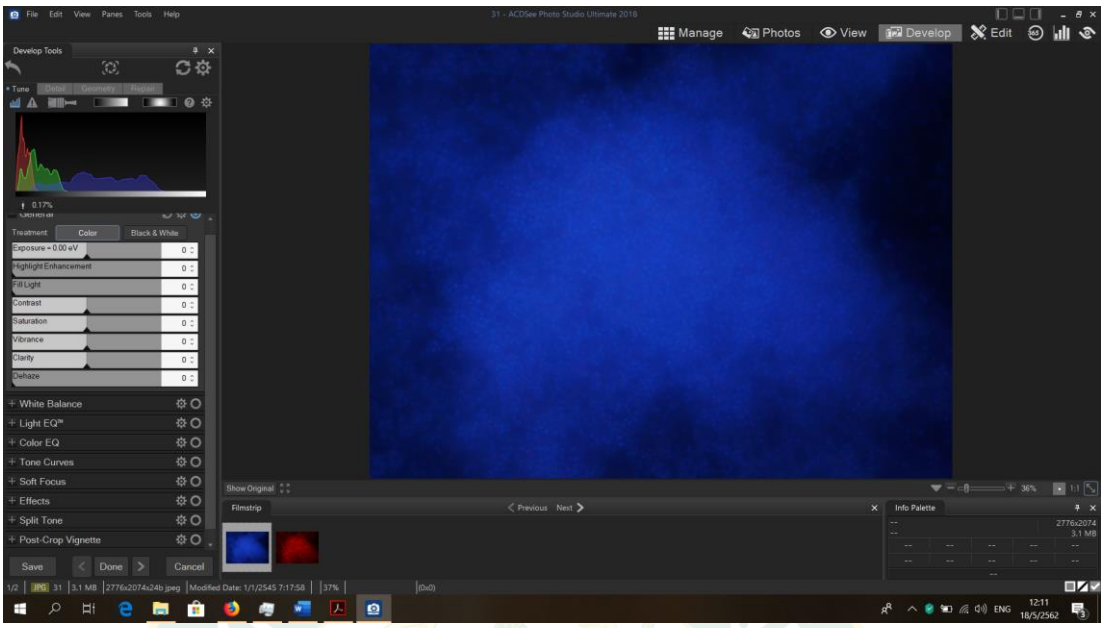

Figure C2 Before customize the image color by ACDSee Photo Studio Ultimate 2018.

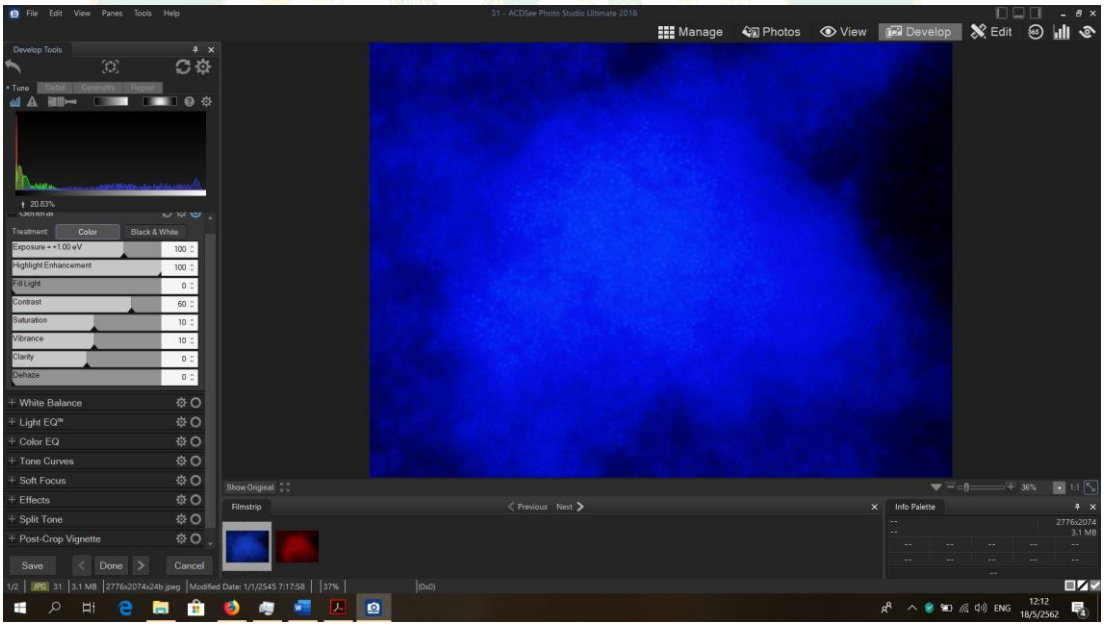

Figure C3 After customize the image color by ACDSee Photo Studio Ultimate 2018.

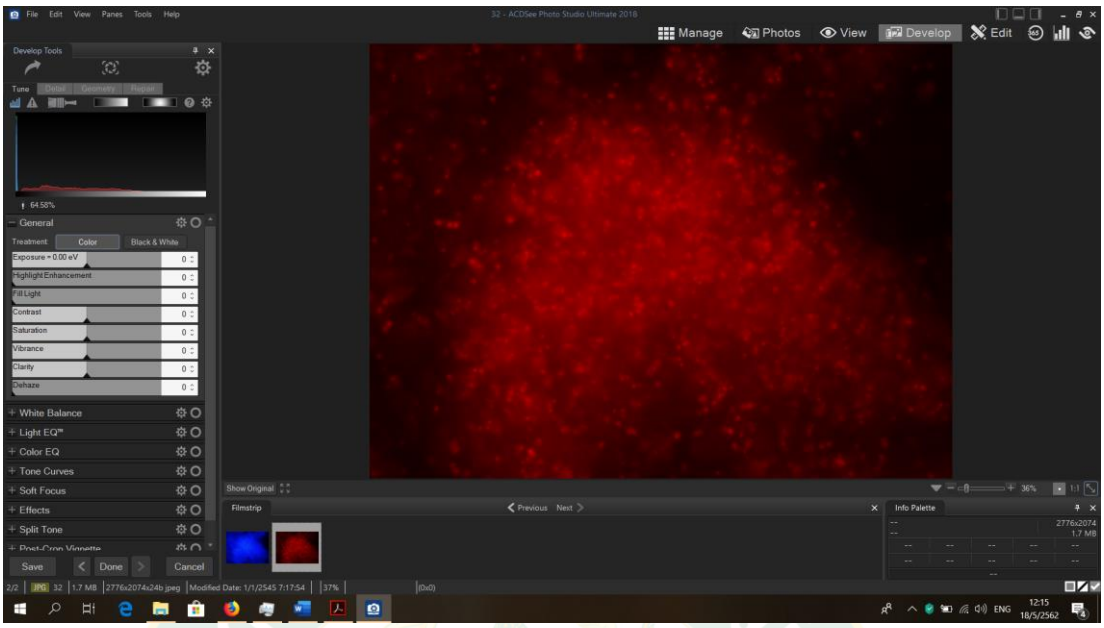

Figure C4 Before customize the image color by ACDSee Photo Studio Ultimate 2018.

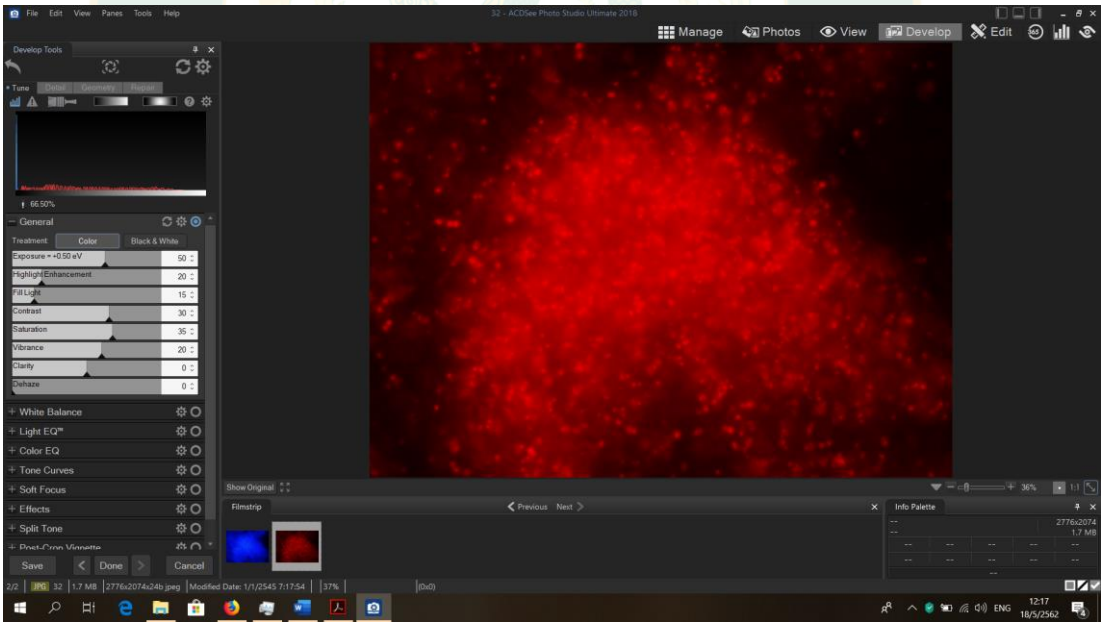

Figure C5 After customize the image color by ACDSee Photo Studio Ultimate 2018.

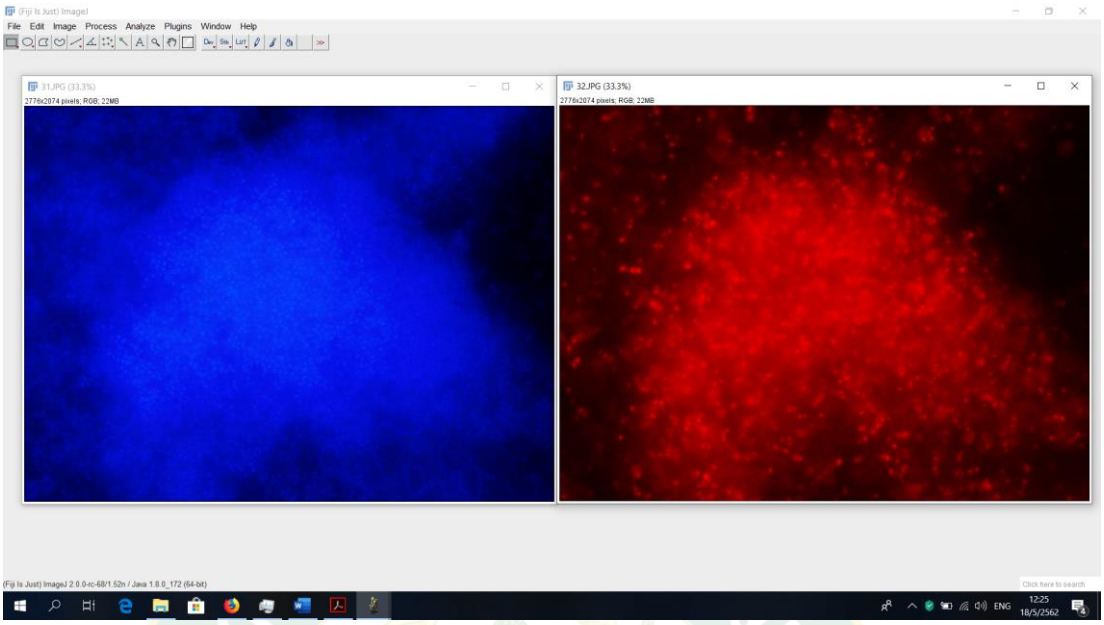

Figure C6 Open image in ImageJ-win64 program.

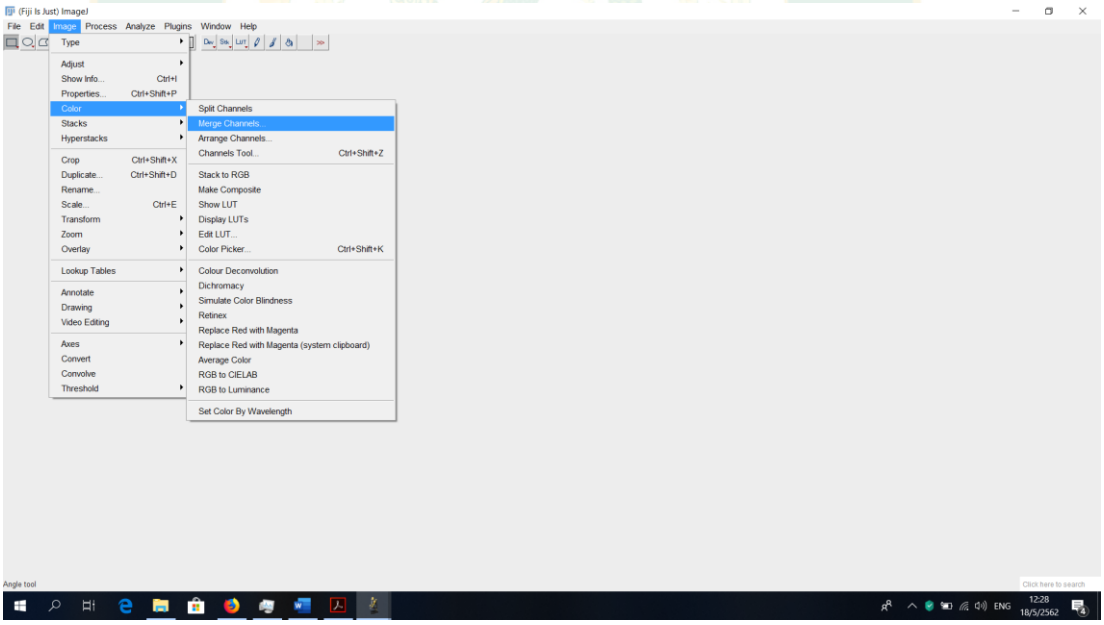

Figure C7 Merge image by Image/Color/Merge Channels and the Merge Channels box.

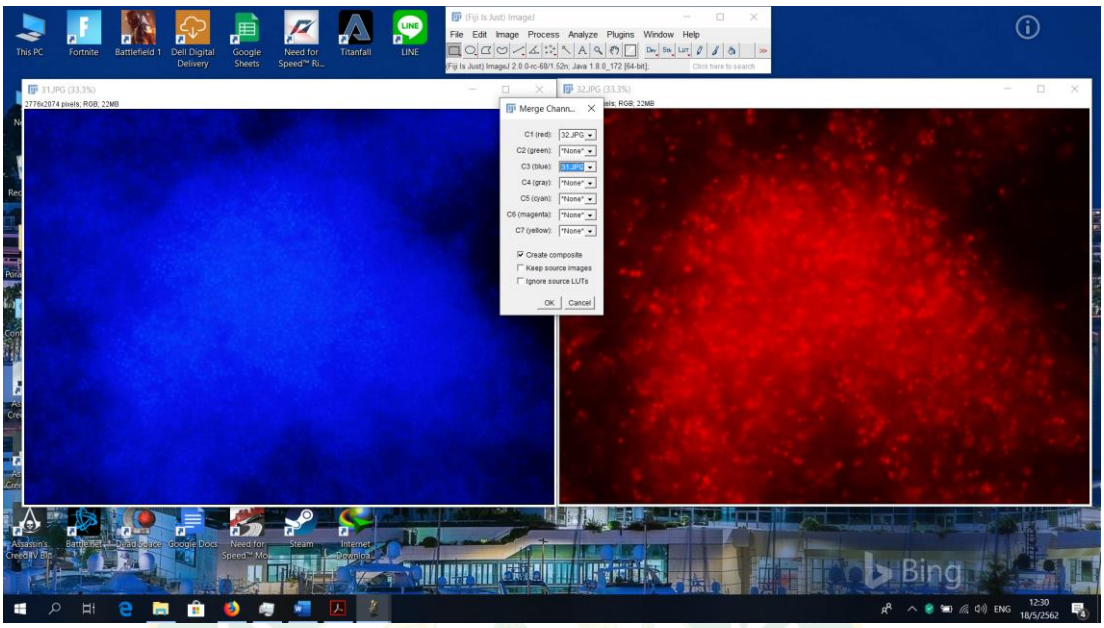

Figure C8 Select the fluorescent images in the appropriate R, G and B channels.

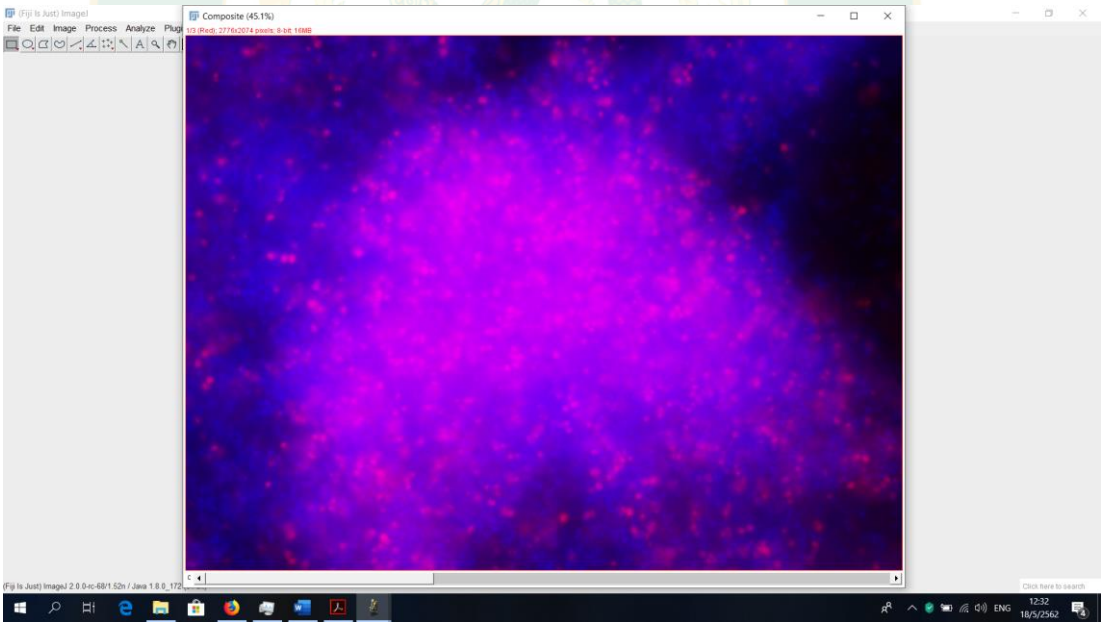

Figure C9 After merge 2 image.

APPENDIX D

CELL CULTURE

D.1 Cell culture

Human Dermal Fibroblasts, adult (HDFa) cells Cat. no. C-013-5C purchased from Cascade Biologics™ invitrogen cell culture (GIBCO invitrogen cell culture). Primary human dermal fibroblasts are isolated from adult skin, cryopreserved at the end of the primary culture. Morphology of HDFa cells are spindle-shaped (cells are bipolar and refractile) and passage of HDFa cell for experimented not more than passage 12. Before plasma exposure, HDFa cells were have 70-80% confluence, media cover around 2 mm. and gab between DBDJ and cells at 5 mm.

HDFa cells were cultured in 10% Fetal Bovine Serum (FBS) with Dulbecco's Modified Eagle Medium (DMEM) high glucose supplemented and Antibiotic-Antimycotic (1X) - Thermo Fisher Scientific (Thermo Fisher Scientific, Inc., Waltham, MA, USA) in a humidified atmosphere containing 95% air/5% CO2 at 37°C. HDFa cells were grown to 70-80% confluence, before removed media and washed by Phosphate Buffered Saline (PBS 1X, pH 7.4) 2 times, harvested by add 1 mL (T-25 flask) or 2 mL (T-75 flask) 0.025% trypsin-EDTA (Thermo Fisher Scientific, Inc.) in PBS incubated for 5 min 95% air/5% CO_2 at 37°C. Add complete media (DMEM+10%FBS), after trypsinization and move cell suspension to tube 15 mL for centrifuge. After centrifuge at 1,000 rpm 7 min was removed media, add fresh media seed cells to 6-well plate at volume 2 mL/well for flowcytometry and 12-well plate at volume 1 mL/well on coverslip glass diameter 10 mm. for Live/Dead assay, HDFa cell had confluence 25-30% and changed media every 48 h. Then HDFa cells before experiment were have confluence, 70-80%.

D.2 Live/Dead assay

After DBDJ experiment was removed media and add 200 uL double stain HO/PI diluted (1 ug/mL in deionized water) on coverslip glass incubated at 37 °C for 30 min to activate double stain HO/PI avoid exposing to light. After incubated was removed solution, washed by PBS 2 times and plate coverslip glass on cleaned microscope slide

with BosterBio antifade mounting medium 20 uL. Live/dead assay of HDFa cell was observed by Olympus BX51 fluorescence microscope. The fluorescent image of HDFa cells were used magnification at 200x and 400x. For fluorescent imaging of HO/PI have to take at the same spot but used different laser source to excitation HO/PI stains. After saved both of HO/PI image, export file, customize the image color in ACDSee Photo Studio Ultimate 2018 and merge or overlap two images by ImageJ-win64 program same as bacteria biofilm (Fluorescence image processing).

D.3 Muse Cell Analyzer

The Muse Cell Analyzer uses miniaturized fluorescence detection and microcapillary cytometry to deliver single-cell analysis, which is highly quantitative especially when compared with traditional bulk methods like microscopy and Western blot. The system delivers high-performance cell analysis using a microcapillary technology and miniaturized optics which occupy one-tenth the space of a typical cytometer. Laser-based fluorescence detection of each cell event can evaluate up to 3 cellular parameters. The Muse Cell Analyzer uses miniaturized fluorescent detection and microcapillary technology to deliver truly accurate, precise, quantitative cell analysis compared to other methods. Laser-based fluorescence detection of each cell event can evaluate up to 3 cellular parameters – cell size (forward scatter) and 2 colors (detected in the red and/or yellow channels). The Muse Cell Analyzer show in Figure D1.

Figure D1 Muse Cell Analyzer.

D.4 Muse Count & Viability Assay

The Muse™ Count & Viability Reagent allows the quantitative analysis of cell count and viability on the Muse™ Cell Analyzer. It is a rapid and reliable alternative to trypan blue exclusion. The Muse™ Count & Viability Reagent provides absolute cell count and viability data on cell suspensions from a variety of cultured mammalian cell lines. Both viable and non-viable cells are differentially stained based on their permeability to the DNA-binding dyes in the reagent. Data generated with the Muse™ Count & Viability Software Module provides: viable cell count (cells/mL), total cell count (cells/mL) and % viability of sample.

D.5 Staining Protocol of Muse Count & Viability Assay

1. Prepare a uniform cell suspension for counting. Be sure adherent cells are completely removed from flasks and are well mixed. NOTE: Accurate cell counting requires the even distribution of the cells within suspensions. Gently but thoroughly mix all suspensions during all dilution and staining steps and before loading samples onto the system for analysis. Do not vortex samples vigorously as sample can splash out, resulting in erroneous cell counts.

2. Prepare stained cell samples by mixing cells with Muse™ Count & Viability Reagent in a sample tube. Accurate cell counting occurs at a concentration range of 1 x 10^4 cells/mL to 5 x 10^5 cells/mL in the stained sample.

- If you know the approximate concentration of the original cell suspension, refer to the following table as a dilution guide.

Table D1 Cell Suspension Dilution Table (recommended volumes).

Concentration of Original Cell Suspension	Dilution Factor	Cell Suspension Volume	Count & Viability Reagent Volume	Concentration of Diluted Cells
$1x10^5$ to $1x10^6$ cells/mL	10	50 uL	450 uL	$<1x10^5$ cells/mL
$1x10^6$ to $1x10^7$ cells/mL	20	20 uL	380 uL	$<5x10^5$ cells/mL
$1x10^7$ to $2x10^7$ cells/mL	40	20 uL	780 uL	$<5x10^5$ cells/mL

- If you do not know the approximate concentration of your original cell suspension, prepare a stained cell sample by mixing with Muse™ Count & Viability Reagent at a 20-

fold dilution (for example, 20 uL of cell suspension into 380 uL of Count & Viability Reagent).

- If the original concentrations are >2 x 10^7 cells/mL, then results are out of the measurement range. Samples can be prepared with an 80-fold dilution of the original cell suspension and reacquired. Or, the original cell sample can be diluted with PBS or media before repeating the assay with the guidelines above. In this case, be sure to account for both dilutions by multiplying the dilution factors. For example, if you dilute your original sample 1:10 with PBS, then dilute the sample 1:10 with Count & Viability reagent during sample preparation, the final dilution factor is 100.

- If the final concentration of the stained cell sample for data acquisition is too concentrated (>5 x 10^5 cells/mL), the cell count may not be accurate.

3. Allow the cells to stain for a minimum of 5 minutes. Run assay start at positive control, negative control, treatment control and plasma treatment respectively.

Table D2 Percentage of viability HDFa cells.

Conditions	%Viability	SD	N	SE
Negative control	97.30	1.09	3	0.63
Positive control	82.15	1.86	3	1.07
Treatment control	97.82	0.34	3	0.20
DBDJ at 0.5 W, 60 s	95.12	1.78	3	1.03

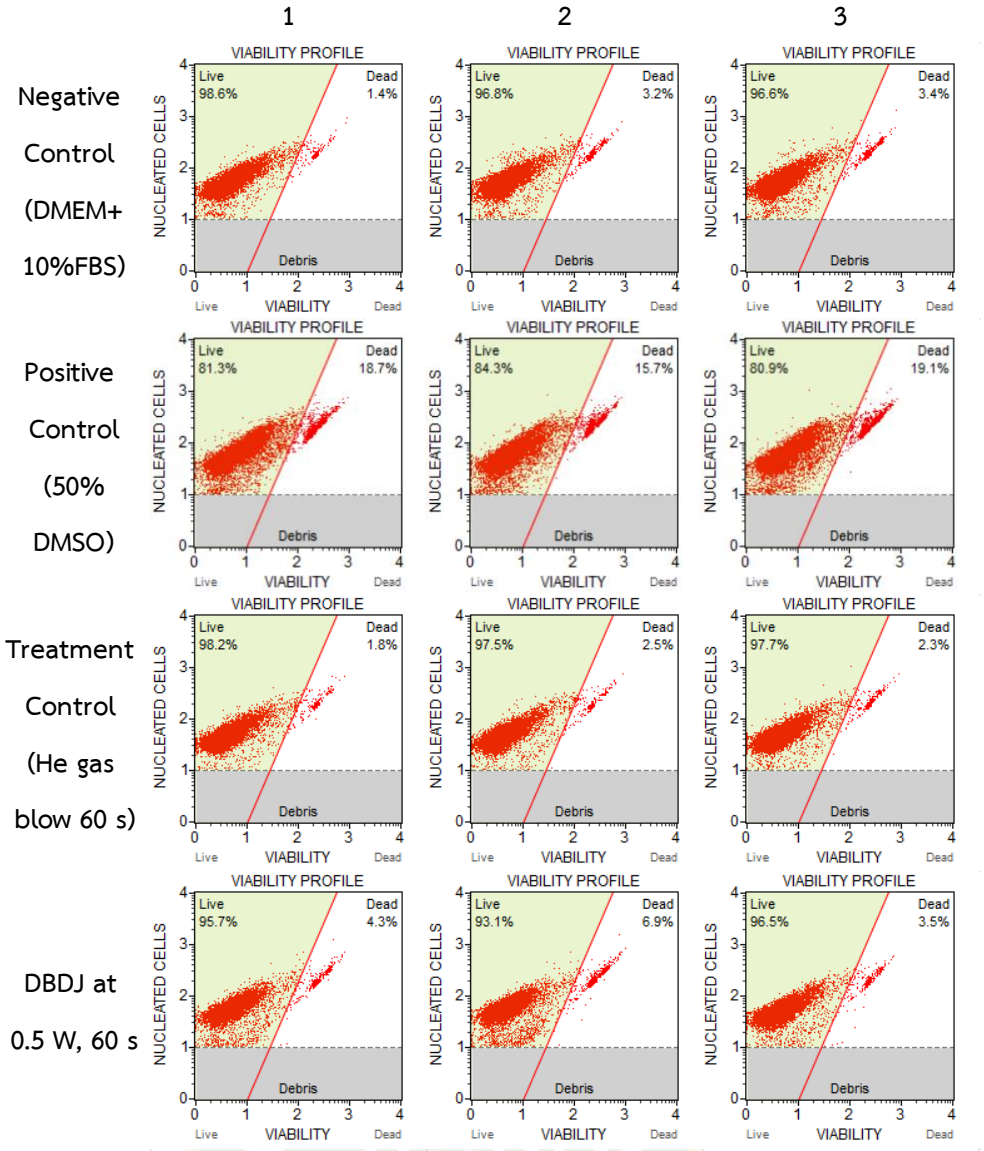

Figure D2 Muse Count & Viability profile.

D.6 Muse Annexin V and Dead Cell Assay

The Muse™ Annexin V & Dead Cell Assay allows for the quantitative analysis of live, early and late apoptosis, and cell death on both adherent and suspension cell lines on the Muse™ Cell Analyzer. Minimal sample preparation is required in this no-wash, mix-and-read assay to obtain accurate and precise results. The software provides: Concentrations (cells/mL) for live, early apoptotic, late apoptotic, total

apoptotic, and dead cells, Percentage of live, early apoptotic, late apoptotic, total apoptotic, and dead cells.

D.7 Staining Protocol of Muse Annexin V and Dead Cell Assay

1. Allow the Muse™ Annexin V & Dead Cell Reagent to warm to room temperature.

2. Add 100 uL of cells in suspension to each tube.

NOTE: You must have cells in suspension with at least 1% BSA, 1%, FBS, or 10% filtered NHS when performing this assay. Make sure to stain positive and negative controls.

3. Add 100 uL of the Muse™ Annexin V & Dead Cell Reagent to each tube.

NOTE: Should your induced cells express large amounts of PS, it may be necessary to add more reagent. You can add up to 150 uL of the Annexin V & Dead Cell Reagent to each tube. If you need to use more reagent for optimal staining, then it is better to decrease the volume of medium that the cells are in from 100 uL to 50 uL and add between 150 uL to 175 uL (up to 200 uL) of the reagent.

4. Mix thoroughly by pipetting up and down or vortexing at a medium speed for 3 to 5 seconds.

5. Stain samples for 20 minutes at room temperature in the dark. Then start assay at positive control, negative control, treatment control and plasma treatment respectively.

Table D3 Percentage of viability, apoptosis and dead cells.

Conditions	Live (LL)	Apoptotic (LR)	Apoptotic/ Dead (UR)	Dead (UL)	Total Apoptotic
Negative control	94.32	2.14	3.01	0.53	5.15
Positive control	50.57	3.80	42.75	2.87	46.56
Treatment control	95.34	1.93	2.33	0.40	4.26
DBDJ at 0.5 W, 60 s	90.99	4.03	4.52	0.46	8.55

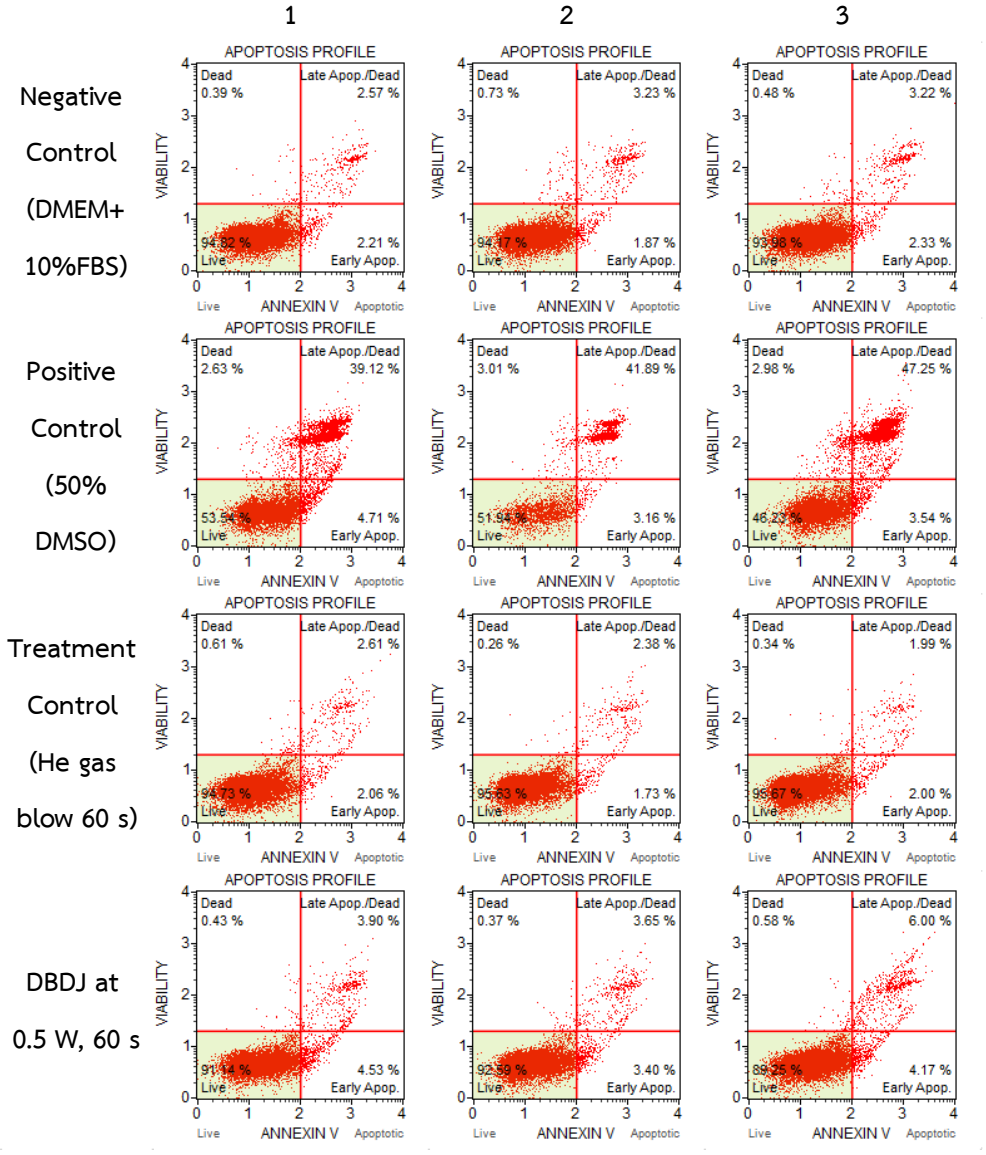

Figure D3 Muse Annexin V and Dead Cell profile.

D.8 Statistical analysis

After export PDF file report of Muse Count & Viability Assay or Muse Annexin V and Dead Cell Assay in Figure D4 and Figure D5, key data from report in Microsoft Excel 2016 and used for calculating mean, standard deviation (SD), number of test (n) and standard error (SE) in Figure D6. Next, export file from Microsoft Excel 2016 in form text file (.txt) by first column is condition number, mean, SD, n, and SE respectively in Figure D7. Then, were used R-program x64 ver.3.5.1 with R-Studio ver.1.1.456. Significant differences were evaluated by using repeated measures one-way ANOVA followed by an appropriate post hoc multiple comparison test (Tukey method). If result compared in each condition, one by one condition have P-value or probability value < 0.01-0.05 is significant mark * and < 0.01 is significantly mark ** in Figure D8 to Figure D11. Therefrom, plot graph data in R-Studio and export graph in form PDF file in Figure D12. Import graph pdf file into Adobe Illustrator CC for editing graph, labeling the X-Axis and Y-Axis, marking significant bar and adjusting graph scale in Figure D13. After editing graph finished save graph in form PDF and PNG file for reported.

07-Jul-2018 05:27:27 Muse Count & Viability 1.4

Acquisition Date and Time : 07-JUL-2018 05:15:03
Analysis Date and Time : 07-JUL-2018 05:15:03
Instrument Serial Number : 7200121308
FileName : HDFa P7 DBDJ 7jul18
Sample # : 7
Sample ID : Nature 1
Annotation :

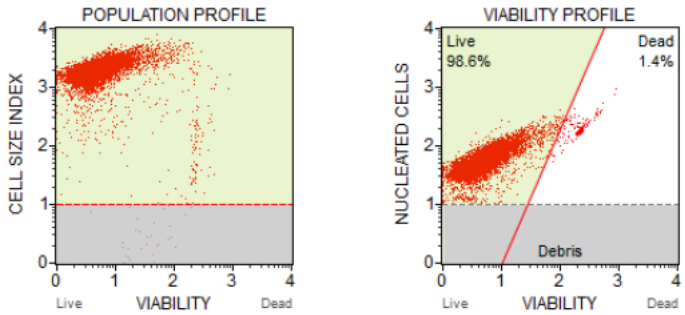

Viable Cells / mL :	1.06E+07
Viability % :	98.55 %
Total Cells / mL :	1.07E+07
Events Acquired :	10032
Dilution Factor :	20.00
Original Volume :	10.00 mL

Figure D4 PDF file report of Muse Count & Viability Assay.

18-Aug-2018 02:25:40 Muse Annexin V & Dead Cell 1.4

Acquisition Date and Time : 18-AUG-2018 02:03:51
Analysis Date and Time : 09-OCT-2066 20:58:40
Instrument Serial Number : 7200121308
FileName : HDFa P12 DBDJ re 18aug18
Sample # : 1
Sample ID : Nature1
Annotation :

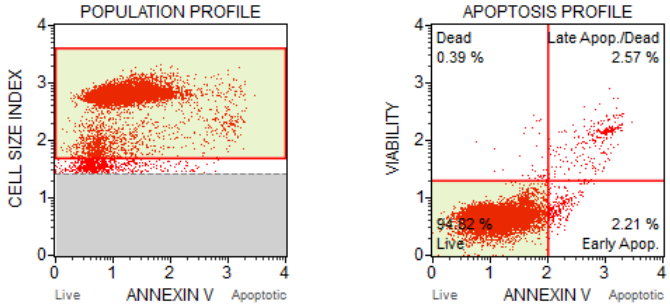

	Cell Conc. (Cells / mL)	% Gated
Live (LL) :	1.50E+06	94.82 %
Early Apoptotic (LR) :	3.50E+04	2.21 %
Late Apop./ Dead (UR) :	4.07E+04	2.57 %
Debris (UL) :	6.14E+03	0.39 %
Total Apoptotic :	7.56E+04	4.79 %

Figure D5 PDF file report of Muse Annexin V and Dead Cell Assay.

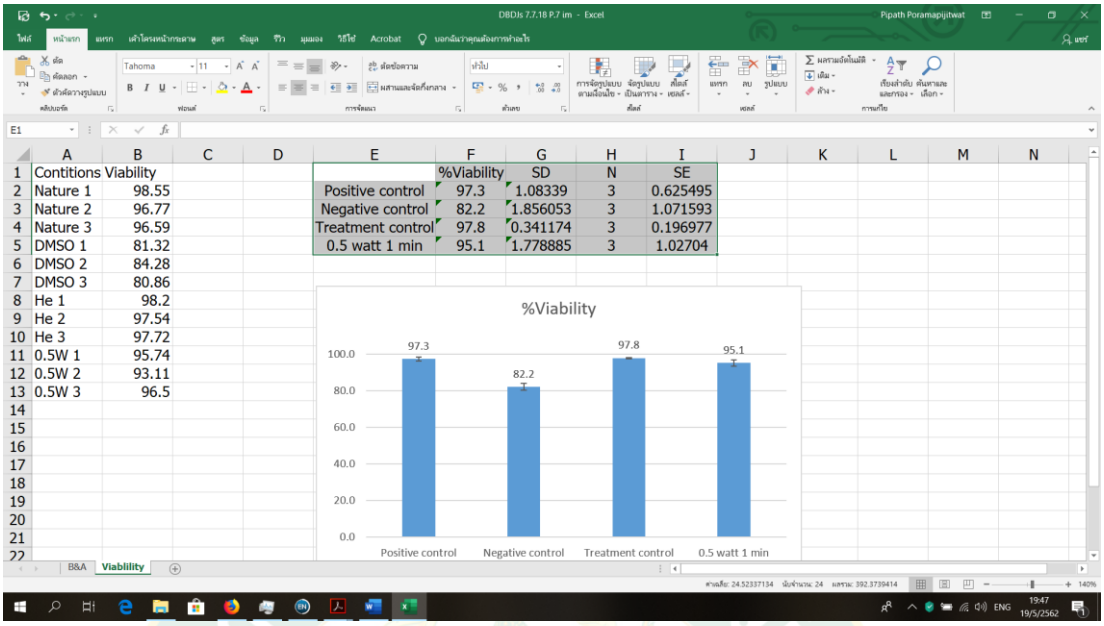

Figure D6 Calculating mean, standard deviation (SD), number of test (n) and standard error (SE) in Microsoft Excel.

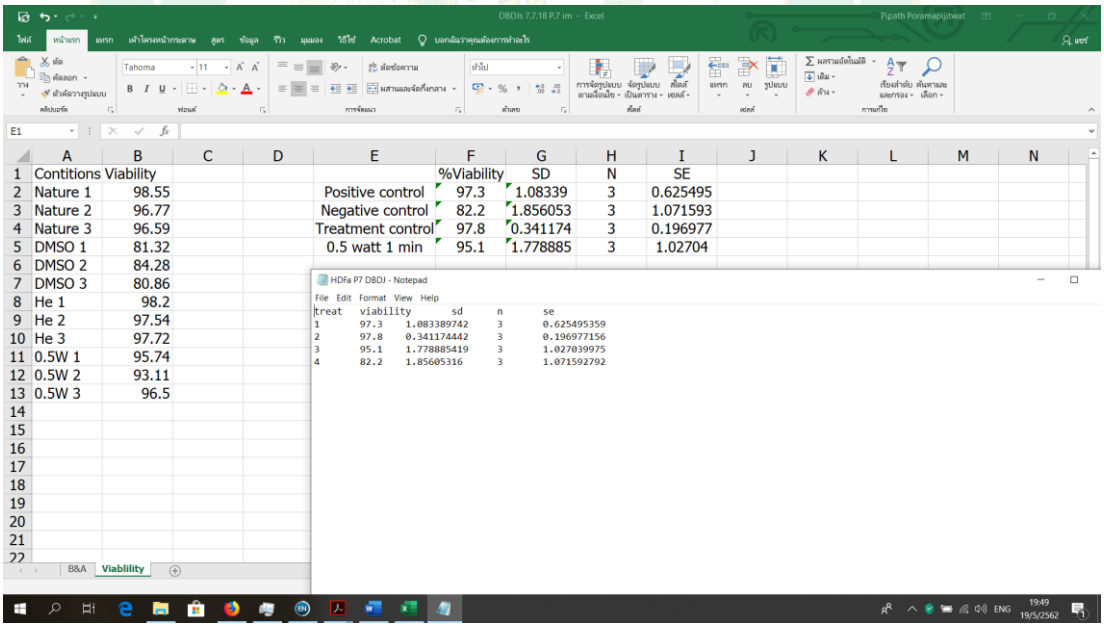

Figure D7 Move data to Notepad in file type.txt before analysis.

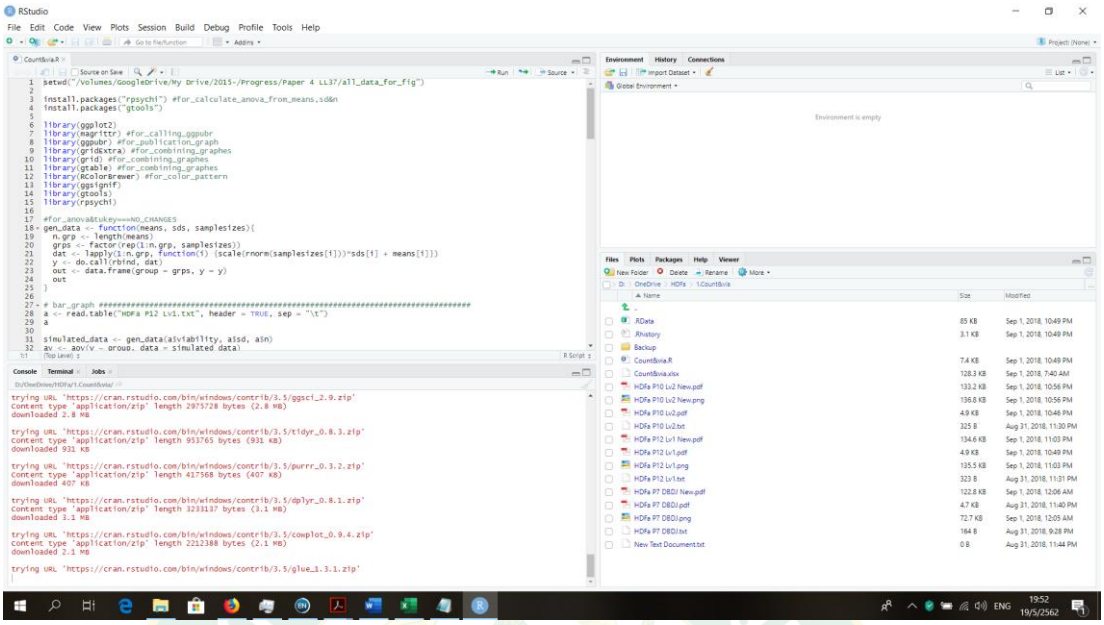

Figure D8 R-program x64 ver.3.5.1 with R-Studio ver.1.1.456.

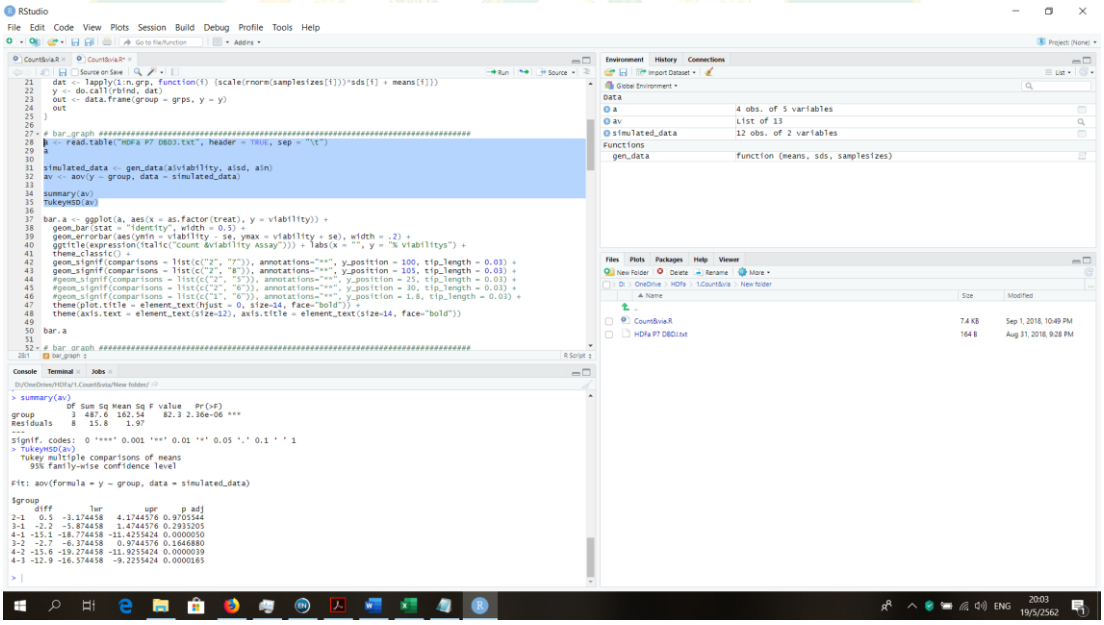

Figure D9 Run code in R-Studio.

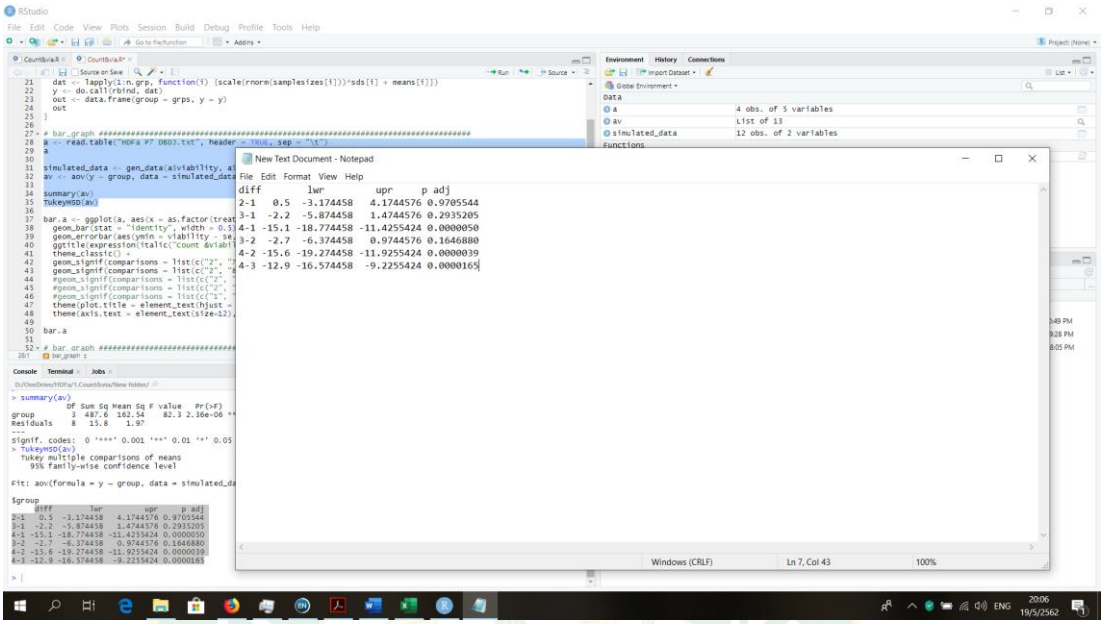

Figure D10 Compared *P*-value each other condition.

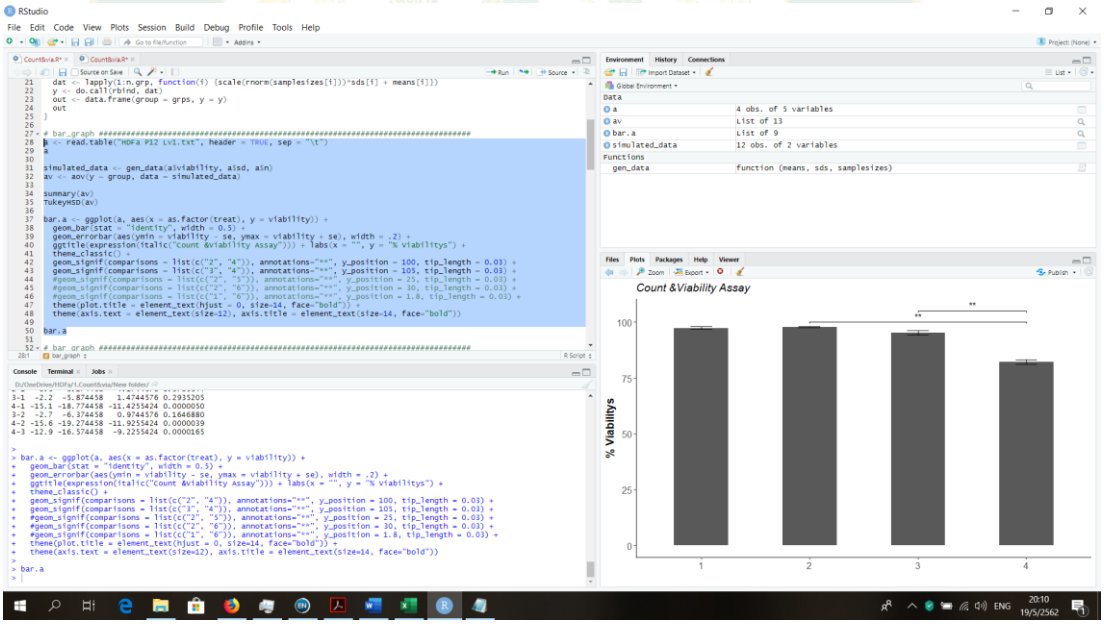

Figure D11 After compared condition mark significant bar and run code for plot graph.

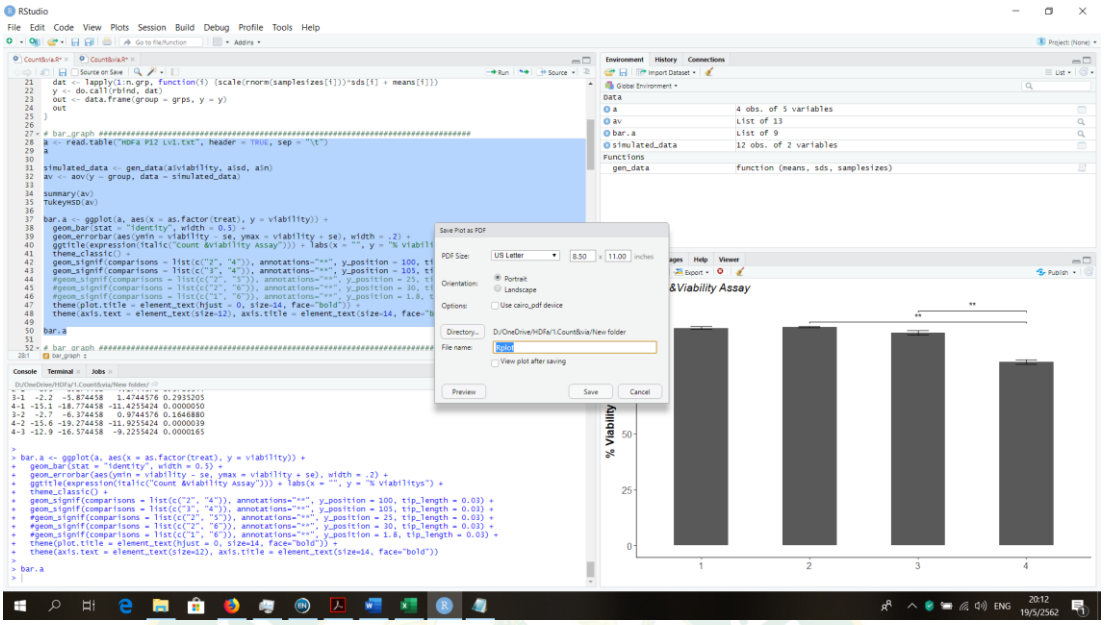

Figure D12 Export graph in PDF file for edit.

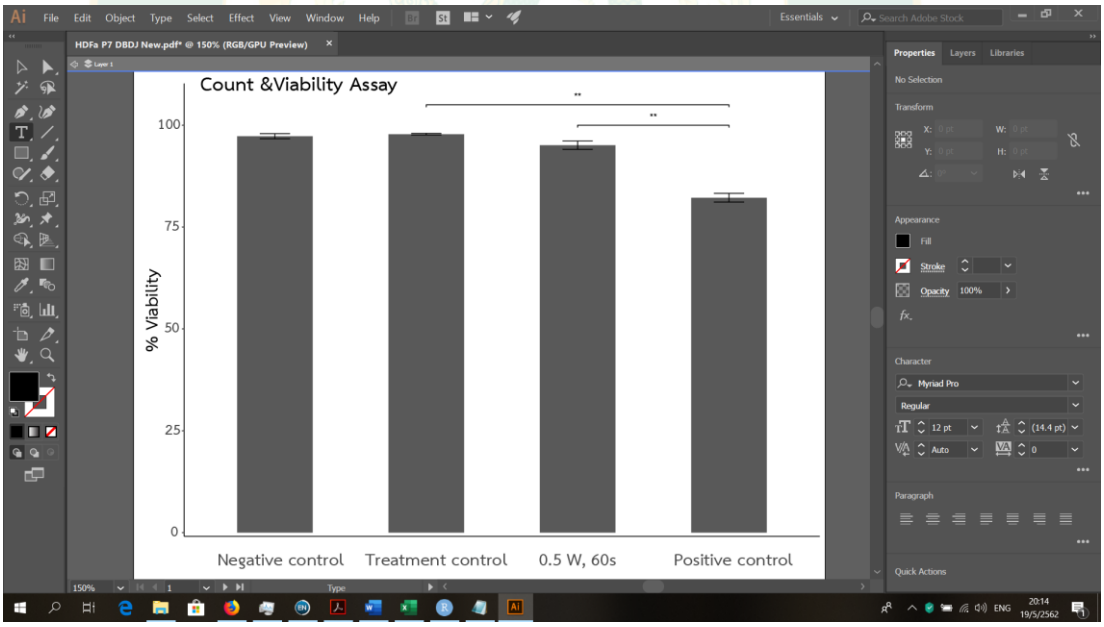

Figure D13 Import graph pdf file into Adobe Illustrator CC for editing graph, labeling the X-Axis and Y-Axis, marking significant bar and adjusting graph scale.

APPENDIX E

PUBLICATION

E.1 Conference

1. 10th INTERNATIONAL CONFERENCE ON PLASMA SCIENCE AND APPLICATIONS (ICPSA) 2017. Topic “The Investigation of Dielectric Barriers Discharge Plasma Jets (DBDJs) for Bactericidal in Chronic Wounds”. 10-12 OCTOBER 2017, Walailak University, Nakhon Si Thammarat, Thailand. (Oral presentation)
2. The 9th RMUTP International Conference on Science, Technology and Innovation for Sustainable Development: Challenges Towards the Digital Society 2018. Topic “The investigation of Dielectric Barriers Discharge Plasma Jet (DBDJ) for bactericidal in wound healing”. The Sukosol, Bangkok, Thailand, 21-22 JUNE 2018. (Oral presentation)
3. 2nd Asia-Pacific Conference on Plasma Physics (AAPPS-DPP 2018). Topic “The Investigation of Dielectric Barriers Discharge Plasma Jet (DBDJ) for Bactericidal in Chronic Wounds”. November 12(Monday) -17(Saturday), 2018. The Kanazawa Chamber of Commerce and Industry & Ishikawa Prefectural Bunkyo Hall, Japan. (Oral presentation)
4. International Conference on Radiation and Emission in Materials, ICREM-2018. Topic “EFFECT OF DIELECTRIC BARRIER DISCHARGE PLASMA JET (DBDJ) ON HUMAN DERMAL FIBROBLAST ADULT (HDFA) CELLS AS IN VITRO CONTAMINATED WOUND HEALING MODEL”. Holiday Inn, Chiang Mai, Thailand. November 20-23, 2018. (Oral presentation)

E.2 Published

1. Walailak Journal of Science and Technology (WJST). Investigation of Dielectric Barriers Discharge Plasma Jets for Bactericidal in Chronic Wounds, Pipath PORAMAPIJITWAT *et al*. Walailak J Sci & Tech 2019; 16(6): 409-414.
2. ICONSCi9 Proceeding Book for Sustainability Science and Engineering. The investigation of Dielectric Barriers Discharge Plasma Jet (DBDJ) for bactericidal in wound healing, Pipath Poramapijitwat *et al*. 2018.

3. PROCEEDINGS OF THE INTERNATIONAL CONFERENCE ON RADIATION AND EMISSION IN MATERIALS (ICREM 2018). PLASMA EFFECT OF DIELECTRIC BARRIER DISCHARGE PLASMA JET (DBDJ) ON HUMAN DERMAL FIBROBLASTS ADULT (HDFa) CELLS: IN VITRO CONTAMINATED WOUND HEALING MODEL, Pipath Poramapijitwat et al. 2018.

E.3 Exchange Program

Sakura Science Plan (Japan-Asia Youth Exchange Program in Science) organized by Japan Science and Technology Agency (JST). Topic “International collaboration program between Japan and Thailand to develop superconducting coils in magnetic confinement fusion”. National Institute for Fusion Science (NIFS) in Toki, Japan, 12 November – 2 December 2017.

WALAILAK JOURNAL
http://wjst.wu.ac.th Engineering and Physical Sciences

Investigation of Dielectric Barriers Discharge Plasma Jets for Bactericidal in Chronic Wounds[†]

Pipath PORAMAPIJITWAT[1,*], Phuthitorn THANA[2], Dheerawan BOONYAWAN[2], Keratiya JANPONG[1,3] and Sureeporn SARAPIROM[1,3,4]

[1]Nanoscience and Nanotechnology, Faculty of Science, Maejo University, Chiang Mai 50290, Thailand
[2]Department of Physics and Materials Science, Faculty of Science, Chiang Mai University, Chiang Mai 50200, Thailand
[3]Applied Physics, Faculty of Science, Maejo University, Chiang Mai 50290, Thailand
[4]Thailand Center of Excellence in Physics, Commission on Higher Education, Bangkok 10400, Thailand

([*]Corresponding author's e-mail: poramapijitwat@yahoo.co.th)

Received: 15 December 2017, Revised: 28 September 2018, Accepted: 20 October 2018

Abstract

The atmospheric pressure plasma technique has been recognized in health care for disinfection in wounds as well as that it can enhance wound healing and reduce pain in patient without side effects. In this study, Dielectric Barrier Discharge Plasma Jets (DBDJs) were used for bactericidal in vitro as well as the efficiency of bacteria killing were investigated using gram positive bacteria, *Staphylococcus Aureus* (*S. Aureus*). The DBDJs plasma used He gas at flow rate at 1 L/min, pulse repetition rate between 50 to 110 Hz and exposure time 15 to 60 s for bactericidal. The studies of DBDJs utilized an Optical Emission Spectroscopy (OES) to identify radical species in the plasma. The results of the OES studies showed in DBDJs plasma N_2, NO, He and OH radical groups were found. These radicals in plasma played an important role in bactericidal, including wound healing. The intensity of radical in plasma depends on the repetition rate applied by the plasma system. After DBDJs plasma exposure, plates were incubated at 37 °C. Repetition rate and time of plasma exposure were drastically reduced. With the increase in the repetition rate over 100 Hz or exposure time up to 60 s for bactericidal, the reduction of bacteria was increased up to 100 %. The large clear zone showed the efficiency of bacteria killed ability of the plasma.

Keywords: Atmospheric pressure plasma, dielectric barrier discharge plasma jets, bactericidal, chronic wounds, *S. Aureus*

Introduction

Bacteria are prokaryotic micro-organisms which have great adaptability to changing environments. They can cause diseases including chronic wound, meningitis, pneumonia etc. Bacteria are divided into 2 major groups: gram positive and gram negative, based on their cell wall structure. Gram-positive bacteria have a relative thick peptidoglycan cell wall, whereas gram-negative bacteria have a thinner peptidoglycan cell wall and an outer membrane containing lipopolysaccharide and protein [1]. One of the gram-positive bacteria is *Staphylococcus Aureus* (*S. Aureus*). *S. Aureus* can cause a broad variety of infections, ranging from minor infections of the skin to post-operative wound infections. The adaptive power of *S. Aureus* to antibiotics leads to the emergence of Methicillin-Resistant *Staphylococcus Aureus* (MRSA). MRSA is the most commonly identified chronic wounds [2] that may cause sepsis and deaths. Therefore, alternative techniques to stop the growing bacteria antibiotic resistant are proposed. One of

[†]Presented at the 10th International Conference on Plasma Science and Applications 2017: October 10th - 11th, 2017

those techniques is Cold Atmospheric Pressure Plasma treatment (CAPP). CAPP was widely studied and reported to have high efficiency to eradicate a wide range of pathogens such as fungi, viruses and bacteria (gram-positive and gram-negative bacteria) including MRSA [2].

The CAPP used in medical field have become a rapidly developing interdisciplinary field that brings a new innovative approach in a broad range of biomedical applications [3]. Atmospheric pressure plasma can be operated at an excitation frequency either in the several tens of kilohertz ac range (or pulsed mode) or in the Radio Frequency (RF) range [4]. It has been shown to inactivate many different animalcules including bacteria, fungus, cancer diseases, proteinaceous matters and genetic DNA [5]. Different designs have been proposed and investigated to utilize CAPP in medical applications. CAPP has to be operated at ambient temperatures and low current without harmful chemicals [6]. It is advisable the basic of physical and chemical properties in plasma including power deposition and consumption, electromagnetic, electrical characteristics, optical emission spectrum, gas temperature and other parameter should be delicately manipulated [7].

Materials and methods

Samples of *S. Aureus* TISTR 2329 were obtained from Thailand Institute of Scientific and Technological Research (TISTR). The *S. Aureus* bacteria were grown in 5 ml nutrient broth (NB) to obtain a bacterial density of approximately 1×10^{7} to 1×10^{8} CFU/ml at 37 °C for 24 h. The grown bacteria were then diluted with serial dilution to 10^{-4} and spread onto nutrient agar plates (NA). Plasma exposure on *S. Aureus* was carried out using a Dielectric Barrier Discharge Plasma Jets (DBDJs) of Photo Bio Care Co. Ltd, Thailand [8]. Plasma was generated at repetition rate between 50 to 110 Hz, time exposure 15 to 60 s and flow rate of He gas of 1 l/min. Optical Emission Spectroscopy (OES, Fiber Optic Spectrometer: AvaSpec-2048) was applied to detect radical species in the plasma frame. The high voltage waveform was determined by use a high-voltage probe (Tektronix, P6015A). The plasma power was estimated by Lissajous figure [9], whiles the discharge charge was determined by a HV probe (Hantek, T3100). Following plasma exposure, the bactericidal efficiency was observed using Colony Forming Unit (CFU) method. Data of bactericidal efficiency was statistically interpreted.

Results and discussion

As seen in **Figure 1**, the strongest OES spectrum of DBDJs corresponding to NO, OH, N_2 and He is found at 297.61, 308.99, 337.54 and 709.54 nm, respectively. The emission spectrum has a broad wavelength ranging from 200 to 900 nm. The NO peaks lying between 200 - 300 nm are primarily from the NO A–X (γ) in the ultraviolet region. However, their intensity is very low. The N_2 C-B (2^{nd} positive system at 334.27 nm) and N^{+}_{2} B-X (1^{st} negative system at 406.24 nm) are observed at wavelength ranging from 300 to 450 nm, which could result from the excitation processes; the electron excitation from the ground state N_2 (X1Σ g+) and the first metastable state N_2 (A3Σ u+) and pooling reaction [10]. The existence of these molecules implied curative properties of the studied plasma because reactive nitrogen species (RNS), reactive oxygen species (ROS) and reactive oxygen nitrogen species (RONS) were found to play an important role in bactericidal reactions [10].

RNS and ROS have 3 important effects on cells including protein oxidation, lipid peroxidation and oxidation of DNA. Regarding protein oxidation, ROS can fragment protein and protein-protien crosslinkages by inducing oxidation in both amino acid side chains and protein backbones. In lipid peroxidation, RNS/ROS can induce electrostatic force in the cell membrane, which therefore steal electron from the lipids in cell membranes, resulting in cell lysis. With regard to DNA, RNS can induce DNA deamination leading to strand breaks [11,12].

In addition, as seen in **Figure 2**, intensity of the OES spectra increases with the applied pulse rate. **Figure 3** shows variation in OES intensity of NO and OH. It is also found that the intensity of both increases with the applied pulse rate. The increase in OES intensity could result from higher decomposition of the active species at higher pulse rate, indicating bactericidal performance of plasma can be increased by increasing the applied pulse rate.

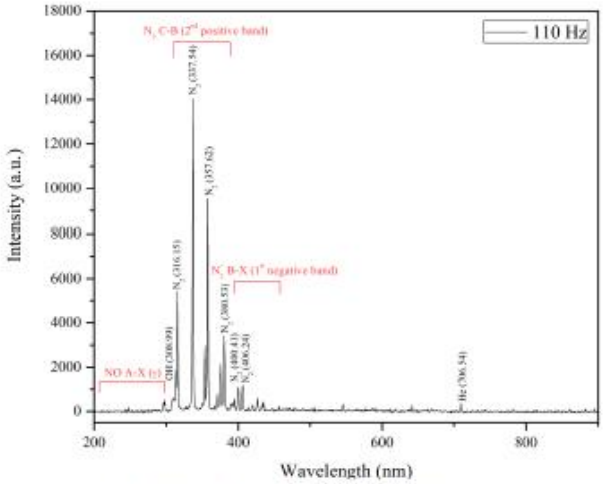

Figure 1 Emission spectra of DBDJs with applied pulse rate at 110 Hz.

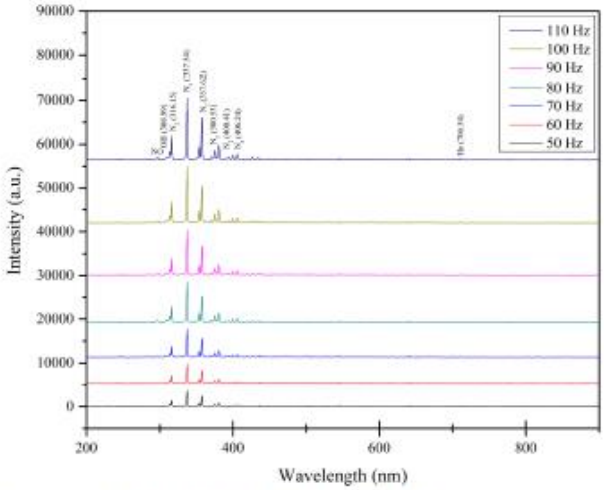

Figure 2 Emission spectra of DBDJs with pulse rate from 50 to 110 Hz.

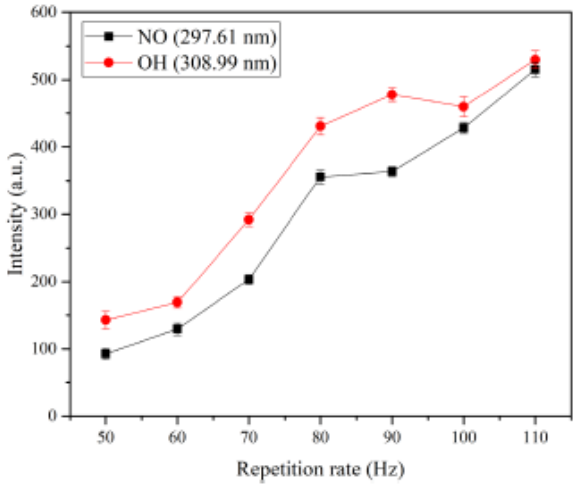

Figure 3 NO and OH intensity and the applied repetition rate.

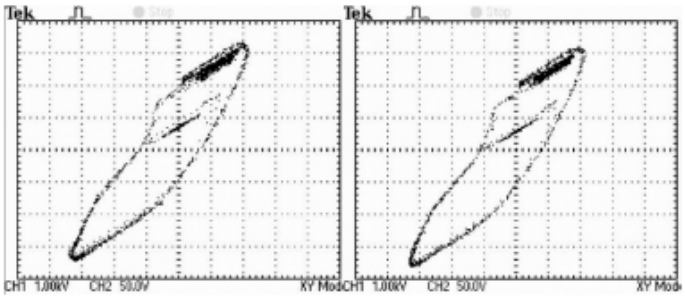

Figure 4 Lissajous figure of DBDJs (a) 50 Hz repetition rate and (b) 110 Hz repetition rate.

The Lissajous figure of DBDJs is shown in **Figure 4**. It is observed that pulse rate at 50 Hz with duty cycle at 36.7 delivered power of 1.96 watt which was equivalent to dose of 1.17 J/cm^2 [9]. Pulse rate at 110 Hz with duty cycle at 43.3 delivered power of 2.31 watt that was equivalent to dose of 2.17 J/cm^2. This suggests that increasing the pulse rate and percentage of duty cycle can increase power and dose of DBDJs, which therefore can increase radicals in DBDJs.

Evaluation of antibacterial activity of DBDJs is shown in **Figure 5**. It is observed that there is no bacteria inhibition zone in **Figures 5a** and **5b**, indicating that DBDJs with pulse rate at 50 Hz and time of exposure of 15-30 s does not exhibit bactericidal manner. However, as seen in **Figures 5c - 5h**, the

bacteria inhibition zone becomes visible and increases with repetition rate and time of exposure. This reveals that DBDJs were potentially effective in suppressing microbial growth when repetition rate and time of exposure was increased. This finding is consistent with bactericidal efficiency which was evaluated by CFU method (**Figure 6**). It is seen that bactericidal efficiency increases with both repetition rate and time of exposure. The increase in antibacterial activity demonstrates an increase of antibacterial species generated by excited plasma.

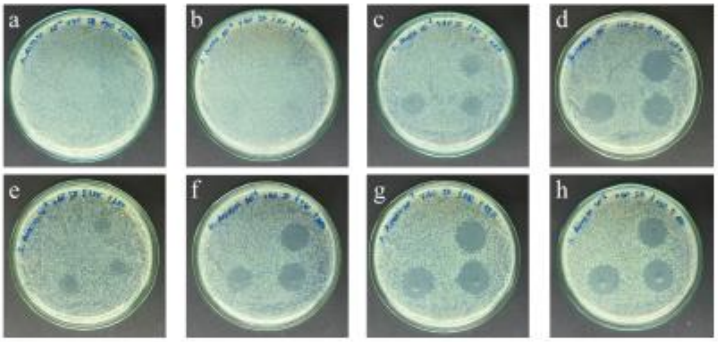

Figure 5 Efficiency of DBDJs to bactericidal (a, b, c and d) at repetition rate 50 Hz and time of exposure 15-60 s, (e, f, g and h) at repetition rate 110 Hz and time of exposure 15 - 60 s.

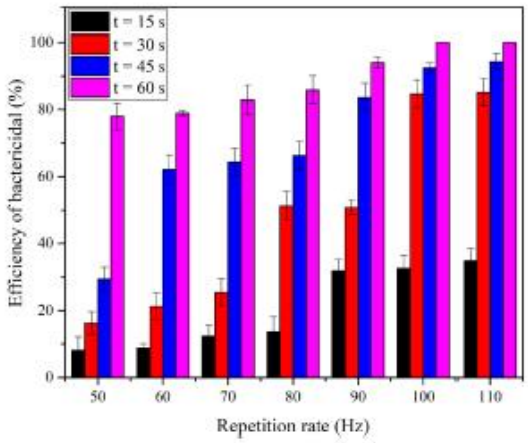

Figure 6 Percentage of bactericidal efficiency.

Conclusions

The DBDJs generated NO, OH, N_2 and He species which belong to RONS group and their intensity increased with plasma power. Bactericidal efficiency was dependent on repletion rate and time of exposure: antibacterial activity of the DBDJs increased with dose rate.

Acknowledgements

We wish to thank C. Kuensaen and C. Yatongchai for research consult, Thailand Center of Excellence in Physics (ThEP) and Graduate School Maejo University for the scholarships. DBDJs has been supported by C. Chutsirimongkol.

References

[1] ZH Lin, CYT Tschang, KC Liao, CF Su, JS Wu and MT Ho. Ar/O_2 argon-based round atmospheric-pressure plasma jet on sterilizing bacteria and endospores. *IEEE Trans. Plasma Sci.* 2016; **44**, 3140-7.

[2] N Mohd Nasir, BK Lee, SS Yap, KL Thong and SL Yap. Cold plasma inactivation of chronic wound bacteria. *Arch. Biochem. Biophys*. 2016; **605**, 76-85.

[3] EM Kulaga, DJ Jacofsky, C McDonnell and MC Jacofsky. The use of an atmospheric pressure plasma jet to inhibit common wound-related pathogenic strains of bacteria. *Plasma Med*. 2016; **6**, 1-12.

[4] S Kubinova, K Zaviskova, L Uherkova, V Zablotskii, O Churpita, O Lunov and A Dejneka. Non-thermal air plasma promotes the healing of acute skin wounds in rats. *Sci. Rep*. 2017; **7**, 451-83.

[5] Y Setsuhara. Low-temperature atmospheric-pressure plasma sources for plasma medicine. *Arch. Biochem. Biophys*. 2016; **605**, 3-10.

[6] YW Hung, LT Lee, YC Peng, CT Chang, YK Wong and KC Tung. Effect of a nonthermal-atmospheric pressure plasma jet on wound healing: An animal study. *J. Chin. Med. Assoc*. 2016; **79**, 320-8.

[7] J Heinlin, G Isbary, W Stolz, G Morfill, M Landthaler, T Shimizu, B Steffes, T Nosenko, J Zimmermann and S Karrer. Plasma applications in medicine with a special focus on dermatology. *J. Eur. Acad. Dermatol. Venereol*. 2011; **25**, 1-11.

[8] C Yaopromsiri, LD Yu, S Sarapirom, P Thopan and D Boonyawan. Effect of cold atmospheric pressure He-plasma jet on DNA change and mutation. *Nucl. Instrum. Meth. Phys. Res. Sect. B* 2015; **365**, 399-403.

[9] KG Kostov, RY Honda, LMS Alves and ME Kayama. Characteristics of dielectric barrier discharge reactor for material treatment. *Braz. J. Phys*. 2009; **39**, 2322-5.

[10] SJ Kim, TH Chung and SH Bae. Characteristic study of atmospheric pressure microplasma jets with various operating conditions. *Thin Solid Films* 2009; **517**, 4251-4.

[11] SK Kang, HY Kim, GS Yun and JK Lee. Portable microwave air plasma device for wound healing. *Plasma Sourc. Sci. Tech*. 2015; **24**, 1-12.

[12] TV Woedtke, S Reuter, K Masur and KD Weltmann. Plasmas for medicine. *Plasma Phys. Rep*. 2013; **530**, 291-320.

© The 9th RMUTP International Conference on Science, Technology and Innovation for Sustainable Development: Challenges Towards the Digital Society, 21-22 June 2018 The Sukosol, Thailand
http://iconsci.rmutp.ac.th/

The investigation of Dielectric Barriers Discharge Plasma Jet (DBDJ) for bactericidal in wound healing

Pipath Poramapijitwat[1,a*], Phuthidhorn Thana[2,b], Dheerawan Boonyawan[2,c], Keratiya Janpong[1,3,d] Wasin Charerntantanakul[4,e] and Sureeporn Sarapirom[1,3,5,f*]

[1]Nanoscience and Nanotechnology, Faculty of Science, Maejo University, Chiang Mai 50290, Thailand

[2]Department of Physics and Materials Science, Faculty of Science, Chiang Mai University, Chiang Mai 50200, Thailand

[3]Applied Physics, Faculty of Science, Maejo University, Chiang Mai 50290, Thailand

[4]Program of Biotechnology, Faculty of Science, Maejo University, Chiang Mai 50290, Thailand

[5]Thailand Center of Excellence in Physics, Commission on Higher Education, Bangkok 10400, Thailand

[a]poramapijitwat@yahoo.co.th, [b]phuthidhorn.thana@gmail.com, [c]dheerawan.b@cmu.ac.th, [d]pimpornjunphong@gmail.com, [e]wasin@mju.ac.th, [f]ssarapirom@gmail.com

Keywords: Atmospheric pressure plasma, Dielectric barrier discharge plasma jets, Wound healing, *Staphylococcus aureus, Pseudomonas aeruginosa*

Abstract. The cold atmospheric pressure plasmas (CAPPs) technique have been recognized in health care for wound healing enhancement while the patient's pain relieving without side effects. In this study, dielectric barrier discharge plasma jet (DBDJ) was used for bactericidal. This cold plasma jet is driven by high voltage dc pulse at 20 kHz and using 1 L/min of helium (He) as plasma gas. The DBDJ plasma was varied the plasma dissipated power from 0.27 to 0.50 watt and the treatment time 15 to 60 s. Plasma radical species were utilized by using an optical emission spectroscopy (OES). The results of the OES study was found NO and OH radical groups which is an important role of bactericidal and wound healing. The increasing of radical plasma density depends on the dissipated power. The Colony Forming unit (CFU) method was used to monitor the efficiency of bacteria killing. *Staphylococcus Aureus* (*S. aureus*) and *Pseudomonas Aeruginosa* (*P. aeruginosa*) were used for in vitro bacteria killing test. The results showed that the dissipated power and treatment time were affectively factors for bactericidal. When increasing the plasma dissipated power at 0.50 watt and treatment time to 60 s, the effect of bacteria killing was increased up to 100%.

Introduction

Bacteria are prokaryotic micro-organisms, it has great adaptability to the environment and is the main cause of illnesses, wound infections, including chronic wound, meningitis, pneumonia etc. The difference of the cell wall structure bacteria can be divide into two groups. Gram-positive bacteria have a relative thick peptidoglycan (20 to 80 nm) cell wall, while gram-negative bacteria have a thinner peptidoglycan (< 10 nm) cell wall [1, 2]. The difference of bacterial cell wall lead to different properties to the cell, especially the cell responses to external stressors such as a heat, UV radiation and also antibiotics [2]. One of the gram-positive bacterial strains is *S. aureus* and gram-negative bacterial strains is *P. aeruginosa*. These are causing public health concerns in the postsurgical patient population. The *S. aureus*, *P. aeruginosa* including methicillin-resistant *Staphylococcus aureus* (MRSA) are the most commonly identified bacterium in wounds [3], including being the cause of a range of sickness from skin and wound infections, pneumonia with empyema and bacteremia that may cause of sepsis and death. Therefore, an alternative technique to

© The 9th RMUTP International Conference on Science, Technology and Innovation for Sustainable Development: Challenges Towards the Digital Society, 21-22 June 2018 The Sukosol, Thailand
http://iconsci.rmutp.ac.th/

stop the growing bacteria antibiotic resistant are required. The physical technique such as the CAPPs technique are report an efficiency against antimicrobial and a wide range of pathogens such as fungi, viruses and bacteria including antibiotic resistant bacteria such a MRSA. The CAPPs in medical field has become a rapidly developing interdisciplinary field that brings a new innovative approach in a broad range of biomedical applications [4]. For medical applications, the plasma temperature should be at room temperature without any electrical and chemical harm. The CAPPs sources have been operated at an excitation frequency, either in the several tens of kilohertz ac range or in the radio frequency (RF) range. Because of various design configurations and operation conditions of plasma, the factors controlling discharges, for instance temperature, charged particle, ion, electromagnetic field and radical species are obvious. For suitable control of the plasma treatment processes, it is important to understand the basics of physical and chemical properties in plasma, such as power deposition and consumption, electromagnetic, electrical characteristics, optical emission spectrum, gas temperature and other parameter in plasma [5]. They play important roles in bactericidal by CAPPs.

Materials and methods

The emission spectrum of this plasma jet was detected by broadband CCD spectrometer (Fiber Optic Spectrometer: AvaSpec-2048). The high voltage waveform was determined by using a high-voltage probe (Tektronix, P6015A). The plasma dissipated power was estimated by using Lissajous figure [6], where the discharge charge was estimated from the voltage across the 1 nF capacitor measured by a HV probe (Hantek, T3100). The NO and O_3 concentration were measurement by using the two gas detectors (Shenzhen YuanTe Technology); model SKY2000-NO for measuring NO concentration and model SKY2000-O_3 for measuring O_3 concentration. The bactericidal efficiency was observed by using Colony Forming unit (CFU) method. Samples of *S. aureus* TISTR 2329 and *P. aeruginosa* TISTR 2370 were obtained from Thailand Institute of Scientific and Technological Research (TISTR). The sample bacteria of *S. aureus* and *P. aeruginosa* will be prepared in nutrient broth (NB) 5 ml and orbital shaker 150 rpm in incubator at 37 °C for 24 hr. After 24 hr. *S. aureus* and *P. aeruginosa* in NB have density of approximately $1x10^7$ to $1x10^8$ CFU/mL and dilute with serial dilution to 10^{-4} before prepared in nutrient agar (NA).

Results and discussion

The Lissajous figure of DBDJ is shown in Fig. 1. At applied frequency 20 kHz, the plasma dissipated power at 0.27 watt. Therefore, when increasing frequency to DBDJ the percentage of duty cycle, power and dose of DBDJ increased. These factors have influence on the intensity of radicals in DBDJ. Intensity of radicals in plasma play an important role for bactericidal.

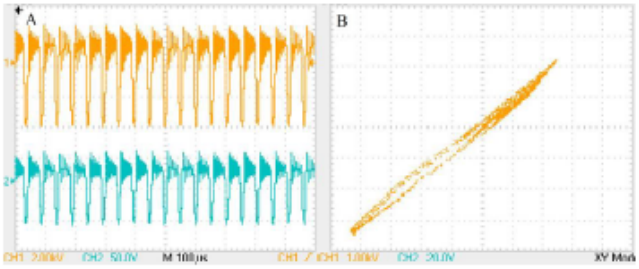

Figure 1 A) The applied voltage signal (channel 1) the voltage across the 1 nF capacitor (channel 2) and **B)** the Lissajous figure of DBDJ the plasma dissipated power at 0.27 watt.

The 9th RMUTP International Conference on Science,
Technology and Innovation for Sustainable Development:
Challenges Towards the Digital Society, 21-22 June 2018
The Sukosol, Thailand
http://iconsci.rmutp.ac.th/

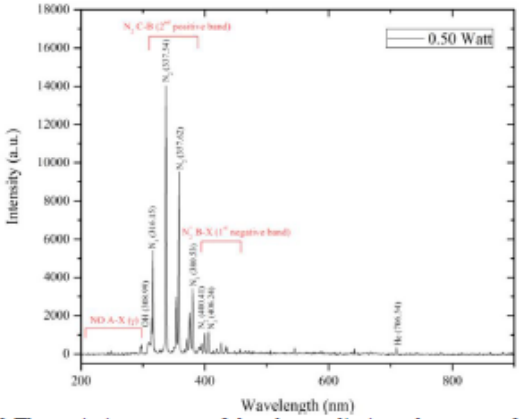

Figure 2 The emission spectra of the plasma dissipated power at 0.50 watt.

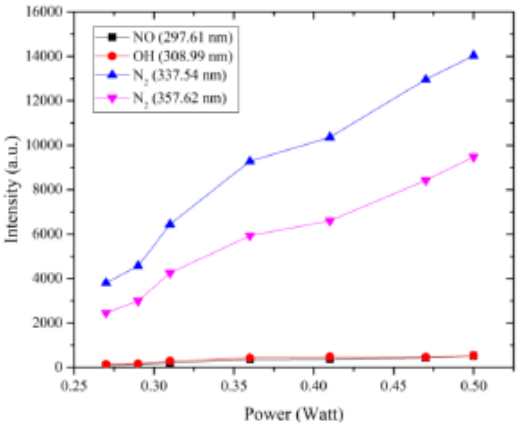

Figure 3 The relative of the RONS intensity and the plasma dissipated power.

The reactive oxygen and nitrogen species (RONS) play an important role in bactericidal [7]. These radicals and electrostatic force of ions break down bacteria cell, DNA damage and charge accumulated leading to cell lysis. The main bactericidal are RONS that could kill bacteria [8, 9]. The OES spectrum of DBDJ found the peak of NO at 297.61 nm, OH at 308.99 nm, N_2 at 337.54 nm and He at 706.54 nm as shown in Fig. 2. The NO lines are primarily from the NO A–X (γ) in the ultraviolet region at wavelength 200 to 300 nm but intensity very low. The N_2 C-B (2^{nd} positive system at 334.27 nm) and N^+_2 B-X (1^{st} negative system at 406.24 nm) are observed between wavelength 300 to 450 nm because the excitation processes like the electron impact excitation from the ground state N_2 (X1Σ g+) and the first metastable state N_2 (A3Σ u+) and pooling reaction [7]. Also found OH at 308.99 nm and He at 706.54 nm. The Fig. 3 shows that when increasing the plasma dissipated power from 0.27 to 0.50 watt the intensity of RONS was increased. The increasing of NO intensity is significant but ineffective for the intensity of OH. The O_3 concentration were increased with the plasma dissipated power. The same trends were observed with significantly higher concentration of NO was show in the Fig. 4. However, the operational condition the O_3 concentration was in the safety regulations of medical devices.

© The 9th RMUTP International Conference on Science, Technology and Innovation for Sustainable Development: Challenges Towards the Digital Society, 21-22 June 2018 Tha Sukosol, Thailand
http://iconsci.rmutp.ac.th/

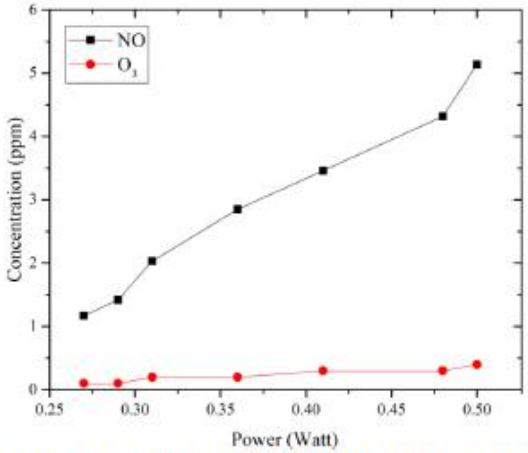

Figure 4 The relative between concentration of NO and O_3 and the plasma dissipated power.

The bactericidal efficiency of DBDJ can be observed in Fig. 5-8. The inactivation areas were clearly increased with the plasma dissipated power and treatment time. At a short exposure time, the inactivation areas were limited only the head zone area. While the longer exposure times, the clear zones were larger and diffused to the neighbor area. It is mainly with the OH and O_3 density. However, the killing zones expanded to cover the neighbor area that related with the long-life time of O_3 and high NO concentration in the superoxide ambient area. There was could be involved in an increased nitroxidative stress which was leading to the formation of highly reactive radicals and oxidative species. RNS induces nitric oxide and nitric acid influences bactericidal [10, 11]. Acidified nitrite has a strong antimicrobial ability on bacteria cell leading to cell death. The CAPPs treatment prompts the acidic conditions and accumulation of nitrite and hydrogen peroxide. Consequently these factors are the main cause for CAPPs to induced toxic effects on bacteria cell [10].

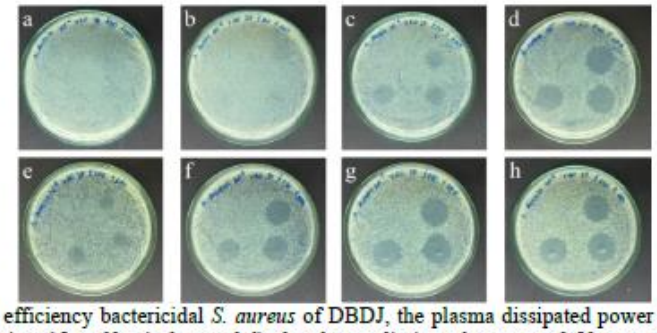

Figure 5 The efficiency bactericidal *S. aureus* of DBDJ, the plasma dissipated power at 0.27 watt and treatment time 15 to 60 s (a, b, c and d), the plasma dissipated power at 0.50 watt and treatment time 15 to 60 s (e, f, g and h).

© The 9th RMUTP International Conference on Science, Technology and Innovation for Sustainable Development: Challenges Towards the Digital Society, 21-22 June 2018 Tha sukosol, Thailand
http://iconsci.rmutp.ac.th/

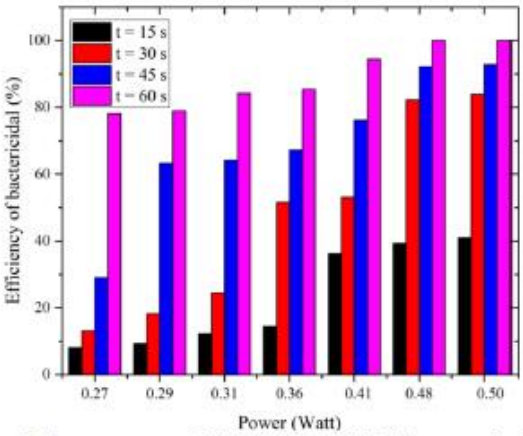

Figure 6 The percentage efficiency of bactericidal *S. aureus* by DBDJ.

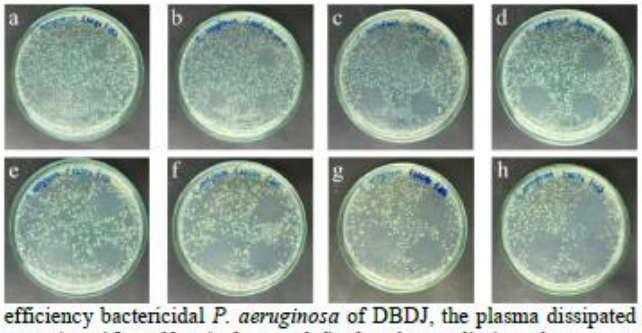

Figure 7 The efficiency bactericidal *P. aeruginosa* of DBDJ, the plasma dissipated power at 0.27 watt and treatment time 15 to 60 s (a, b, c and d), the plasma dissipated power at 0.50 watt and treatment time 15 to 60 s (e, f, g and h).

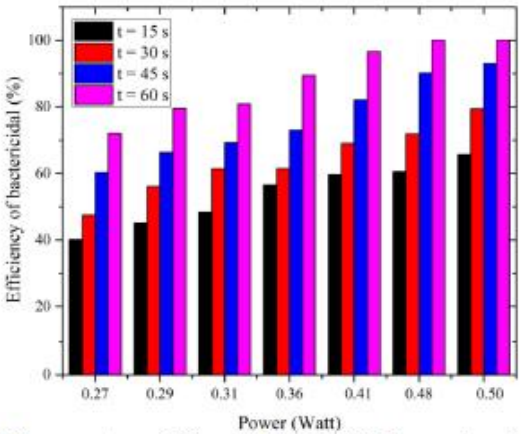

Figure 8 The percentage efficiency of bactericidal *P. aeruginosa* by DBDJ.

© The 9th RMUTP International Conference on Science, Technology and Innovation for Sustainable Development: Challenges Towards the Digital Society, 21-22 June 2018 The Sukosol, Thailand
http://iconsci.rmutp.ac.th/

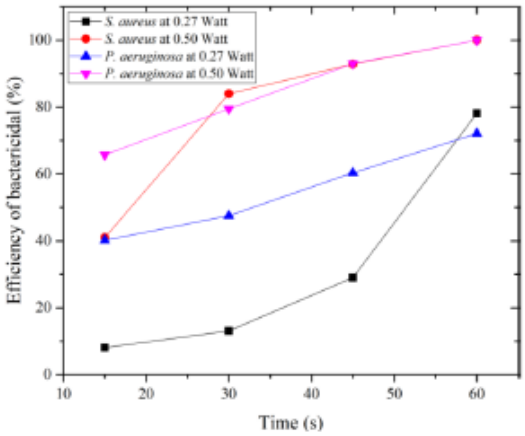

Figure 9 The percentage efficiency of bactericidal *S. aureus* and *P. aeruginosa* by DBDJ the plasma dissipated power at 0.27 and 0.50 watt, treatment time 15 to 60 s.

Comparing the bacterial efficiency of *S. aureus* and *P. aeruginosa* are shows in Fig. 9. It was found that the *P. aeruginosa* have a higher bactericidal efficiency than *S. aureus* under the same condition. Because of the main difference of the cell wall structure of bacteria. The outer structure of *S. aureus* cell wall is the multi layers of peptidoglycan which is the stronger bonding than the *P. aeruginosa* cell wall. *P. aeruginosa* cell wall consists of phospholipids and lipopolysaccharides, there are have an influence of the polarity. Destruction of peptidoglycan through external stresses will lead to cell lysis. Therefore, the different thickness of cell wall between two group of bacteria, the outer membrane of gram-negative as well as cell appendices of gram-positive bacteria play an important role for bactericidal in DBDJ [2, 12]. The inactivation of CAPPs to bacterial well-know is peroxidation of lipids [13] and membrane lipids are the most vulnerable to physical stresses because the position is outside of the cell envelope and it is sensitive to RONS. Furthermore, the charged particles in plasma played an important role for bactericidal with the rupture of bacteria cells wall [14, 15]. When the charge particles accumulated on outer surface of the membrane being more than the tensile strength of the membrane lead to cell rupture by electrostatic force [16]. If no force exists, the repulsive force will only impact on the charges and little damage to the cell membrane. The electric field generated between charge particles have non-uniformity. When time of charge accumulate the transmembrane potential increases. On the other hand, the ions generated in the CAPPs cannot get through the cell membrane. Hence, charge accumulation is still execution. If the intensity of electric field generated form charge particles strong enough it could change the three dimensional of the proteins structure, separate out the cell membrane and be forceless. Thus, the charge particles forming CAPPs have ability and destroy the proteins and enzymes activity into the cell. Most likely the cytoplasm will leaks out the cell through these holes, which is the reason leading the cell death why the cell dies [9, 15]

Conclusions

The DBDJ have a high efficiency on bactericidal both of *S. aureus* and *P. aeruginosa* at 20 kHz, plasma dissipated power 0.41 to 0.50 watt and treatment time 45 to 60 s. All the death of bacteria was increased with plasma dissipated power and treatment time. The lager clear zones affected by RONS and charge particles. Electrostatic force of ions in plasma play an important role for bactericidal leading to cell lysis. Moreover, the difference of cell wall structure between gram-positive and gram-negative bacteria leading to difference sensitivity by DBDJ. Hence, the DBDJ have a high bactericidal efficiency and assist in wound healing.

© The 9th RMUTP International Conference on Science, Technology and Innovation for Sustainable Development: Challenges Towards the Digital Society, 21-22 June 2018 The Sukosol, Thailand
http://iconsci.rmutp.ac.th/

Acknowledgements

The authors are thankful to Plasma medicine project in supporting the equipment. The Dielectric Barriers Discharge Plasma Jets (DBDJ) from Dr.Chanchai Chutsirimongkol to investigate the bactericidal. Thailand Institute of Scientific and Technological Research (TISTR) for bacterial stain in my research. Mr.Chakkrapong Kuensaen for consultation and suggestion to improve my research. Thailand Center of Excellence in Physics (ThEP) and Graduate School Maejo University for my scholarships. Plasma and Beam Physics Research Facility, Department of Physics and Materials Science, Faculty of Science, Chiang Mai University, Nanoscience and Nanotechnology, Faculty of Science and laboratory of Maejo University in supporting my research.

References

[1] Z.H. Lin, C.Y.T. Tschang, K.C. Liao, C.F. Su, J.S. Wu, M.T. Ho. Ar/O2 Argon-Based Round Atmospheric-Pressure Plasma Jet on Sterilizing Bacteria and Endospores, IEEE Transactions on Plasma Science 44 (2016) 3140-3147.
[2] A. Mai-Prochnow, M. Clauson, J. Hong, A.B. Murphy. Gram positive and Gram negative bacteria differ in their sensitivity to cold plasma, Sci Rep 6 (2016) 38610.
[3] N. Mohd Nasir, B.K. Lee, S.S. Yap, K.L. Thong, S.L. Yap. Cold plasma inactivation of chronic wound bacteria, Arch Biochem Biophys 605 (2016) 76-85.
[4] S. Kubinova, K. Zaviskova, L. Uherkova, V. Zablotskii, O. Churpita, O. Lunov, A. Dejneka. Non-thermal air plasma promotes the healing of acute skin wounds in rats, Sci Rep 7 (2017) 45183.
[5] S.J. Kim, T.H. Chung, S.H. Bae. Characteristic study of atmospheric pressure microplasma jets with various operating conditions, Thin Solid Films 517 (2009) 4251-4254.
[6] K.G. Kostov, R.Y. Honda, L.M.S. Alves, M.E. Kayama. Characteristics of dielectric barrier discharge reactor for material treatment, Brazilian Journal of Physics 39 (2009) 322-325.
[7] S.K. Kang, H.Y. Kim, G.S. Yun, J.K. Lee. Portable microwave air plasma device for wound healing, Plasma Sources Science and Technology 24 (2015).
[8] T. von Woedtke, S. Reuter, K. Masur, K.D. Weltmann. Plasmas for medicine, Physics Reports 530 (2013) 291-320.
[9] M.G. Kong, G. Kroesen, G. Morfill, T. Nosenko, T. Shimizu, J. van Dijk, J.L. Zimmermann. Plasma medicine: an introductory review, New Journal of Physics 11 (2009).
[10] C.V. Suschek, C. Opländer. The application of cold atmospheric plasma in medicine: The potential role of nitric oxide in plasma-induced effects, Clinical Plasma Medicine 4 (2016) 1-8.
[11] J. Heinlin, G. Morfill, M. Landthaler, W. Stolz, G. Isbary, J.L. Zimmermann, T. Shimizu, S. Karrer. Plasma medicine: possible applications in dermatology, J Dtsch Dermatol Ges 8 (2010) 968-976.
[12] W. Vollmer, D. Blanot, M.A. de Pedro. Peptidoglycan structure and architecture, FEMS Microbiol Rev 32 (2008) 149-167.
[13] F. Vatansever, W.C. de Melo, P. Avci, D. Vecchio, M. Sadasivam, A. Gupta, R. Chandran, M. Karimi, N.A. Parizotto, R. Yin, G.P. Tegos, M.R. Hamblin. Antimicrobial strategies centered around reactive oxygen species--bactericidal antibiotics, photodynamic therapy, and beyond, FEMS Microbiol Rev 37 (2013) 955-989.
[14] G. Fridman, A.D. Brooks, M. Balasubramanian, A. Fridman, A. Gutsol, V.N. Vasilets, H. Ayan, G. Friedman. Comparison of Direct and Indirect Effects of Non-Thermal Atmospheric-Pressure Plasma on Bacteria, Plasma Processes and Polymers 4 (2007) 370-375.
[15] J. Guo, K. Huang, J. Wang. Bactericidal effect of various non-thermal plasma agents and the influence of experimental conditions in microbial inactivation: A review, Food Control 50 (2015) 482-490.
[16] M. Laroussi, D.A. Mendis, M. Rosenberg. Plasma interaction with microbes, New Journal of Physics 5 (2003) 41-41.

PLASMA EFFECT OF DIELECTRIC BARRIER DISCHARGE PLASMA JET (DBDJ) ON HUMAN DERMAL FIBROBLASTS ADULT (HDFa) CELLS: IN VITRO CONTAMINATED WOUND HEALING MODEL

Pipath Poramapijitwat[a*], Phuthidhorn Thana[b], Dheerawan Boonyawan[b], Keratiya Janpong[a,c], Chakkrapong Kuensaen[d], Wasin Charerntantanakul[e] and Sureeporn Sarapirom[a,c*]

[a]*Nanoscience and Nanotechnology, Faculty of Science, Maejo University, Chiang Mai 50290, Thailand*

[b]*Department of Physics and Materials Science, Faculty of Science, Chiang Mai University, Chiang Mai 50200, Thailand*

[c]*Applied Physics, Faculty of Science, Maejo University, Chiang Mai 50290, Thailand*

[d]*Department of Biology, Faculty of Science, Chiang Mai University, Chiang Mai 50200, Thailand*

[e]*Program of Biotechnology, Faculty of Science, Maejo University, Chiang Mai 50290, Thailand*

**Corresponding author Email Address: Poramapijitwat@yahoo.co.th, Ssarapirom@gmail.com*

Abstract

The dielectric barrier discharge plasma jet (DBDJ) was used to study the effect of plasma radicals on *S. aureus*, *P. aeruginosa*, biofilm and Primary Human Dermal Fibroblasts adult (HDFa) cells. The He plasma was generated by high voltage dc pulse. Plasma radical species were obverved. The N_2, NO, He and OH radical groups were found. The intensity of radical in plasma depends on the repetition rate applied by the plasma system. After treatment with plasma at 0.50 watt and exposure time at 60 s, the result showed that it was the best condition for killing bacteria up to 100%. Therefore, this condition was chose to study the effect of plasma on biofilm and HDFa cells. The result showed that DBDJ had high efficiency to removed biofilm. After plasma treatment the shape of HDFa cells was unchanged. The results of Muse Count & Viability Assay Kit and Muse Annexin V & Dead Cell Assay Kit showed plasma had slightly effect on HDFa cell viability. Therefore, the DBDJ has a high efficiency to kill bacteria, destroy biofilm and assist in contaminated wound healing without damage to skin cells.

Keywords: Dielectric Barrier Discharge Plasma Jet; Human Dermal Fibroblasts adult cells; Bactericidal; Wound Healing; Bacterial Biofilms

1. Introduction

Bacteria is the main cause of illnesses, wound infections, chronic wound etc. These are causing public health concerns in postsurgical patients. The *S. aureus*, *P. aeruginosa* and methicillin-resistant *Staphylococcus aureus* (MRSA) are the most commonly identified bacterium in wounds [1]. Physical techniques were recruited to stop growing antibiotic-resistant bacteria. One of those physical techniques is cold atmospheric pressure plasma (CAPP). CAPP can be operated at body temperature without any electrical and chemical harm and it was reported to have an efficiency gainst a wide range of pathogens such as fungi, viruses and bacteria including MRSA. CAPP has become a rapidly developing interdisciplinary field that brings a new innovative approach in a broad range of biomedical applications [2]. Various of plasma factors including temperature, charged particle, ion and radical species can be manipulated to fine a suitable condition. In this study, DBDJ was used to generate plasma and effects of plasma radicals on *S.aureus*, *P. aeruginosa*, biofilm and HDFa were investigated.

2. Experimental Procedure

The DBDJ plasma device operated in a pure He mode, described elsewhere [3]. The emission spectrum of this DBDJ was obtained by broadband CCD spectrometer (Fiber Optic Spectrometer: AvaSpec-2048). The high voltage waveform was determined using a high-voltage probe (Tektronix, P6015A). The plasma dissipated power was estimated by Lissajous figure [4], where the discharge charge was estimated from the voltage across the 1 nF capacitor measured by a HV probe (Hantek, T3100). The NO and O_3 concentration were measured using the two gas detectors (Shenzhen YuanTe Technology): model SKY2000-NO and SKY2000-O_3.

Preparation of *S. aureus* and *P. aeruginosa*

Bactericidal efficiency was observed by Colony Forming unit (CFU) method. Samples of TISTR 2329 *S. aureus* and TISTR 2370 *P. aeruginosa* were obtained from Thailand Institute of Scientific and Technological Research (TISTR). The *S. aureus* and *P. aeruginosa* were grown in 5 ml nutrient broth (NB). The grown bacteria was spread onto nutrient agar plates (NA). The DBDJ plasma operated at plasma dissipated 0.27 to 0.50 watt and exposure time 15 to 60 s.

Preparation of Biofilms

The bacterial biofilms both of *S. aureus* and *P. aeruginosa* were prepared in NB and then moved to 12-well plate at 1 mL/well on the coverslip glass. The bacteria samples were incubated for 48 hr. After that, plasma exposure on bacteria samples was carried out at plasma dissipated 0.50 watt and exposure time 60 s. Live/Dead assay method with double stain Hoechst 33342 and Propidium iodide (PI) was used. Bactericidal perfomance of the studied plasma was observed under fluorescence microscope.

Preparation of HDFa

Human Dermal Fibroblasts, adult (HDFa) Cat. no. C-013-5C was purchased from Cascade Biologics™ invitrogen cell culture (GIBCO invitrogen cell culture). Effect of DBDJ on HDFa cells was also studied using Live/Dead assay method. In addition, Muse Cell Analyzer with the Muse Count & Viability Assay Kit and Muse Annexin V & Dead Cell Assay Kit was utilized to find survivalability. One-way ANOVA in R-program x64 ver.3.5.1 with R-Studio ver.1.1.456 was used for data interpretation. Post hoc multiple comparison test (Tukey method) was applied at 99% confidence level (α=0.01) [5].

3. Results and Discussion

Plasma properties

The reactive oxygen and nitrogen species (RONS) played an important role in bactericidal [10]. These radicals and electrostatic force of ions break down bacteria cell, DNA damage and charge accumulated leading to cell lysis. The main bactericidal was RONS that could kill bacteria [11, 12].

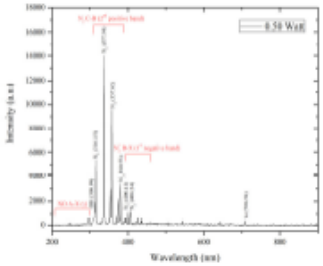

Figure 1 The emission spectra of the plasma dissipated power at 0.50 watt.

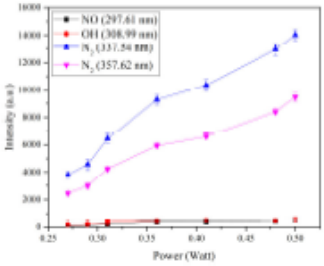

Figure 2 The relative of the RONS intensity and the plasma dissipated power.

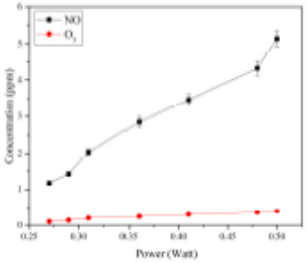

Figure 3 The relative between NO and O_3 concentration and the plasma dissipated power.

The OES spectrum of DBDJ is presented in Fig. 1. It is found the strongest peak of NO at 297.61 nm, OH at 308.99 nm, N_2 at 337.54 nm and He at 706.54 nm. Fig. 2, intensity of N_2 shows a steady increase with intensity with the plasma dissipated power, while intensity of OH and NO presents a slight increase when the plasma dissipated power increase.

Regarding NO, as seen in Fig. 3, NO concentration exhibits a remarkable increase with the plasma power, which is incresed from 1 ppm at 0.25 watt to 5 ppm at 0.5 watt. Whereas, O_3 concentration shows an infinitesimal value less than 0.5 ppm. In biomedical applications, concentration of O_3 and NO should not be higher than 8 hr TWA 0.1 ppm [6] and TWA 25 ppm [7], respectively, otherwise it could adversely affect the respiratory system.

Bactericidal efficiency

Evaluation of antibacterial activity of DBDJ to *S. aureus* is shown in Fig. 4. It is observed that there is no bacteria inhibition zone in Fig. 4a and 4b, indicating that DBDJ with plasma dissipated power at 0.27 watt and time of exposure of 15-30 s does not exhibit bactericidal manner. However, as seen in Fig. 4c-4h, the bacteria inhibition zone becomes visible and increases with plasma dissipated power and time of exposure. This reveals that DBDJ were potentially effective in suppressing microbial growth when plasma dissipated power and time of exposure was increased. This finding is consistent with bactericidal efficiency which was evaluated by CFU method (Fig. 5). It is seen that bactericidal efficiency increases with both plasma dissipated power and time of exposure.

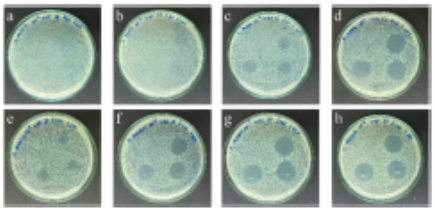

Figure 4 The *S. aureus* bactericidal efficiency of DBDJ, the plasma dissipated power at 0.27 watt and exposure time 15 to 60 s (a, b, c and d), the plasma dissipated power at 0.50 watt and exposure time 15 to 60 s (e, f, g and h).

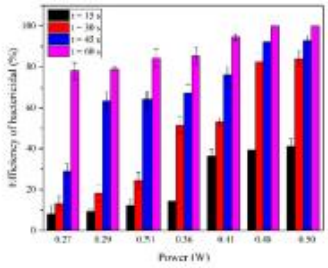

Figure 5 The percentage of *S. aureus* bactericidal efficiency by DBDJ.

Bactericidal effect of DBDJ on *P. aeruginosa* is presented in Fig. 6 and 7. Similar to *S. aureus* results, plasma from DBDJ can cause apoptosis of *P. aeruginosa* and bactericidal performance increases with plasma dissipated power and time of exposure. It is found that bactericidal effect of DBDJ on *P. aeruginosa* shows more effective than that on *S. aureus*. The difference in antibacteria activity of DBDJ on both bacteria could be caused by the difference in the cell wall structure. The outer structure of *S. aureus* cell wall is multi layers of peptidoglycan which has stronger bonding than *P. aeruginosa* outmost cell wall of which consists of phospholipids and lipopolysaccharides. Destruction of peptidoglycan through external stresses will lead to cell lysis [8, 9].

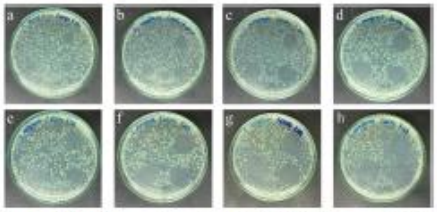

Figure 6 The *P. aeruginosa* bactericidal efficiency of DBDJ, the plasma dissipated power at 0.27 watt and exposure time 15 to 60 s (a, b, c and d), the plasma dissipated power at 0.50 watt and exposure time 15 to 60 s (e, f, g and h).

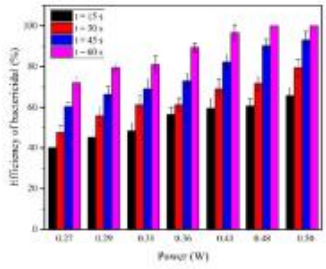

Figure 7 The percentage of *P. aeruginosa* bactericidal efficiency by DBDJ.

Effect of DBDJ on Bacterial Biofilms

DBDJ plasma operated at 0.5 watt and exposure time 1 min have high ability to eradicate bacteria as show in Fig. 4-7, the Fig. 8 show the fluorescent image. The result has shown this condition have high enough to eradicate bacterial and destroy bacterial biofilm [10] both of *S. aureus* and *P. aeruginosa*.

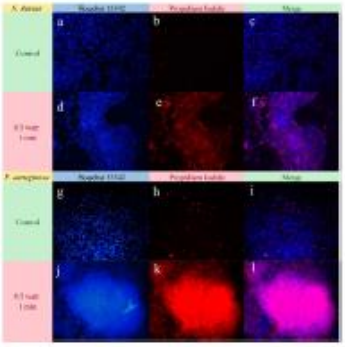

Figure 8 Bacterial biofilms of *S. aureus* and *P. aeruginosa* by Live/Dead assay with double stain Hoechst 33342 and Propidium iodide (PI). Control sample *S. aureus* (a, b and c) and *P. aeruginosa* (g, h and i). Plasma power at 0.5 watt and exposure time 1 min for removed bacterial biofilm *S. aureus* (d, e and f) and *P. aeruginosa* (j, k and l).

Furthermore, the charged particles in plasma played an important role for bactericidal with the rupture of bacteria cells wall [11, 12]. When the charge particles accumulated on outer surface of the membrane being more than the tensile strength of the membrane lead to cell rupture by electrostatic force [13]. CAPPs has the ability to destroy the proteins and enzymes activity into the cell. Most likely the cytoplasm will leaks out the cell through these holes, which was the reason leading the cell death why the cell dies [12, 14].

Cytotoxicity of HDFa Cells

Fig. 9 show the fluorescent image of HDFa cells. After treated HDFa cell with DBDJ plasma dissipated power at 0.5 watt and exposure time 1 min, the Fig. 9j to 9l show the plasma was not damage to the cells.

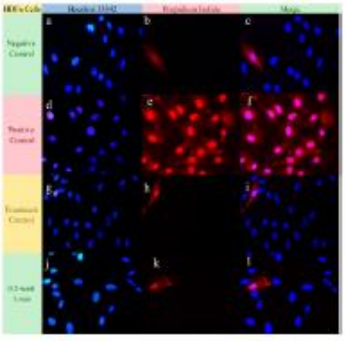

Figure 9 HDFa cells by Live/Dead assay with Hoechst 33342 and Propidium iodide (PI). Negative control as 10% FBS+DMEM (a, b and c), positive control as 50% DMSO +DMEM (d, e and f), treatment control as He gas blow (g, h and k) and plasma treated at 0.5 watt in 1 min (j, k and l).

The viability percentage of HDFa cells : negative control, positive control and treatment control show in Fig. 10A. The result shows that HDFa cells was not dead-induced by DBDJ with plasma dissipated power at 0.5 watt and exposure time 1 min. Fig. 10B statistical analysis of cell viability percentage. The result has shown this condition has a high ability to eradicate bacterial and destroy bacterial biofilms without effect to the viability percentage of HDFa cells. The total apoptosis percentage of HDFa cells shows in Fig. 11. Accordingly, the apoptosis profile could distinguish 4 cell populations by this method: Live cells; early apoptotic cells; late apoptotic/dead cells; and necrotic cells. Fig. 11A presents DBDJ with plasma dissipated power at 0.5 W and exposure time at 1st min. increasing the total apoptosis percentage of HDFa cells slightly but this is not significant after used statistical analysis (see Fig. 11B). The result shows DBDJ plasma was not induced apoptosis and leading cell to death when compared with negative control and treatment control. In positive control was used DMEM +10% DMSO 2 hr for induced cells to apoptosis and dead cells.

The result from Live/Dead assay, Muse Count & Viability Assay and Muse Annexin V & Dead Cell Assay shown in the same direction is DBDJ without side effect to viability cell and not inducing apoptosis leading cell to death cell of HDFa cell shown in Fig. 9-11.

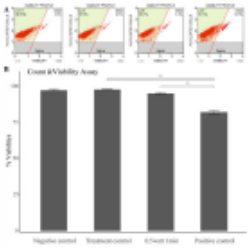

Figure 10 A. Representative figures from flow cytometry of HDFa cells with negative control, treatment control, plasma dissipated power at 0.5 watt with exposure time 1 min and positive control. **B.** Quantitative analysis of percentage cell viability from flow cytometry. Data are means of 3 replicates and expressed as means ± SD. ** indicates $P<0.01$.

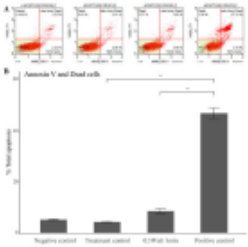

Figure 11 A. Representative figures from flow cytometry of HDFa cells with negative control, treatment control, plasma dissipated power at 0.5 watt with exposure time 1 min and positive control. **B.** Quantitative analysis of percentage total apoptosis from flow cytometry. Data are means of 3 replicates and expressed as means ± SD. ** indicates $P<0.01$.

4. Summary

The DBDJ have a high bactericidal efficiency to *S. aureus* and *P. aeruginosa* at plasma dissipated power 0.41 to 0.50 watt and exposure time 45 to 60 s. The bacteria inhibition zone affected by RONS and charge particles. Electrostatic force of ions in plasma played an important role for bactericidal leading to cell lysis. The difference of cell wall structure bacteria leading to difference DBDJ sensitivity. DBDJ with plasma dissipated power at 0.5 watt and exposure time 1 min have high potential to killed bacteria, eliminate bacterial biofilms by without damage or side effect to cell viability, apoptosis and death of HDFa cells in vitro is essential for clinical use [5] which it have a high bactericidal efficiency and assist in wound healing.

Acknowledgements

The authors are thankful to C. Chutsirimongkol for the Dielectric Barriers Discharge Plasma Jet (DBDJ). C. Yatongchai for consultation and suggestion to improve my research. Thailand Center of Excellence in Physics (ThEP) and Graduate School Maejo University for my scholarships.

References

[1] N. Mohd Nasir, B.K. Lee, S.S. Yap, K.L. Thong and S.L. Yap, Cold plasma inactivation of chronic wound bacteria. *Arch. Biochem. Biophys.*, **605** (2016) 76-85.

[2] S. Kubinova, K. Zaviskova, L. Uherkova, V. Zablotskii, O. Churpita, O. Lunov and A. Dejneka, Non-thermal air plasma promotes the healing of acute skin wounds in rats. *Sci. Rep.*, **7** (2017) 45183.

[3] C. Chutsirimongkol, D. Boonyawan, N. Polnikorn, W. Techawatthanawisan, T. Kundilokchai, C. Bunsaisup, P. Rummaneethorn, W. Kirdwichai, A. Chuangsuwanich and P. Powthongg, Non-Thermal Atmospheric Dielectric Barrier Discharge Plasma, Medical Application Studies in Thailand. *Plasma Medicine*, **6** (2016) 429-446.

[4] K.G. Kostov, R.Y. Honda, L.M.S. Alves and M.E. Kayama, Characteristics of dielectric barrier discharge reactor for material treatment. *Braz. J. Phys.*, **39** (2009) 322-325.

[5] J. Balzer, K. Heuer, E. Demir, M.A. Hoffmanns, S. Baldus, P.C. Fuchs, P. Awakowicz, C.V. Suschek and C. Oplander, Non-Thermal Dielectric Barrier Discharge (DBD) Effects on Proliferation and Differentiation of Human Fibroblasts Are Primary Mediated by Hydrogen Peroxide. *PLoS One*, **10** (2015) e0144968.

[6] S.D. Sheet. *OZONE*. 2012. p.1.

[7] S.D. Sheet. *NITRIC OXIDE*. 2003. p.1.

[8] A. Mai-Prochnow, M. Clauson, J. Hong and A.B. Murphy, Gram positive and Gram negative bacteria differ in their sensitivity to cold plasma. *Sci Rep.*, **6** (2016) 38610.

[9] W. Vollmer, D. Blanot and M.A. de Pedro, Peptidoglycan structure and architecture. *FEMS Microbiol. Rev.*, **32** (2008) 149-167.

[10] D. Dobrynin, G. Fridman, G. Friedman and A. Fridman, Physical and biological mechanisms of direct plasma interaction with living tissue. *New J. Phys.*, **11** (2009).

[11] G. Fridman, A.D. Brooks, M. Balasubramanian, A. Fridman, A. Gutsol, V.N. Vasilets, H. Ayan and G. Friedman, Comparison of Direct and Indirect Effects of Non-Thermal Atmospheric-Pressure Plasma on Bacteria. *Plasma Process. Polym.*, **4** (2007) 370-375.

[12] J. Guo, K. Huang and J. Wang, Bactericidal effect of various non-thermal plasma agents and the influence of experimental conditions in microbial inactivation: A review. *Food Control*, **50** (2015) 482-490.

[13] M. Laroussi, D.A. Mendis and M. Rosenberg, Plasma interaction with microbes. *New J. Phys.*, **5** (2003) 41.

[14] M.G. Kong, G. Kroesen, G. Morfill, T. Nosenko, T. Shimizu, J. van Dijk and J.L. Zimmermann, Plasma medicine: an introductory review. *New J. Phys.*, **11** (2009).

CERTIFICATE OF ACHIEVEMENT

This is to certify that

Mr. Pipath Poramapijitwat

has successfully achieved the course of Japan-Asia Youth Exchange program in Science(SAKURA Exchange Program in Science) administered by Japan Science and Technology Agency. National Institute for Fusion Science ran the course from November 12 to December 2 in 2017. We welcome you as a member of the Sakura Science Club.

SAKURA SCIENCE Exchange Program in Science

M Hamaguchi

HAMAGUCHI MICHINARI, MD., PH.D.
PRESIDENT
JAPAN SCIENCE AND TECHNOLOGY AGENCY

Date: December 2, 2017

No: 17104466

PW : ssc46617

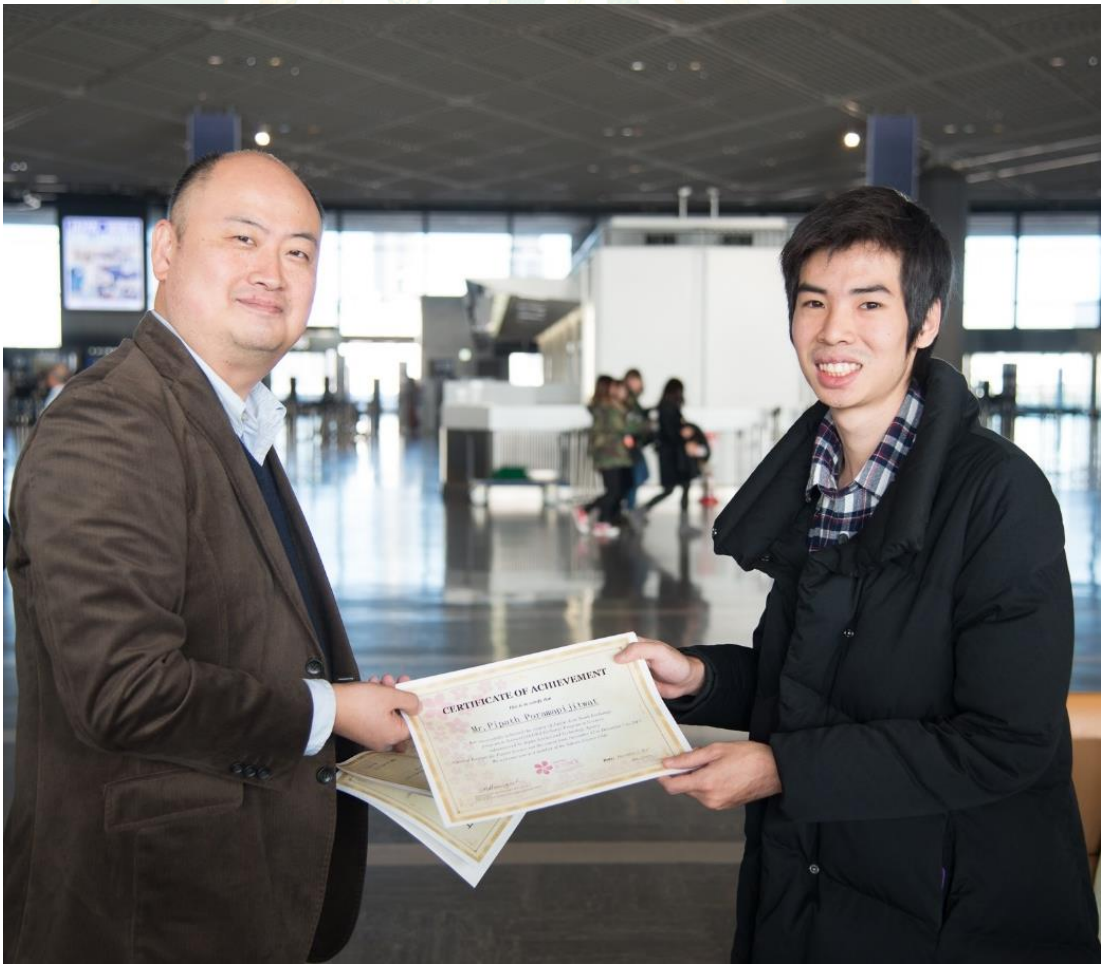

CURRICULUM VITAE

NAME Mr.Pipath Poramapijitwat

DATE OF BIRTH 25 January 1993

EDUCATION 2016-2019 Master of Science Program in Nanoscience and Nanotechnology, Maejo University, Chiang Mai, Thailand.
2011-2015 Bachelor of Science Program in Materials Science, Maejo University, Chiang Mai, Thailand.
2008-2011 High-School Certificate, Kawilawitayalai School, Chiang Mai, Thailand.
2005-2008 Middle-School Certificate, Kawilawitayalai School, Chiang Mai, Thailand.